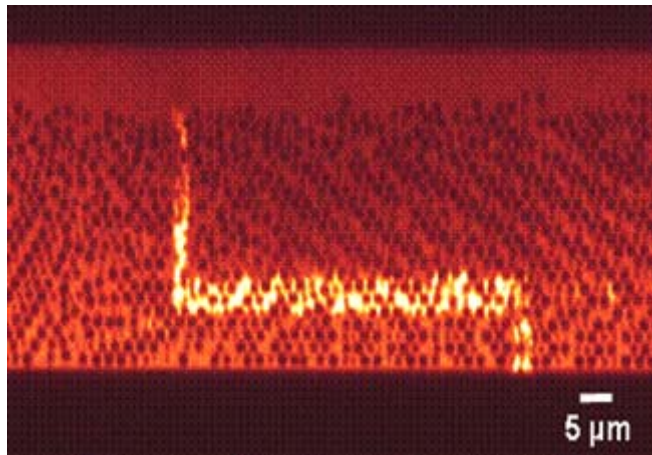
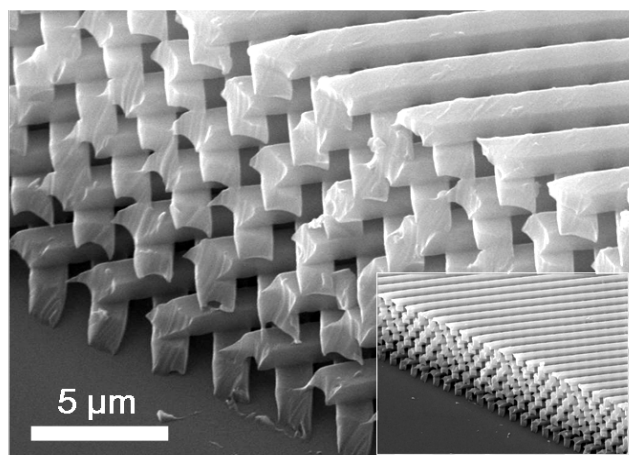
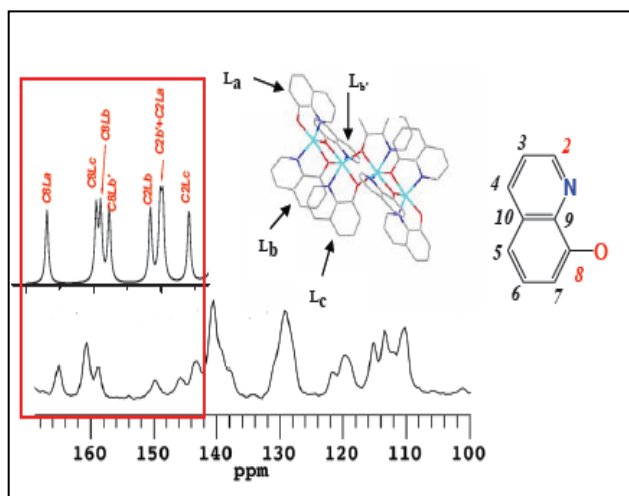


2006 Fundamental Research Underlying Solid-State Lighting Contractors Meeting

February 1, 2006, Grosvenor Hotel, Lake Buena Vista, Florida



Cover

Top Left: Solid State ^{13}C CP-MAS NMR spectrum for Zn(II)(8-quinolinoato) tetramer showing C8 and C2 resonances are different depending on the mode and environment of ligand chelation. (Inset: Simulated spectrum showing C8 and C2 resonances from DGAIO-SCFF Calculations).
Courtesy: *Linda Sapochak, Pacific Northwest National Laboratory*

Top Right: Excited light from quantum dots solutions
Courtesy: *J.P. Wilcoxon, Paula Provencio and Billie Abrams, Sandia National Laboratories*

Bottom Left: 12-layered polymer microstructure by 2P- μTM .
Courtesy: *Kai-Ming Ho, Ames Laboratory, Iowa State University*

Bottom Right: Laser scanning confocal microscope image of a three-dimensional waveguide embedded within a self-assembled photonic crystal. The substrate-photonic crystal interface is at the bottom of the image, and the waveguide is the z-bend structure running from the bottom to the top of the photonic crystal.
Courtesy: *Paul Braun, Wonmok Lee, and Stephanie Pruzinsky, University of Illinois*

Foreword

This volume highlights the scientific content of the 2006 Fundamental Research Underlying Solid-State Lighting Contractors Meeting sponsored by the Division of Materials Sciences and Engineering (DMS&E) in the Office of Basic Energy Sciences (BES) of the U. S. Department of Energy (DOE). This meeting is the second in a series of research theme-based Contractors Meetings and will focus on BES/DMS&E-funded research that underpins solid-state lighting technology. The meeting will feature research that cuts across several DMS&E core research program areas. The major programmatic emphasis is on developing a fundamental scientific base, in terms of new concepts and new materials that could be used or mimicked in designing novel materials, processes or devices.

The purpose of the 2006 Fundamental Research Underlying Solid-State Lighting Contractors Meeting is to bring together researchers funded by BES in this new and emerging research area to facilitate the exchange of new results and research highlights, to foster new ideas and collaborations among the participants, and to identify needs of the research community. The meeting will also help DMS&E in assessing the state of the program, charting future directions and identifying programmatic needs. The agenda reflects some of the major research themes that have potential contributions to make toward the science underlying solid-state lighting.

Many of the BES Contractors Meetings are passing the quarter-century mark in longevity and are very highly regarded by their participants. We sincerely hope that the 2006 Fundamental Research Underlying Solid-State Lighting Contractors Meeting will join the others in keeping with the long-standing BES tradition.

We thank all of the invited speakers and meeting attendees for their active participation in sharing their ideas and research results. The dedicated efforts of the Meeting Chair, Valy Vardeny, in organizing and coordinating the meeting are sincerely appreciated. We also extend our thanks to Jim Brodrick and his colleagues in the Office of Energy Efficiency and Renewable Energy (EERE) at DOE for the invitation to hold our meeting in conjunction with the 2006 EERE Solid-State Lighting Workshop. Thanks also go to Christie Ashton from DMS&E, Brian Herndon and colleagues from the Oak Ridge Institute of Science and Education, Karen Marchese from Akoya and the staff of Sage Technologies for their fine work in taking care of logistical aspects of the meeting.

Tim Fitzsimmons, Arvind Kini, and Dick Kelley
Division of Materials Sciences and Engineering
Office of Basic Energy Sciences
Office of Science
U.S. Department of Energy

2006 DOE SOLID-STATE LIGHTING WORKSHOP

February 1-3, 2006
Grosvenor Hotel
Lake Buena Vista, Florida

Preliminary Agenda

February 1, 2006 – Basic Energy Science Contractor Meeting

7:30 Registration and Coffee

8:00 **Welcome**

Valy Vardeny, University of Utah
Tim Fitzsimmons, DOE
James Brodrick, DOE

8:20 **Keynote Address: Electrophosphorescent Organic Light Emitting Devices, and their Application to Solid-State Lighting**

Stephen Forrest, Princeton University

9:00 **Interfaces of Polymer Electronic Devices**

Antoine Kahn, Princeton University

9:30 **Spin Transport in Organic Semiconductors**

Jing Shi, University of California, Riverside

10:00 Coffee Break

10:20 **Electronic Processes in Solid State Organic Electronic Materials**

Darryl Smith, Los Alamos National Laboratory

10:50 **Transport Fundamentals in Crystalline Organic Semiconductor Devices**

Arthur Ramirez, Lucent Technologies

11:20 **Behavior of Charges, Excitons and Plasmons at Organic/Inorganic Interfaces**

Michael McGehee, Stanford University

11:50 **Design, Synthesis, and Structuring of Functional Polymers and Dendrimers with Potential in Solid-State Lighting Technologies**

Jean Fréchet, University of California and Lawrence Berkeley National Laboratory

12:20 Lunch

The DOE Nanoscience Centers and Solid State Lighting

Paul Alivisatos, University of California, Berkeley and Lawrence Berkeley National Laboratory

2:00 **How to Dope Wide-Gap Materials: Basic Design Rules**

Alex Zunger, National Renewable Energy Laboratory

2:30 **Optical Properties of Semiconductors from Crystals to Nanocrystals**

James Chelikowsky, University of Texas

- 3:00 **Synthesis of Nanoclusters for Energy Applications**
Jess Wilcoxon, Sandia National Laboratories
- 3:30 *Coffee Break*
- 3:50 **Photonic Crystals and Negative Index Materials**
Costas Soukoulis, Iowa State University, Ames Laboratory
- 4:20 **Programming Function in Photonic Crystals**
Paul Braun, University of Illinois
- 4:50 **Biased Self-Assemblies in Block Copolymers and Nanorods**
Tom Russell, University of Massachusetts, Amherst
- 5:30 **Wrap-Up and Day 2 Preview**
Valy Vardeny, University of Utah
Tim Fitzsimmons, DOE, James Brodrick, DOE
- 5:40 **Adjourn**
- 6-8:30 **Poster Session and Reception with hors d'oeuvre stations and cash bar**

Table of Contents

Foreword	i
Agenda	iii
Table of Contents	iv
Poster Sessions	vi
Abstracts	
Electrophosphorescent Organic Light Emitting Devices and Their Application to Efficient Solid State Lighting	1
<i>Stephen Forrest</i>	
Interfaces of Polymer Electronic Devices.....	2
<i>Antoine Kahn, Princeton University</i>	
Spin Transport in Organic Semiconductors.....	6
<i>Jing Shi, University of California, Riverside</i>	
Electronic Processes in Solid State Organic Electronic Materials.....	7
<i>Darryl Smith, Los Alamos National Laboratory</i>	
Transport Fundamentals in Crystalline Organic Semiconductor Devices.....	11
<i>Arthur Ramirez, Lucent Technologies</i>	
Behavior of Charges, Excitons and Plasmons at Organic/Inorganic Interfaces	12
<i>Michael McGehee, Stanford University</i>	
Design, Synthesis, and Structuring of Functional Polymers and Dendrimers with Potential in Solid- State Lighting Technologies	15
<i>Jean Fréchet, University of California and Lawrence Berkeley National Laboratory</i>	
The DOE Nanoscience Centers and Solid State Lighting	19
<i>Paul Alivisatos, University of California and Lawrence Berkeley National Laboratory</i>	
How to Dope Wide-Gap Materials: Basic Design Rules.....	20
<i>Alex Zunger, National Renewable Energy Laboratory</i>	
Optical Properties of Semiconductors from Crystals to Nanocrystals.....	21
<i>James Chelikowsky, University of Texas</i>	
Synthesis of Nanoclusters for Energy Applications	25
<i>Jess Wilcoxon, Sandia National Laboratories</i>	

Photonic Crystals and Negative Index Materials.....	26
<i>Costas Soukoulis, Iowa State University, Ames Laboratory</i>	
Programming Function in Photonic Crystals.....	27
<i>Paul Braun, University of Illinois</i>	
Biased Self-Assemblies in Block Copolymers and Nanorods.....	31
<i>Tom Russell, University of Massachusetts, Amherst</i>	
Posters	32

POSTER SESSION
Wednesday, February 1, 2006

P-1

Optical, Electrical and Magnetic Studies of Ordered π -Conjugated Systems
Z. Valy Vardeny

P-2

The Organic Chemistry of Conducting Polymers: From Molecular Wires to Photovoltaics
Laren M. Tolbert and Janusz Kowalik

P-3

Combinatorial Fabrication and Screening of Organic Light-Emitting Device Arrays
Joseph Shinar

P-4

Charge Injection and Transport in Polyfluorenes
Alexis Papadimitratos, Hon Hang Fong, and George G. Malliaras

P-5

Spectroscopic Study on Sputtered PEDOT-PSS: Role of Surface PSS Layer
Jaehyung Hwang, Fabrice Amy and Antoine Kahn

P-6

White-Light Emission from Ultra-small Cadmium Selenide Nanocrystals
Michael J. Bowers II; James R. McBride and Sandra J. Rosenthal

P-7

Enhanced Light Emission from Lu_2SiO_5 Induced by Ion Irradiation
Luiz G. Jacobsohn, Ross E. Muenchausen and D. Wayne Cooke

P-8

Nanophosphors
Ross E. Muenchausen, Luiz. G. Jacobson, and D. Wayne Cook

P-9

In-Situ Synchrotron X-ray Studies of Metal Organic Chemical Vapor Deposition of $\text{In}_x\text{Ga}_{1-x}\text{N}$
G. Brian Stephenson, Fan Jiang, Stephen K. Streiffer, Anneli Munkholm

P-10

Luminescence, Structure, and Growth of Wide-Bandgap InGaN Semiconductors
S. R. Lee, D. D. Koleske, S. R. Kurtz, R. J. Kaplar, M. H. Crawford, D. M. Follstaedt, and A. J. Fischer

P-11

Overcoming Doping Bottlenecks in Semiconductors and Wide-gap Materials

Shengbai Zhang and Su-Huai Wei

P-12

Theoretical and Experimental Study of Solid Composition and Ordering in III/V Systems

G. B. Stringfellow, F. Liu, A. Howard, and J. Zhu

P-13

Many Body Effects in Nanotube Fluorescence Spectroscopy

E. J. Mele and C. L. Kane

P-14

Solid-State MAS NMR Studies of Supramolecular Zinc Chelates and ZnO Nanorods

Linda Sapochak, Li-Qiong Wang, Kim Ferris, Chunhua Yao, Greg Exarhos

P-15

Theoretical Investigations of Nanoscale Structures and Semiconductor Surfaces

J. Bernholc and C. Roland

P-16

Theory of Surface and Interface Properties of Correlated Electron Materials

Andrew Millis and Satoshi Okamoto

P-17

Metal-Insulator-Semiconductor Photonic Crystal Fibers: A New Paradigm for Optoelectronics

Y. Fink and J. D. Joannopoulos

P-18

Three-Dimensional Photonic Crystals by Soft Lithographic Technique

Jae-Hwang Lee, Yong-Sung Kim, Joong-Mok Park, Wai-Y. Leung, Chang-Hwan Kim, Ping Kuang, Rana Biswas, Kristen Constant, Kai-Ming Ho

Abstracts

Electrophosphorescent Organic Light Emitting Devices and Their Application to Efficient Solid State Lighting

Stephen Forrest

Departments of Electrical Engineering and Computer Science, and Physics
University of Michigan
Ann Arbor, MI 48109 USA

A significant challenge facing human kind in the 21st Century is how to address the ever decreasing supply of depletable and renewable energy. One approach to this problem is to decrease our usage. For this reason, considerable attention has been focused on more efficient means for room lighting which currently consumes approximately 20% of the energy used in buildings. Organic light emitting devices (OLEDs) provide a unique opportunity to provide this high efficiency solid state lighting at very low cost. In this talk, I will discuss several strategies for achieving very high efficiency white light emission at high brightnesses for the next generation of efficient solid state lighting sources based on small molecular weight, vapor deposited OLED structures. Key to our approach is the use of electrophosphorescence as a means for converting all electrical into optical energy. We show that the highest luminance efficiencies can be obtained by a combination of fluorescence and phosphorescence in a unique OLED structure. Furthermore, the highest brightnesses are achieved (without a significant loss in power efficiency) by stacking several fluorescent/phosphorescent elements in a single OLED structure (called a SOLED), with each emitting element in the stack separated by a transparent charge generation layer. Prospects for OLEDs as the next practical generation of interior illumination sources will be reviewed.

Interfaces of Polymer Electronic Devices

Antoine Kahn, Princeton University (kahn@princeton.edu); Jean-Luc Brédas, Georgia Institute of Technology; Anil Duggal, General Electric Global Research; and George Malliaras, Cornell University

Program Scope

The field of organic molecular thin films and devices is developing extremely fast, driven by the enormous potential that small molecule and polymer semiconductors have for applications in large-scale electronic and optoelectronic devices. The most rapid development of the past decade has been in the area of organic light emitting diodes (OLED) and field effect transistors (FET). Considerable effort has also been spent on the development of OLEDs for general lighting and heterojunction photovoltaic cells. The endless choice of molecules and the range of organic film processing techniques (from vacuum deposition to printing from solvent solutions) allow a degree of originality that cannot be matched with inorganic semiconductor technology. In the same time, the multiplicity of compounds and processing techniques places considerable demands on our ability to understand and control the structural and electronic properties of these materials and their interfaces.

Interfaces of organic materials with inorganic and organic solids play a central role in charge injection and transport, and are exceedingly important for device performance and lifetime. Technologically important organic semiconductors have large energy gaps (≥ 2 eV), making injection barriers potentially large. A detailed understanding of the mechanisms that control interface energetics and chemistry, and of methods to modify the electrical behavior of these interfaces is therefore of paramount importance.

Much has also been done on polymer interfaces¹⁻³, although experimental constraints due to (mostly) ex-situ film formation methods have somewhat limited the scope of investigations of the basic bulk and interface energetics. Interface energy level alignment mechanisms and link between transport levels and interface injection barriers are not as well understood as in molecular films. Yet, the ability to predict and control interface electronic structures and injection efficiency in polymers films requires a clear connection between: (i) interface electrical properties (injected current vs. applied bias); (ii) transport electronic levels, i.e. highest occupied and lowest unoccupied molecular orbitals (HOMO, LUMO) and injection barriers, i.e. the “Schottky barriers”; and (iii) theoretical electronic structure of the material and its interfaces. The purpose of the work supported by DOE has been to establish a concerted experimental, theoretical and device effort aimed at addressing this crucial connection for model polymer systems.

Recent Progress

Two fluorene-based polymers – the fluorene homopolymer poly(dioctylfluorene) (F8) and the fluorene-triarylamine poly(dioctylfluorene-co-N-(4-butylphenyl) diphenylamine) (TFB) – were chosen for this work (Figure 1). High performance blue-emitting devices can be made when these two polymers are blended together. A “standard” fabrication protocol was developed at GE that yields devices representative of what is typically accomplished in industrial settings, but which

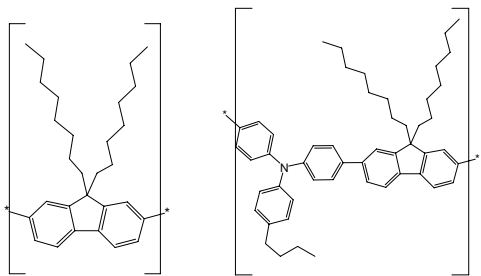


Fig. 1: chemical structure of the two polymers F8 (left) and TFB (right)

utilized only “university-scale” equipment that is available at the participants’ laboratories.

The initial focus was on electron spectroscopy of the polymer films and modeling to extract precise position of the electron and hole transport states. Thin films (~150Å) were prepared by spin-casting from solution on substrates of indium tin oxide (ITO) covered by a layer of the hole injector poly(3,4-ethylenedioxythiophene) / poly(styrenesulfonate) (PEDOT:PSS). Ultra-violet photoemission and inverse photoemission spectroscopy (UPS, IPES) measurements were performed to measure the density of filled and empty states, respectively, and the associated ionization energy (IE) and electron affinity (EA) of the material (Table below).

	IE (eV)	EA (eV)	Vacuum level shift from substrate (eV)	E_F -HOMO (eV)	LUMO- E_F (eV)	Transport gap (eV)
F8	5.75	2.4	0.0	0.6~0.65	2.7	3.35
TFB	5.50	2.35	0.3	0.6~0.7	2.45	3.15
1:1 blend	5.60	N/A	0.1	0.6~0.65	N/A	N/A

Theoretical computations of density of states were performed to interpret the spectroscopic data. F8 was modeled by a pentamer of fluorene and TFB by a trimer of the two comonomers, fluorene and triphenylamine⁴. The trimer was built in a symmetric fashion by attaching an additional fluorene to the triphenylamine terminus. Diocetyl side- groups, which do not affect electronic structure of interest, were omitted from the models and replaced with hydrogen atoms. A plane-wave, pseudopotential Density Functional Theory (DFT) method within the generalized-gradient approximation (GGA) with the BLYP functional was used for all geometry and wavefunction calculations⁵.

An example of the simulation of UPS and IPES spectra of F8 and TFB is given in Figure 2. The agreement between theory and experiment allows a detailed interpretation of the experimental features. One notable feature in the UPS spectrum of TFB is the appearance of an additional peak as the highest occupied band. Examination of the molecular orbitals indicates that this peak originates from the triphenylamine moieties, whereas the second peak of TFB and the first of F8 share a similar origin. This feature explains the destabilization of the HOMO level when incorporating triphenylamine units, which leads to an ionization potential of about 5.3 eV;

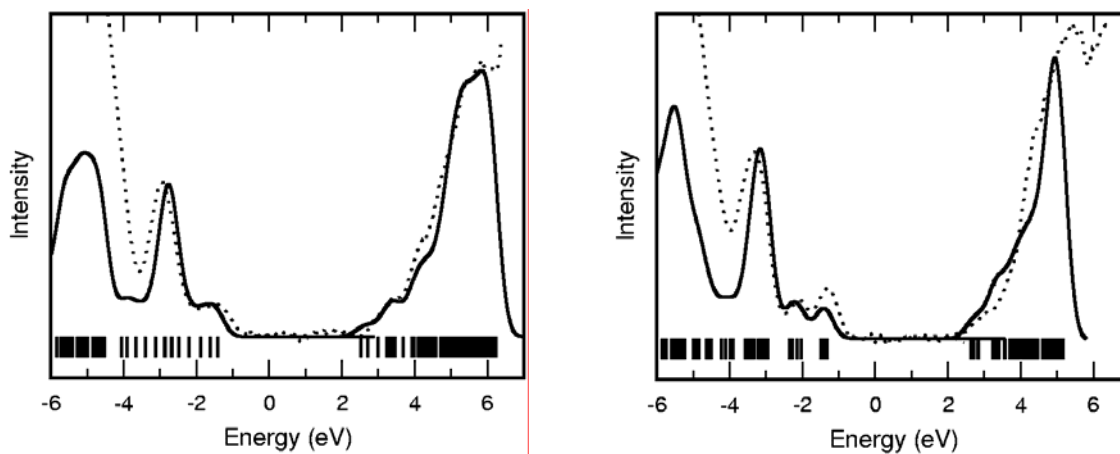
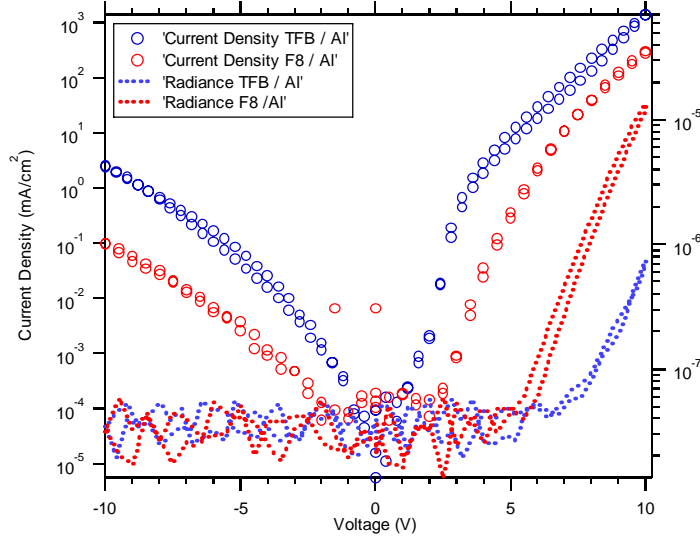


Fig. 2: Simulated UPS and IPES spectra of F8 (left) and TFB (right). The calculated energy spectra (bar curves) are convolved by a Gaussian function with a FWHM of 0.55 eV. The dotted line represents the experimental data.

as a result, hole injection from the anode can be significantly improved since the ionization potential is lowered by about 0.25 eV with respect to F8. From the point of view of defining key transport states in these polymers, the combination, and alignment, of experimental and theoretical spectra (Fig. 2) allows a precise determination of the HOMO and LUMO positions and of the transport gap of the material.

Simple devices were made to test for injection efficiency from various metals into F8 and TFB. In agreement with the UPS measurements of interface barriers, it was found that the barrier for hole injection is considerably smaller than the barrier for electron injection. Using PEDOT:PSS/polymer/Al devices, it was shown that the current is mostly a hole current, but the



radiance is controlled by electron injection from the Al electrode. Higher current was found for the TFB device, in accord with a lower barrier for hole injection for this polymer, while the higher radiance found for F8 is consistent with a lower barrier for electron injection for this polymer (Fig.3).

Fig. 3: Current-voltage and Radiance-Voltage characteristics of ITO/PEDOT:PSS/PFO/Al light emitting diodes, where PFO is F8 and TFB

In order to relate measured injected current to interface electronic barriers, initial hole mobility measurements were performed with time-of-flight (TOF) measurements. Various approaches were tried, leading to the successful casting of films with thickness in the several microns range. TOF measurements on TFB yielded a hole mobility of 10^{-4} cm^2/Vsec . The trace was dispersive, indicating considerable hole-trapping. At this point, it is unclear whether the traps are intrinsic or extrinsic, as the sample was handled and measured in air.

Finally, a basic OLED device structure (Fig.4) was used as a standard baseline to test these polymers. Devices with this structure were made with variable light-emitting polymer layer thickness and F8:TFB ratios of 1:0, 1:1, and 0:1. A substantial analysis by the team, drawing on all information available on interface electronic structure, injection barriers and charge carrier transport will be required to understand these devices. However, in rough terms, the F8 device has the highest efficiency values, the TFB has the lowest,

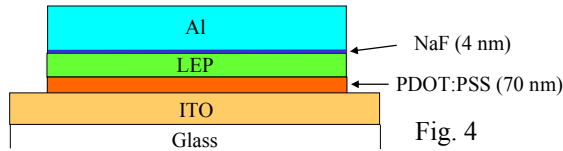


Fig. 4

while the mixture exhibits values in between the two extremes. This relative ordering of the efficiency as a function of the F8:TFB ratios suggests a trivial “law of mixing” result with no complex interactions. However, it is unlikely that the physics is so simple. For instance, the shape of the efficiency curves at low current density is substantially different for the three blend ratios. Similarly, the color stability of the three different LEP blends exhibits a different ordering. This can be seen in the output spectrum (not shown here) of the same devices before and after a single current-voltage measurement cycle. One can see that the pure F8 and pure TFB exhibit noticeable changes in their spectrum whereas the mixture exhibits no such change. Hence there

must be some beneficial change in the charge, energy transfer, or morphology dynamics that occurs with the mixture of these two materials. Over the course of this program, we expect to uncover numerous phenomena like this and it is expected that teasing out the explanations will provide important insights into the physics of polymer based OLEDs.

Future plans

The following research on these materials and devices will be developed in the next two years.

- continuation of theoretical work on electronic structure of pristine polymer chains (both occupied and unoccupied levels) as well as PEDOT:PSS, with simulation of UPS and IPES spectra. Simulation of optical absorption spectra and evaluation of exciton binding energy including effects of surrounding. Initial work on electronic structure of polymer interfaces with metal electrodes
- initial UPS/IPES and Kelvin probe-Contact Potential Difference investigations of interfaces between polymer films and a range of metals
- TOF experiments to determine intrinsic limits to carrier mobility in the model system polymers. The film casting technique has been improved to allow for preparation and characterization of samples in the absence of oxygen and moisture.
- injection experiments and correlation to transport, spectroscopy and theory
- continued fabrication and testing of devices utilizing the model system polymers and identification and supply of polyfluorene model system variations that exhibit contrasting electronic and morphological properties

References

1. *Conjugated Polymer and Molecular Interfaces*, W.R. Salaneck, K. Seki, A. Kahn and J.-J. Pireaux, editors, Marcel Dekker, Inc. (2001).
2. W.R. Salaneck, S. Stafström and J.-L. Brédas, *Conjugated Polymer Surfaces and Interfaces*, Cambridge University Press, 1996
3. M. Lögdlund, G. Greczynski, A. Crispin, M. Fahlman, W.R. Salaneck and T. Kugler in [1], p. 73.
4. *Electronic Materials—The Oligomer Approach*, edited by G. Wegner and K. Müllen (VCH, Weinheim, 1998).
5. CPMD, version 3.9.1, IBM and MPI-Stuttgart, 2004.

DOE Sponsored publications (2005)

1. Electrical doping of Poly(9,9-dioctylfluorenyl-2,7-diyl) with tetrafluoro-tetracyanoquinodimethane by solution method, J. Hwang and A. Kahn, *J. Appl. Phys.* **97**, 103705 (2005)
2. Composition and electronic structure of PEDOT:PSS surfaces: the role of the segregated PSS layer, J. Hwang, F. Amy and A. Kahn, *Org. Electronics* (submitted)
3. Fundamental study on electron band structure of polyfluorene and its derivative polymer, J. Hwang, E. Kim, J.-L. Brédas and A. Kahn (in preparation)

Spin transport in organic semiconductors

Jing Shi¹ and Valy Vardeny²

1. Department of Physics, University of California at Riverside
2. Department of Physics, University of Utah

Spin degree of freedom plays an important role in exciton formation and resulting light emission in ordinary organic light emitting devices. Spin injection and coherent transport in organic semiconductors could in principle be exploited to enhance the quantum efficiency of the light emission. To explore this possibility, we have first fabricated simple spin valve devices which consist of two ferromagnetic electrodes (e.g. LaSrMnO and Co) and an organic semiconductor (e.g. Alq₃ or NPD) spacer layer. The well-defined switching between “on” and “off” states corresponds well to the switching of the magnetization of the two ferromagnetic layers, indicative of the well-known spin valve effect. The inverse magnetoresistance is consistent with the fact that the spin polarization of the two ferromagnetic electrodes is opposite to each other. The magnitude of the spin valve magnetoresistance decreases as the organic semiconductor spacer layer becomes thicker due to increased spin scattering. By measuring the spin valve magnetoresistance between the parallel and anti-parallel magnetization states as a function of the spacer layer thickness, we can extract the spin diffusion length in organic semiconductors, which decreases rather rapidly as the temperature increases. We have been working with different small molecule materials in order to understand the physical origin of this temperature dependence. In addition to the low field magnetoresistance, we have also observed another kind of magnetic field dependence in both resistance and electroluminescence at high magnetic fields. We attribute these high field effects to an enhanced carrier injection at the LSMO/organic interface due to an upshift of the Fermi level in LSMO at high magnetic fields.

* Research supported by NSF, DARPA and DOE.

Electronic Processes in Solid State Organic Electronic Materials

Darryl L. Smith, Ian H. Campbell, Brian K. Crone, and Richard L. Martin
Los Alamos National Laboratory, Los Alamos, NM 87545
dsmith@lanl.gov, campbell@lanl.gov, bcrone@lanl.gov, rlmartin@lanl.gov

Program Scope

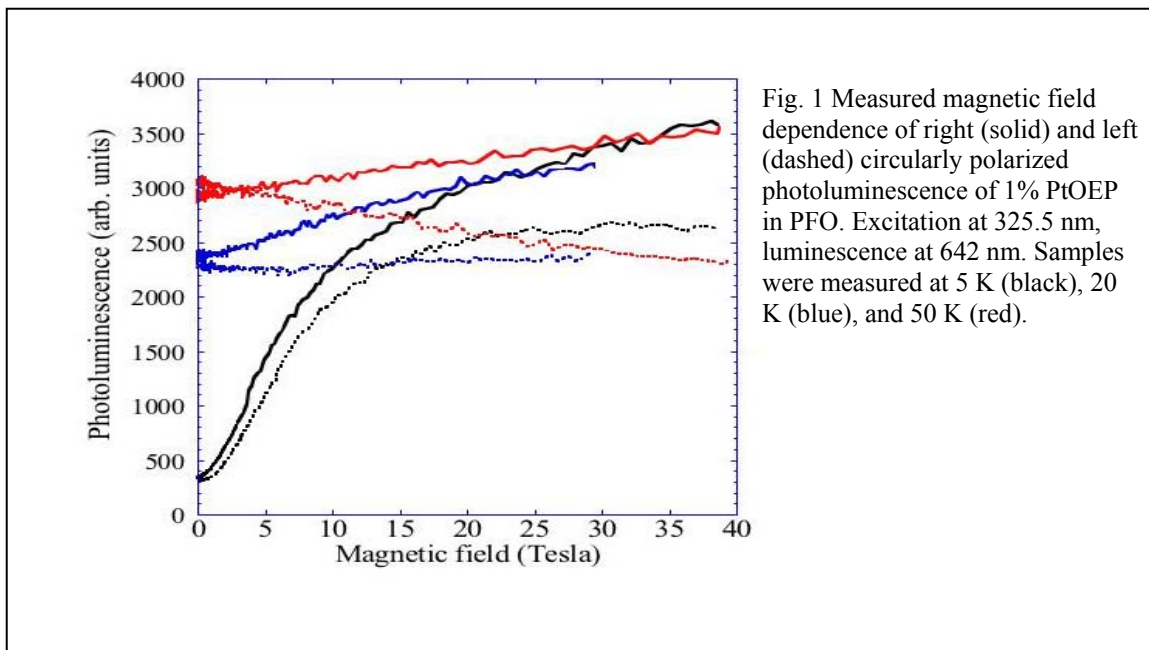
Organic electronic materials are of great intrinsic scientific interest. In these materials there is strong coupling of electron charge, spin, and lattice degrees of freedom, and the resulting rich spectrum of tunable ground and excited states makes them an ideal vehicle for the study of flexible strongly correlated systems. Organic electronic materials are also becoming technologically important for a broad class of applications. Factors motivating the technological development of organic electronic materials include: their ability to be processed economically in large areas and at low temperature; the unprecedented tunability of their electronic properties; facile thin film and heterostructure fabrication; and the possibility of creating nanoscale structures and devices through molecular assembly techniques. To date, the development of organic electronic materials has primarily followed an Edisonian approach. Because of the very large material and device structure phase space, there is a critical need for basic scientific research on the fundamental physical properties of organic electronic materials. Organic electronic materials are a condensed phase (i.e., thin films, single crystals, and nanoscale molecular assemblies) of π -conjugated molecules. Intermolecular interactions are critical in determining the condensed phase properties and the electronic properties of the dense films are typically not the same as those of the isolated molecules or of single polymer chains. A major theme of this research is aimed at determining which features of the electronic structure of the isolated molecules are maintained and which are modified in the condensed phase and to use our understanding of molecular electronic structure to describe the behavior of the condensed phases. The overall goal is to provide an understanding of the fundamental physical processes that are important in determining the properties of organic electronic materials. We are focusing on representative materials, including both conjugated polymers and smaller conjugated molecules, which provide model systems with which to understand these fundamental physical processes. We are using an integrated theory, fabrication, and measurement approach to: 1) study electron charge injection at metal/organic and organic/organic interfaces; 2) investigate electron charge transport in organic electronic materials; 3) investigate exciton formation and dissociation in heterogeneous organic systems; 4) study electron spin injection, detection, and transport.

Recent Progress

Since the start of the program on 4/05 we have focused on electron spin processes in organic electronic materials. The prospect of using the electron spin degree of freedom in a new generation of electronic and electro-optic spintronic devices is an exciting possibility. Realization of spintronic devices relies on three basic processes: a) the establishment of a non-equilibrium electron or hole spin distribution; b) transport and

manipulation of the spin distribution; and c) detection of the spin distributions. Recently there has been dramatic progress in understanding electron spin-based phenomena in inorganic semiconductors. Conjugated organic semiconductors are especially promising for non-equilibrium electron spin based phenomena because: 1) they have extremely small spin-orbit interactions and small hyper-fine interactions so that both electron and hole spin lifetimes are long; 2) organometallic compounds with strong spin-orbit interactions can be included at specific spatial locations in an organic semiconductor based structure to permit manipulation of spin-orbit coupling without adverse effects on spin lifetimes elsewhere in the structure; and 3) self-assembled monolayers can be used to tailor interface properties for spin injection and electrical spin detection using ferromagnetic contacts.

Spin-orbit coupling is essential for optical spin detection because it is the origin of the spin dependence of the optical selection rules [1]; however, it also provides spin relaxation mechanisms that greatly reduce spin lifetimes. Typical organic semiconductors have negligible spin-orbit coupling because they consist of very light elements. This is a great advantage to obtain the long spin-lifetimes required in most spintronic structures; however it does not permit optical injection or detection of spins. Organometallic compounds such as platinum octaethylporphine (PtOEP) have substantial spin-orbit coupling because they contain a heavy atom (Pt) and permit optical injection and detection of spins. Oriented spins in the organic host can be transferred to the organometallic guest to form excitations whose circularly polarized optical properties can be detected. A great advantage of organic semiconductors is that the spin-orbit coupling



can be engineered into the device structure selectively by placing the organometallic compounds in positions where significant spin-orbit coupling is desired but exclude them from other regions where long spin lifetimes are needed.

Recently we have demonstrated that photoluminescence from PtOEP in a magnetic field can be more than 20% circularly polarized [2]. Figure 1 shows the measured photoluminescence intensity (vertical axis) as a function of magnetic field (horizontal axis) for right and left circularly polarized luminescence. The difference in

intensity between the right (solid line) and left (dashed line) circularly polarized luminescence is due to the spin polarization of the emitting state. In these initial experiments we use a high magnetic field to rapidly determine the materials spin dependent properties. We have surveyed several organometallic compounds, including Ir and Eu containing organic phosphors, and PtOEP is a promising organic molecule for spin manipulation. We have begun a theoretical investigation of these compounds in order to fully understand the electronic structure that controls their spin dependent properties.

Future Plans

We have demonstrated that PtOEP is a promising material for investigating the spin physics of organic semiconductors. We will concentrate our research in the coming year on optical and electrical methods to establish non-equilibrium electron and hole spin distributions using this model compound. Non-equilibrium spin distributions can be established by: 1) polarized optical techniques based on spin dependent optical selection rules; and 2) spin polarized electrical injection from ferromagnetic contacts [1]. We will detect the spin distribution using the polarization of the photoluminescence discussed above.

(a) Optical Injection

The absorption of circularly polarized light can be used to create a non-equilibrium spin distribution because of spin dependent optical selection rules [1]. Spin-orbit coupling is essential for optical spin injection because it is the origin of the spin dependence of the optical selection rules. Spin oriented excitations can be formed on organometallics such as PtOEP using circularly polarized light because the spin-orbit interaction couples light to spin, and then the oriented spins can be transferred to the host organic semiconductor. This is the reverse of the luminescence process used to detect the spin polarizations.

(b) Electrical Injection

Recent results for electrical spin injection into inorganic semiconductors

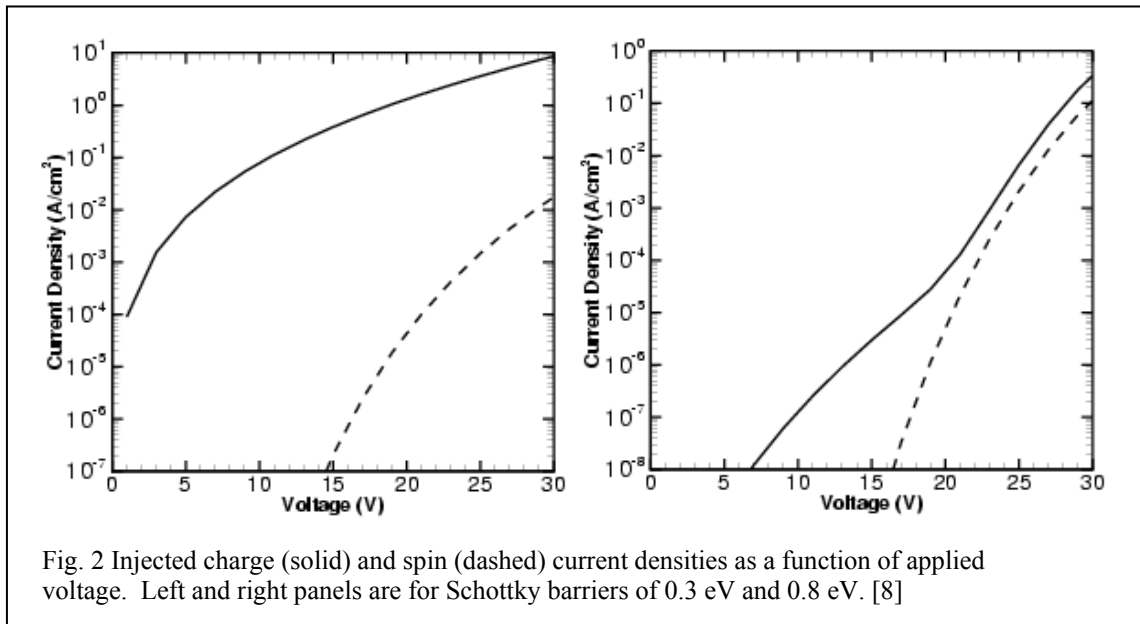


Fig. 2 Injected charge (solid) and spin (dashed) current densities as a function of applied voltage. Left and right panels are for Schottky barriers of 0.3 eV and 0.8 eV. [8]

demonstrate the importance of driving the semiconductor (whose equilibrium state is non-magnetic) out of local equilibrium with the injecting magnetic contact [3-5]. Two routes to achieving this goal are: incorporation of an insulating tunnel barrier at the contact/semiconductor interface or engineering of existing Schottky energy barriers to provide spin dependent tunneling [6]. In π -conjugated organic semiconductors, the Schottky energy barrier is not pinned and a wide range of barrier energies can be realized for a given organic semiconductor by using contacts with different work functions. We have recently completed a theoretical analysis of spin injection from ferromagnetic contacts into conjugated organic semiconductors [7]. Figure 2 shows our calculated results for injected charge and spin current densities near the injecting contact as a function of bias voltage in a 100 nm structure for Schottky barrier heights of 0.3 eV (left panel) and 0.8 eV (right right). The larger Schottky barrier leads to a smaller current density for a given applied voltage, but the spin polarization of the current density, for a given charge current density, is greater for the structure with the large Schottky barrier than for the one with the small Schottky barrier. The greater spin polarization at high voltages is due to spin selective tunneling through the Schottky barrier region. At high voltages spin polarization of the injected current approaches the spin polarization of the tunneling current. Efficient spin injection can also be achieved by incorporating spin selective tunnel barriers at the injecting interface. Spin selective tunnel barriers can be introduced at a magnetic contact/organic semiconductor interface using, for example, self-assembly techniques. SAMs can be used both to shift the effective injection energy barrier (by incorporating molecules with dipole moments) and to control the interface resistance of the contact (by incorporating insulating molecules of different lengths or partially conjugated molecules). We will use SAMs to provide the tunnel barriers necessary to achieve efficient spin injection.

References

- (1) F.X. Bronold, A. Saxena, and D.L. Smith, *Solid State Physics* **58**, 73 (2004).
- (2) B.K. Crone, S.A. Crooker, R.L. Martin, and D.L. Smith, to be published
- (3) D.L. Smith and R. N. Silver, *Phys. Rev. B* **64**, 045323 (2001).
- (4) J. D. Albrecht, and D. L. Smith, *Phys. Rev. B* **66**, 113303 (2002).
- (5) E. I. Rashba, *Phys. Rev. B* **62**, 16267 (2000).
- (6) J.D. Albrecht and D.L. Smith, *Phys. Rev. B* **68**, 035340 (2003).
- (7) P.P. Ruden and D.L. Smith, *J. Appl. Phys.* **95**, 4898 (2004).

DOE Sponsored Publications in 2005

Spin dependent luminescence in organometallic compounds, to be published

Transport Fundamentals in Crystalline Organic Semiconductor Devices

Arthur P. Ramirez^{1,2}, Colin P. Nuckolls¹, David Lang¹, Woo-Young So¹, Theo Siegrist²,
Christian Kloc²

Columbia University¹
Bell Laboratories, Lucent Technologies²

The recent progress in organic light emitting diodes suggests that this class of devices may be important for solid state lighting due to the potential for low cost and ease of fabrication. However, the process of light emission in organic molecular solids is much more complex than in inorganic semiconductors and -- to make matters worse -- our understanding of organic semiconductors is still very primitive compared to the present state-of-the-art in silicon and III-V semiconductors. We still do not understand even the most basic semiconductor properties of organics, such as doping, contacts, and the origins and properties of defect-related gap states. The physical origin of light emission is also quite different in the organics, being dominated by the luminescence of molecular excited states, not by the recombination of mobile electrons and holes as in inorganic semiconductors. We are studying the fundamental properties of organic semiconductors by using purified single crystals of pentacene, tetracene, and rubrene. In almost all cases the transport and optical properties are dominated by extrinsic factors, such as impurities and native defects, even though the material has been extensively purified. We have also observed a novel defect in pentacene that can be reversibly generated by voltage-bias-stress and has been correlated with the disruption of the π -electron system resulting from the bonding of an additional hydrogen on the pentacene molecule. This defect can be removed by photo-excitation above the HOMO-LUMO bandgap. The spectrum of this photoquenching process gives us some additional insight into the localized defect states of pentacene crystals and shows that even good quality crystals have a broad bandtail similar to inorganic amorphous material. These results imply that the efficiency of organic light-emitting devices can be improved by understanding and controlling the reaction paths for free electron-hole pairs to light-emitting molecular states versus competing non-radiative recombination processes at defects and impurities.

Behavior of Charges, Excitons and Plasmons at Organic/Inorganic Interfaces

Michael D. McGehee, Nicholas Melosh, Mark Brongersma
Department of Materials Science, Stanford University
mmcgehee@stanford.edu, nmelosh@stanford.edu, brongersma@stanford.edu

Program Scope

As electronic device dimensions shrink to nanometer scales and the range of desirable applications grows, two trends are emerging. First, the range of materials under serious development is growing, and many device structures consist of both organic and inorganic building blocks. Second, many physical phenomena that were heretofore only observed within academic experiments are becoming important for technologically relevant devices. Consequently, there are a large number of technical issues that need to be solved before these new possibilities become technologically viable. These include reproducible device performance on this lengthscale, sample heterogeneity, interface state control, defect properties, thermal transport and surface roughness. In addition, physical phenomena such as electron tunneling, Förster coupling, and plasmon-excitation quenching begin to severely impact device behavior at length scales less than 10 nm. This is particularly true within the emerging subset of structures that utilize both organic and inorganic materials, such as solar cells, electronic paper, molecular electronics, and organic light emitting displays. Within this rather broad collection of challenges, our team has identified the need to understand excited state behavior within organic species close to inorganic surfaces as a key problem for future applications of these materials.

Excited state phenomena within organic materials are often complicated by the multiple lengthscales, morphology, multiple competing decay processes, and inorganic surface interactions that affect the overall behavior of the system. Current studies of realistic devices are complicated by simultaneous excitation decay via a number of different processes within different regions of the sample. These decay processes, in which the charge or energy of an excited state in a molecule is transferred to an adjacent metal electrode, depend strongly upon the molecule to metal spacing.

In order to address these issues systematically, our team examines exciton transfer and decay within organic systems on a hierarchy of lengthscales. Melosh studies exciton transport and molecular wavefunction coupling to metal electrodes on the molecular level (~1 nm). McGehee examines exciton and charge transport within conducting polymer films close to metallic electrodes or dielectric films (5-100 nm). Brongersma investigates how excitons couple to surface plasmon waves on metal surfaces within the 10-500 nm range. Collectively, these measurements provide a better overall understanding of the behavior and importance of charges, excitons and plasmons within electrically active organic-inorganics than would be possible from a single study alone.

Recent Progress

Low operating voltages, a wide range of emission wavelengths, and solution processing make polymer light-emitting diodes attractive for high-growth markets including flexible displays, large-area displays, and solid-state lighting. However, the external efficiencies of these devices must be improved in order to compete with existing technologies. Currently, the majority of the light generated inside polymer LEDs remains trapped within the device by total internal reflection. By using an appropriate extraction technique, this trapped light can be a source for significantly increasing the external efficiency.

We have increased the power efficiency of polymer LEDs by using Bragg gratings to extract light from waveguide modes in the polymer/ITO layers. The gratings were fabricated by holographic and soft lithography techniques. In order to optimize the outcoupling efficiency of the grating, we have empirically varied the thickness, grating depth, grating location, and optical properties of the semiconducting layers and electrodes. We have modeled the structures to determine the waveguide modes and absorption loss. We have also increased efficiencies by using microlenses to extract light from waveguide modes located in the substrate. The microlenses have the potential to be fabricated using low-cost soft lithography and ink-jet printing techniques. By using numerical modeling, we have been able to gather information on how dipole emission is modified by the LED structure. We will use this model and our experimental results to compare and contrast the extraction methods we have studied.

We have characterized the structure and measured the charge carrier mobility of films of regioregular poly (3-hexylthiophene) P3HT as a function of molecular weight, casting solvent, annealing temperature and surface treatment. We have seen that when low molecular weight polymers and low boiling point solvents are used crystals form rapidly in the bulk of the film. Consequently the crystals do not align with each other and the conjugated parts of the polymer chains do not stack up against each other at the grain boundaries. The charge carrier mobility can be as low as 10^{-6} cm²/Vs. On the other hand, when higher molecular weight polymer and higher boiling point solvents are used, crystallization tends to occur only at the surface of the gate dielectric. Consequently, the crystals all tend to have the same orientation and charge carriers can easily hop from one crystal to another. The mobility in this case can be as high as 10^{-1} cm²/Vs. These studies highlight how critical it is to optimize the structure of organic semiconductor films when assessing new molecules for applications.

Almost all organic photovoltaic cells are based on either planar or bulk heterojunctions of two semiconductors. After light is absorbed, excitons must get to the interface between the two semiconductors to dissociate by electron transfer. In some cases, such as in dye-sensitized cells or polymer-fullerene bulk heterojunctions with very high fullerene concentrations, excitons are formed right at the interface and exciton transport is therefore not a limiting factor on the performance of the cells. In many other cases, such as in polymer-nanowire or polymer-titania cells, excitons need to travel at least five nanometers, if not more. For this reason exciton diffusion is a very important process to

understand and optimize. Exciton diffusion must also be avoided in light-emitting diodes so that excitons do not reach quenching sites. We have carefully measured the exciton diffusion length in several polymers and found that the values are less than reported in the literature. Common sources of error in diffusion length measurements are neglecting interdiffusion between the donor and acceptor, interference effects and resonance energy transfer. Since the diffusion length in most polymers is 6 nm or less, we have explored ways to enhance exciton transport. One is to use resonance energy transfer from a donor to an acceptor with a slightly smaller energy gap. We will show an example where the effective diffusion length and consequently the efficiency of the photovoltaic cell is enhanced by a factor of three. We will also show that resonance energy transfer occurs in many previously studied donor-acceptor blends, including polymer-fullerene blends with low fullerene concentrations. Finally we will discuss how high the effective diffusion length could be if the donor-acceptor pair were optimized for resonance energy transfer.

Publications Related to this Project

1. "Synthesis, characterization, and field-effect transistor performance of carboxylate-functionalized polythiophenes with increased air stability," A.R. Murphy, J.S. Liu, C. Luscombe, D. Kavulak, J.M.J. Fréchet, R.J. Kline, M.D. McGehee, *Chemistry of Materials*, 17 (2005) p. 4892-9.
2. "Using Resonance Energy Transfer to Improve Exciton Harvesting in Organic-Inorganic Hybrid Photovoltaic Cells," Y. Liu, M.A. Summers, C. Edder, J.M.J. Fréchet, M.D. McGehee, *Advanced Materials*, 17, (2005) 2960-4.
3. "Enhanced Hole Mobility in Regioregular Polythiophene Infiltrated in Straight Nanopores," K.M. Coakley, B.S. Srinivasan, J. M. Ziebarth, C. Goh, Y. Liu, M.D. McGehee, *Advanced Functional Materials*, 15 (2005) p. 1927-32.
4. "The Dependence of Regioregular Poly(3-hexylthiophene) Film Morphology and Field Effect Mobility on Molecular Weight", R.J. Kline, M.D. McGehee, E.N. Kadnikova, J. Liu, J.M.J. Fréchet, M.F. Toney, *Macromolecules*, 38 (2005) 3312-9.
5. "A Theoretical and Experimental Investigation of Light Extraction from Polymer Light-emitting Diodes", J. M. Ziebarth and M. D. McGehee, *Journal of Applied Physics*, 97 (2005) 064502.
6. "Extracting Light from Polymer Light-Emitting Diodes with Stamped Bragg Gratings", J.M. Ziebarth, A.K. Saafir, M.D. McGehee, S. Fan, *Advanced Functional Materials*, 14 (2004) 451-6.
7. "Controlling the Field-Effect Mobility of Regioregular Polythiophene by Changing the Molecular Weight" R.J. Kline, M.D. McGehee, E.N. Kadnikova, J. Liu, J.M.J. Fréchet, *Advanced Materials* 15 (2003) 1519-22.

Design, synthesis, and structuring of functional polymers and dendrimers with potential in solid state lighting technologies

Jean M.J. Fréchet, Rachel Segalman,
Lan Deng, Frank Lauterwasser, Daniel Poulsen, Justin Virgili
Division of Material Sciences, Lawrence Berkeley National Laboratory,
Berkeley, CA. 94720 J.Frechet@lbl.gov

Program Scope

Our fundamental research effort in the area of materials with relevance to solid state lighting is part of our larger program in plastic electronics initiated in 2005. This abstract will therefore focus exclusively on our current targets in the area of new materials for organic light emitting diodes.

Our program is focused on the exploration of fundamental structure-property relationships in electroactive polymer systems in which the control of functionality, architecture and morphology translates into functional properties within the framework of the conversion of electricity into light. In the early phases of this OLED sub-program the following targets have been identified:

- The development of organic bipolar materials with optimized electronic and self-assembly properties.
- The control of morphology within layers and at interfaces in organic optoelectronic devices
- The discovery and development of novel electron transporters (n-type) since most organic materials available to date are far better hole transporters than electron transporters.
- The physical and chemical tuning of novel electroactive materials for solution processing or direct patterning methods.

Recent Progress

(a) Controlling nanoscale morphology in electroactive polymers for better electron and hole conduction. (Poster presentation by Rachel Segalman)

Most luminescent organics have very low electron mobilities, so multiple component structures must be employed which allow for separate materials to transport electrons and holes in efficient light emitting devices. The current state of the art commercial OLEDs consist of several layers of material deposited by vacuum evaporation. From a technological point of view, multilayer structures are very difficult to solution process and since low-cost processing is a major goal in solid state displays, this is a major concern. From a more fundamental point of view, recombination tends to occur at the

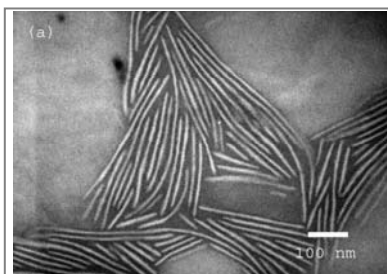


Figure 1: TEM of a 100nm thick film of symmetric rod-coil block copolymer on SiN. Lamellae are oriented both parallel (solid) and perpendicular (striped) to the substrate.

interfaces between layers and we understand little about the fundamental effects of interfacial geometry on device function. In fact, the planar layer geometry inherent in vacuum evaporation minimizes interfacial area. We are developing strategies to harness the unique self-assembly properties of polymers to control interfacial geometry and optimize recombination in polymer light emitting devices.

Several groups have suggested single-layer alternatives with varying degrees of success. Block copolymers are expected to self-assemble into regularly sized, regularly shaped, nearly pure nanodomains. If the nanoscale morphology may be controlled, these materials have the potential to allow us to *design* pathways for electron and hole conduction and recombination. Control over this

nanometer length scale in functional block copolymers presents a new challenge due to non-idealities in molecular conformation and mixing interactions that are present in these materials (as compared to

classical insulating block copolymers), and as a result no phase diagram or predictive model of self-assembly was previously available. We have designed the first conjugated block copolymer system which is capable of equilibrium phase transitions between nanostructures at experimentally accessible temperatures¹⁴. We see nanoscale lamellar structures at low temperatures at almost all volume fractions, a transition to a nematic phase stabilized by the attractive interactions between the rods, and finally a high temperature isotropic phase.

While studies of conjugated polymers in the bulk state are of fundamental interest, the structure near the electrodes of an OLED is of crucial interest to devices since the confining surfaces (electrodes) of a block copolymer film will play an integral role in controlling the long-range order nanodomains. We have recently demonstrated that rod-coil block copolymers in the thin film state take on a highly unusual mixed orientation¹⁶. In Figure 1, black and white striped regions are lamellae oriented upwards from the substrate (though their exact orientation is unknown). Regions which appear a solid shade of gray in this view are lamellae oriented parallel to the substrate. The individual lamellae formed from these rod-coil diblock copolymers are very long and align with a high degree of orientational order and very little bend. This mixed orientation is not observed in classical unconjugated block copolymer thin films where parallel orientations are stabilized by preferential surface interactions. The thin film structure in the conjugated polymer systems is directly influenced by the unusual chain conformation and a number of competing, unexplored interactions may be occurring. However, we anticipate that this mixed orientation may be ideal for device active layers, as it will allow for both optimal transport of charge as well as providing interfaces for recombination in the direction perpendicular to the electric field. The success we have had with this model system is a springboard for a systematic study of the fundamental properties that control rod-coil block copolymers.

We have synthesized a variety of new bipolar system (*vide infra*) which contains both electron and hole transporting blocks and have demonstrated that the self-assembly rules of our model systems are applicable to these novel structures.

(b) Developing novel systems based on bipolar copolymers

The most efficient OLED devices to date are based on evaporated multilayer structures in which an emitting layer of phosphorescent metal complexes (Baldo, Thompson, and Forrest, Nature 2000, 403, 750) is sandwiched between hole and electron transporting layers based on small molecules. As mentioned above, the use of polymers or copolymers capable of performing all of these functions, preferably in a single layer, would enable solution processing or even the direct patterning methods that would be best suited for solid-state lighting applications.

We have now initiated a program involving the design, synthesis, and fundamental study of novel bipolar copolymers that combine in a single chain the functions of hole and electron transport. In order to access a variety of morphologies and nanodomain shapes and dimensions, and thus maximize our abilities to understand structure property relationships as well as focus on the best performing structures, our approaches are not limited to structures involving conjugated polymers or a single type of architecture.

In the past year we have designed a library of non-conjugated bipolar polymers including random and block copolymers with structure of type A (Figure 2), as well as a rod-coil block copolymer with structure B. In order to accurately control polydispersity, the relative amounts of hole and electron transporting moieties or, where appropriate, block dimensions, alkoxyamine initiated living radical polymerization was used for all copolymers of type A using a diversity of hole and electron transporting vinyl monomers. Copolymer B was prepared by a coupling process using the functionalized initiating end of a polyvinylloxadiazole and a suitable modified PPV type hole conductor.

The non-conjugated bipolar copolymers of type A could be solution cast or spin-coated after doping with appropriate amounts of the light emitting Pt or Ir complexes. Our library approach allowed us to test the importance of variables such as the ratio of hole to electron transporting moieties, and to

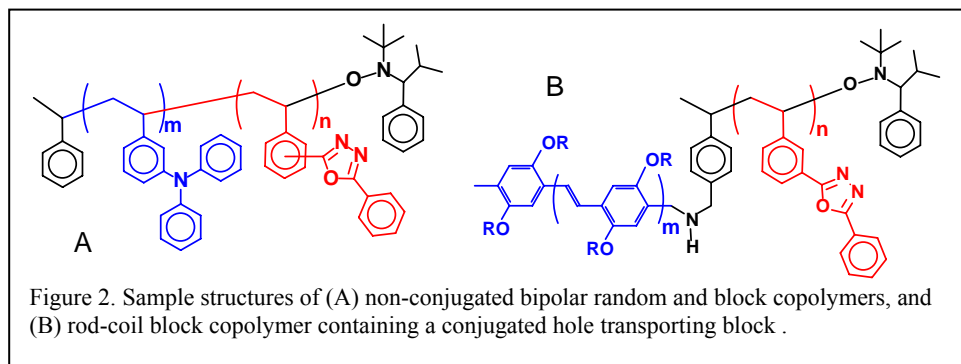


Figure 2. Sample structures of (A) non-conjugated bipolar random and block copolymers, and (B) rod-coil block copolymer containing a conjugated hole transporting block .

compare the performance of random vs. block copolymers in experimental OLED devices. Extremely encouraging results with front-face efficiencies of over 10% were obtained with these phosphorescent polymer-based devices. Early

data suggest that best results in terms of turn-on voltage and brightness are obtained with the block copolymers as shown in Figure 3. It must be emphasized that these results were obtained with spin-

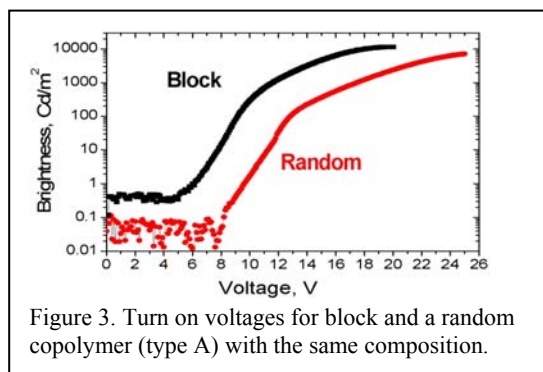


Figure 3. Turn on voltages for block and a random copolymer (type A) with the same composition.

coated polymer layers have not undergone any type of processing in order to optimize morphology.

Future Plans

Based on the results obtained in the first year of this study, we plan to further expand out study of bipolar copolymers by exploring promising new electroactive monomers and optimizing the balance of electron and hole transporting moieties. Our search for better electron transporters includes the development and preliminary evaluation of a series of novel vinyl monomers with pendant heterocyclic moieties. We are also exploring

several very promising copolymer structures containing fullerenes¹⁰ as fullerenes are well known

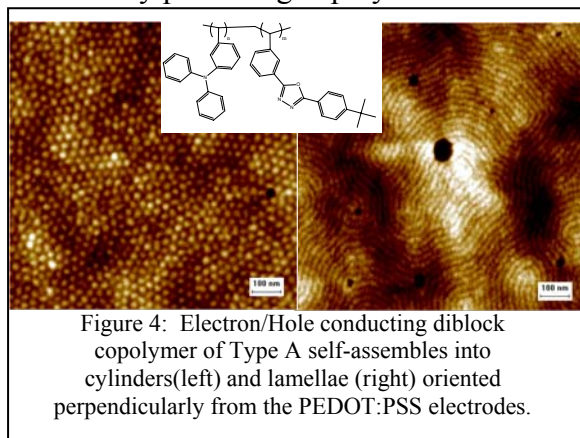


Figure 4: Electron/Hole conducting diblock copolymer of Type A self-assembles into cylinders(left) and lamellae (right) oriented perpendicularly from the PEDOT:PSS electrodes.

electron transporters. An additional area of interest is the fundamental investigation of highly novel terpolymers containing all three functions (hole transport, phosphorescent emitter, and electron transport) in both random and block architectures. To facilitate changes in composition and the establishment of structure-property relationships, these terpolymers (or precursors thereof containing as a middle block the ligands for the emitter complex rather than the complex itself) are prepared using living radical polymerization. Another important area of activity concerns the elucidation of mechanisms to obtain and control long

range order from the non-conjugated bipolar block copolymers of type A. Early results shown in Figure 4, show that the block copolymer self-assembles into cylinders or lamellae (depending on the relative lengths of the blocks) with their axes perpendicular to the electrode surfaces. We postulate that these cylinders and lamellae will act as conduits for charge transport to ensure high efficiency transport of holes and electrons. We are in the process of further tuning the orientation and morphology of these nanoscale patterns to optimize OLED performance. Our library approach to copolymers should prove invaluable as overall composition, block length, molecular weight, etc. are important variables we can control. Finally, we plan to begin the exploration of approaches towards

the direct patterning of our electroactive polymers as such an approach would be invaluable for lighting applications.

Publications in 2005 (DOE Supported program in Pastics Electronics)

1. Deng, L.; Furuta, P.T.; Garon, S.; Li, J.; Kavulak, D.; Thompson, M.E.; Fréchet, J.M.J. Living Radical Polymerization of Bipolar Transport Materials for Highly Efficient Light Emitting Diodes. *Chem Mater.* 2005, ASAP edition.
2. Ratera, I.; Chen, J.; Murphy, A.; Ogletree, D. F.; Fréchet, J.M.J.; Salmeron, M. Atomic force microscopy nanotribology study of oligothiophene self-assembled films. *Nanotechnology*, 2005, 16(5), S235-S239.
3. Murphy, A. R.; Liu, J.; Luscombe, C.; Kavulak, D.; Fréchet, J. M. J.; Kline, R. J.; McGehee, M. D. Synthesis, Characterization, and Field-Effect Transistor Performance of Carboxylate-Functionalized Polythiophenes with Increased Air Stability. *Chem.Mater.* (2005), 17(20), 4892-4899.
4. Goh, Chiatzun; Kline, R. Joseph; McGehee, Michael D.; Kadnikova, Ekaterina N.; Fréchet, Jean M. J.. Molecular-weight-dependent mobilities in regioregular poly(3-hexyl-thiophene) diodes. *Appl. Phys. Lett.* (2005), 86(12), 122110/1-122110/3.
5. Kline, R. J.; McGehee, M. D.; Kadnikova, E. N.; Liu, J.; Fréchet, J. M. J.; Toney, M. F. Dependence of Regioregular Poly(3-hexylthiophene) Film Morphology and Field-Effect Mobility on Molecular Weight. *Macromolecules*, 2005, 38, 3312-3319.
6. Chen, J.; Ratera, I.; Ogletree, D.F.; Salmeron, M., Murphy, A.R.; Fréchet, J.M.J. AFM Study of β -substituted T7 Oligothiophene Films on Mica: Mechanical Properties and Humidity Dependent Phases. *Langmuir*, 2005, 21, 1080-1085.
7. DeLongchamp, D.M.; Sambasivan, S.; Fischer, D. A.; Lin, E. K.; Chang, P.; Murphy, A. R.; Fréchet, J M. J.; Subramanian, V. Direct correlation of organic semiconductor film structure to field-effect mobility. *Adv. Mat.* 2005, 17(19), 2340-2344.
8. Murphy, AR; Chang, P. C.; VanDyke, P.; Liu, J.; Fréchet, J.M.J.; Subramanian, V.; DeLongchamp, D.M.; Sambasivan, S.; Fische, D.A.; Lin E.K. Self-Assembly, Molecular Ordering, and Charge Mobility in Solution-Processed Ultrathin Oligothiophene Films. *Chem Mater.* 2005, 17, 6033-41.
9. Sivula, K.; Ball, Z.T.; Watanabe, N.; Fréchet, J.M.J. Amphiphilic Diblock Copolymer Compatibilizers and Their Effect on the Morphology and Performance of Polythiophene:Fullerene Solar Cells. *Adv. Mat.* 2005, in press (see DOI: 10.1002/adma.200501787 on the web)
10. Ball, Z. T.; Sivula, K.; Frechet, J. M. J.. Well-Defined Fullerene-Containing Homopolymers and Diblock Copolymers with High Fullerene Content and Their Use for Solution-Phase and Bulk Organization. *Macromolecules* 2006, 39, 70-72
11. Subramanian, V.; Fréchet, J. M. J.; Chang, P. C.; de la Fuente Vornbrock, A.; Huang, D. C.; Lee, J. B.; Mattis, B. A.; Molesa, S.; Murphy, A. R.; Redinger, D. R.; Volkman, S. K. Printed organic transistors for low-cost RFID applications. *Proceedings of SPIE-The International Society for Optical Engineering* 2005, 5940, (594013/1-594013/9) 170-178.
12. Subramanian, V.; Fréchet, J.M. J.; Chang, P. C.; Huang, D. C.; Lee, J. B.; Molesa, S. E.; Murphy, A. R.; Redinger, D. R.; Volkman, S.K. Progress toward development of all-printed RFID tags: Materials, processes, and devices. *Proceedings of the IEEE* (2005), 93(7), 1330-1338.
13. Fréchet, J.M.J. Functional Polymers: from Plastic Electronics to Polymer-assisted Therapeutics. *Progr. Polym. Sci.* 2005, 30, 844-857.
14. Olsen, B. D. and Segalman, R. A. Structure and Thermodynamics of Weakly Segregated Rod-Coil Block Copolymers. *Macromolecules* 38, 10127 - 10137 (2005).
- (15) Olsen, B. D., Luning, J. M. and Segalman, R. A. Higher Order Liquid Crystalline Structure in Low Polydispersity DEH-PPV. *Macromolecules* submitted (2005).
- (16). Olsen, B. D. and Segalman, R. A. Thin Film Structure of Conjugated Rod-Coil Block Copolymers. *Macromolecules* in preparation (2005).

The DOE Nanoscience Centers and Solid State Lighting

Paul Alivisatos

University of California, Berkeley and Lawrence Berkeley National Laboratory

The ability to pattern and control matter on the nanoscale can play an important role in the creation of new solid state lighting technologies. Quantum confinement effects, control of the density of electronic, vibrational, and photonic degrees of freedom, and the processing techniques that are used in fabrication will all be impacted by advances in nanoscience.

The new DOE NSRCs are poised to broadly assist the science and technology community to tackle a wide range of important issues, such as those related to solid state lighting. This talk will describe advances which have already occurred at these laboratories and will also provide information for how members of the research community can access the centers to enhance their own research in the area of solid state lighting.

How to Dope Wide-Gap Materials: Basic Design Rules

Alex Zunger, Institute Research Fellow

National Renewable Energy Laboratory, Golden, Co 80401, <http://www.sst.nrel.gov>

Abstract

When one dopes externally an insulator or a semiconductor, at some critical position of the Fermi level, "Pinning Level", doping is spontaneously halted. We now understand that this occurs by the self-regulating, spontaneous formation of "killer defects." In effect, the system protects itself from the perturbing effect of doping by rearranging its bonds to minimize the perturbation, i.e., a manifestation of the Le Chatellier effect. For example, when a solid is doped intentionally n-type so the Fermi level moves toward the conduction band, at some point, cation vacancies form spontaneously. Being acceptors, they "kill" the intentionally-introduced doped electrons. Different materials differ by the position of the critical Fermi level at which this happens. In easy-to-dope materials (Si, GaAs, InAs), this level is located inside the host bands, so doping stops only after the system is already well-doped. On the other hand, in wide gap materials needed for solid state lighting, this critical level might be inside the band gap, so doping stops before the Fermi level reaches its target position near band edges.

In this talk, I will explain the ensuing physics of such self-limiting behavior, and formulate empirical rules as to how one might overcome some of these limits. I will then turn to another design problem -- "impurity design." Assuming, for the sake of discussion, that you could position impurities (such as Nitrogen in III-V's) at any relative geometry in the lattice (isolated impurities, clusters consisting of pairs or of triplets; random impurities, etc), which configuration will yield target physical properties, i.e., deepest levels or shallowest levels; or largest oscillator strength or minimum strain, etc? I will describe how this Inverse Band Structure approach can be performed to the benefit of III-V nitride alloys for Solid State Lighting.

TI 303-384-6672

Fax 303-384-6432

Optical Properties of Semiconductors from Crystals to Nanocrystals

James R. Chelikowsky, jrc@ices.utexas.edu, Center for Computational Materials, Institute for Computational Engineering and Sciences, Departments of Physics and Chemical Engineering, University of Texas, Austin, TX 78712

Program Scope

One of the primary means for learning about the electronic structure and chemical bonding of electronic materials is *optical spectroscopy*. For example, measuring and comparing the reflectivity spectrum to theoretical predictions let to the first accurate energy bands of semiconductors such as silicon. Initial theoretical work was performed with *empirical* potentials, which were adjusted to yield the correct response functions.¹ In particular, the normal incident reflectivity of a solid is given by

$$R = \left| \frac{1 - N}{1 + N} \right|^2 \quad (1)$$

where N is the complex index of refraction, which is related to the complex dielectric function via $N^2 = \epsilon_1 + i\epsilon_2$. One can use the Ehrenreich-Cohen² form for the imaginary part of the dielectric function to relate optical spectra to energy bands in crystals:

$$\epsilon_2(\omega) = \frac{4\pi^2 e^2 \hbar}{3m^2 \omega^2} \sum_{cv} \frac{2}{(2\pi)^3} \int_{BZ} \left| M_{cv}(\vec{k}) \right|^2 \delta(\omega_{cv}(\vec{k}) - \omega) d^3k \quad (2)$$

where e is the charge on the electron, m is the mass of the electron, \hbar is Planck's constant divided by 2π , \vec{k} is the wave vector, the sum is over all the valence (v) to conduction (c) band transitions, the integration is over the Brillouin zone (BZ), the n th band energies, $E_n(\vec{k})$. The transition frequencies are given by

$\omega_{cv}(\vec{k}) = \left(E_c(\vec{k}) - E_v(\vec{k}) \right) / \hbar$. The matrix elements are given by

$$\left| M_{cv}(\vec{k}) \right|^2 = \left| \left\langle u_c(\vec{k}) \left| \nabla \right| u_v(\vec{k}) \right\rangle \right|^2 \quad (3)$$

where u_n is the periodic part of the Bloch function for the n th band. Eq. (2) has a simple physical interpretation. Optical transitions must *conserve energy* and the radiation field can couple only two states with the *correct symmetry*, i.e., the states must permit dipole coupling. The delta function in Eq. 2 assures energy conservation and the matrix elements account for symmetry. If the wave functions and energy bands are known, then Eq. (2) can be evaluated. Once the imaginary part of ϵ is known, then the real part of ϵ can be obtained from a Kramers-Kronig transformation, N is then determined as is the reflectivity.¹ If good agreement is obtained between the calculated optical properties and the measured reflectivity, one can have confidence in the energy bands.

While this approach is correct in spirit, its application to materials in general is oversimplified and complex, especially to systems of interest at the nanoscale where the

optical properties of materials can be quite different than those of the bulk owing to the role of quantum confinement. For example, many materials of interest are not crystalline and lack symmetry. It is often not easy to fit a few potential parameters. As such, empirical potentials are problematic, particularly if there may be hundreds, if not thousands, of atoms involved. In such situations, solving for the energy levels and corresponding wave functions is difficult and computationally intensive. Moreover, the Ehrenreich-Cohen dielectric function is very approximate and does not yield an accurate description of excitons and local fields.

Recent Progress

We have made significant progress in two areas: (1) We have developed new algorithms to examine the electronic structure of materials at the nanoscale. (2) We have implemented existing formalisms to predict optical properties. These include: time dependent density functional theory³ and the GW-Bethe-Salpeter approach.⁴

The electronic structure of materials can be accurately described using the following approximations: the Born-Oppenheimer approximation, the pseudopotential approximation and the local density approximation.⁵ The Born-Oppenheimer approximation allows one to separate the nuclear and electronic degrees of freedom. The pseudopotential approximation allows one to separate the chemically active electron states (valence states) from the chemically inert core state. The local density approximation with density functional theory allows one to map the many electron problem on a one-electron problem. The electronic states of interest can be obtained from the *Kohn-Sham* equation^{5,6}:

$$\left[\frac{-\hbar^2 \nabla^2}{2m} + V_{ion}^p + V_H + V_{xc} \right] \Psi_n = E_n \Psi_n \quad (4)$$

where V_{ion}^p is the ionic pseudopotential, V_H is the Hartree potential and V_{xc} is the exchange-correlation potential. The Hartree potential is solved by computing the electrostatic potential arising from the charge density of the valence electrons, the exchange-correlation potential also depends solely on the charge density. This equation is solved self-consistently so that the calculated density is consistent with the screening potentials. The eigenvalues E_n and eigenfunctions Ψ_n give the energetic and spatial distributions of the electrons. We solve this problem in *real space* using an iterative diagonalization procedure. Our method is ideally suited for localized systems such as large clusters, quantum dots and nanowires.

Time dependent density functional theory provides a unified formalism for computing both the ground state and excited state properties. There are several modes of implementation for this theory. One of the simplest is to integrate the time dependence of the wave functions after the system has been excited by a electromagnetic pulse.⁷ Using the resulting information on the induced dipole, one can extract the absorption spectrum of the system of interest. This method works best for localized systems such as molecules and clusters. The only additional approximation besides the local density

approximation is an adiabatic approximation, *i.e.*, the system responds instantaneously to the electromagnetic field. Our current implementation of this method is capable of describing systems with several hundred atoms.

The GW-Bethe-Salpeter approach⁴ is believed to be one of the most accurate “*ab initio*” methods for predicting the optical spectra of materials. It is capable of handling both localized and extended systems. The method is composed of two steps: the GW part is used to find the excitation energy of a *non-interacting* electron-hole pair. The Bethe-Salpeter equation is used to find the exciton energy or the electron-hole interaction energy. Currently, we have the capability of examining systems with about a hundred atoms with this technique.

Future Plans

Our immediate goal is to extend our real space methods to consider much larger systems, *i.e.*, nanocrystalline matter with several thousands of atoms, and examine the role of dopants and the evolution of shallow dopants. This is an important issue as the properties of electronic materials depend crucially on our ability to alter their electronic characteristics by the controlled introduction of impurities or dopants.

Our longer-range goal is to study the optical properties of materials in other nanoscale configurations such as nano-wires. We have preliminary calculations on the role of doping in these systems where the role of quantum confinement is highly anisotropic.

References

- (1) M.L. Cohen, and J.R. Chelikowsky: *Electronic Structure and Optical Properties of Semiconductors*, (Springer-Verlag, 1989), 2nd edition.
- (2) H. Ehrenreich and M. H. Cohen: *Phys. Rev.* **115**, 782 (1959).
- (3) M.E. Casida: *Recent Developments and Applications of Modern Density Functional Theory*, Editor: J.M. Seminario, Elsevier, Amsterdam, 1996, p. 391.
- (4) M. Rohlfing and S.G. Louie: *Phys. Rev. B* **62**, 4927 (2000).
- (5) J.R. Chelikowsky: *J. Phys. D* **33**, R33 (2000).
- (6) W. Kohn and L. Sham, *Phys. Rev.* **140**, A1133 (1965).
- (7) K. Yabana and G. F. Bertsch, *Int. J. Quant. Chem.* **75**, 55 (1999).

DOE Sponsored Publications in 2003-2005

- (1) W. R. Burdick, Y. Saad, L. Kronik, M. Jain, I. Vasiliev and J.R. Chelikowsky: “Parallel Implementation of Time-Dependent Density Functional Theory,” *Comp. Phys. Comm.* **156**, 22 (2003).
- (2) D.V. Melnikov and J.R. Chelikowsky: “Ab Initio Absorption Spectra of Germanium Nanocrystals,” *Solid State Comm.* **127**, 361 (2003).
- (3) C. Troparevsky, L. Kronik, and J.R. Chelikowsky: “Optical Excitations in CdSe Quantum Dots,” *J. Chem. Phys.* **119**, 2284 (2003)
- (4) S. Ogut, R. Burdick, Y. Saad, and J.R. Chelikowsky: “*Ab Initio* Calculations for the Large Dielectric Matrices of Confined Systems,” *Phys. Rev. Lett.* **90**, 127401 (2003).
- (5) L. Kronik, R. Fromherz, E. Ko, G. Ganteflor, and J.R. Chelikowsky: “Photoemission spectra of deuterated silicon clusters: experiment and theory,” *Euro. Phys. J. D* **24**, 33 (2003).

- (6) M.M.G. Alemany and James R. Chelikowsky: "Edge-sharing tetrahedra: Precursors of the E_g defects in amorphous silica," *Phys. Rev. B* **68**, 054206 (2003).
- (7) J.R. Chelikowsky, L. Kronik and I. Vasiliev: "Time dependent density functional calculations for the optical spectra of molecules, clusters and nanocrystals," *J. Phys. Cond. Matt.* **15**, R1517 (2003).
- (8) D.V. Melnikov and J.R. Chelikowsky: "Electron affinities and ionization energies of semiconductor nanocrystals," *Phys. Rev. B* **69**, 113305 (2004).
- (9) D.V. Melnikov and J.R. Chelikowsky: "Quantum confinement in phosphorus-doped silicon nanocrystals," *Phys. Rev. Lett.* **92**, 046802 (2004).
- (10) M.M.G. Alemany, M. Jain, J.R. Chelikowsky and L. Kronik: "A real space pseudopotential method for computing the electronic properties of periodic systems," *Phys. Rev. B* **69**, 075101 (2004).
- (11) F.-C. Chuang, C.Z. Wang, S. Ogut, J.R. Chelikowsky and K.M. Ho: "Melting of small Sn clusters by *ab initio* molecular dynamics simulations," *Phys. Rev. B* **69**, 165408 (2004).
- (12) S. Li, M.M.G. Alemany and J.R. Chelikowsky: "Ab initio calculations for the photoelectron spectra of vanadium clusters," *J. Chem. Phys.* **121**, 5893 (2004).
- (13) E. L. de la Grandmaison, S.B. Gowda, Y. Saad, M. Tiago, and J.R. Chelikowsky: "An Efficient Computation of the Coupling Matrix in Time Dependent Density Functional Theory," *Comp. Phys. Comm.* **167**, 7 (2005).
- (14) L. Kronik, M. Jain, and J.R. Chelikowsky: "Electronic structure and spin-polarization of MnGaP," *Applied Phys. Lett.* **85**, 2014 (2004).
- (15) G. Neshet, L. Kronik and J.R. Chelikowsky: "Ab initio absorption spectra of Ge nanocrystals," *Phys. Rev. B* **71**, 035344 (2005).
- (16) X. Huang, Eric Lindgren and J.R. Chelikowsky: "Surface passivation method for semiconductor nanostructures," *Phys. Rev. B* **71**, 165328 (2005).
- (17) S. Li, M.M.G. Alemany, and J.R. Chelikowsky: "Ab initio calculations of the photoelectron spectra of transition metal clusters," *Phys. Rev. B* **71**, 165433 (2005).
- (18) M.L. Tiago and J.R. Chelikowsky: "First-principles GW-BSE excitations in organic molecules," *Solid State Comm.* (in press).
- (19) X. Huang, A. Makmal, J. R. Chelikowsky, , and L. Kronik: "Size dependent spintronic properties of dilute magnetic semiconductor nanocrystals," *Phys. Rev. Lett.* **94**, 236801 (2005)
- (20) K.S. Nakayama, M.M.G. Alemany, H. Kwak, T. Sugano, K. Ohmori, J.R. Chelikowsky and J.H. Weaver: "Electronic Structure of Si(001)-c(4×2) Analyzed by Scanning Tunneling Spectroscopy and Ab Initio Simulations," *Phys. Rev. B* (in press).
- (21) C. Bekas, Y. Saad, M.L. Tiago and J.R. Chelikowsky: "Computing Charge Densities with Partially Reorthogonalized Lanczos," *Comp. Phys. Commun.* (in press).
- (22) M. Lopez del Puerto, M.L. Tiago, I. Vasiliev and J.R. Chelikowsky: "Real Space Pseudopotential Calculations of the Ground State and Excited State Properties of the Water Molecule," *Phys. Rev. A* **72**, 052504 (2005).

Synthesis of Nanoclusters for Energy Applications

Jess P. Wilcoxon, (Dept. 1126) Billie L. Abrams, (Dept. 1126), Steven G. Thoma (Dept. 6245), and Paula P. Provencio (Dept. 1111), Sandia National Laboratories, Albuquerque, N.M. 87185-1421, jpwilco@sandia.gov

The large surface area, unusual surface chemistry, and surface morphologies of nanoclusters imbue them with physical properties differing significantly from their bulk counterparts. Of direct significance to next generation lighting technologies we describe our BES supported work concerning the synthesis and optical properties of a new class of extremely small, $d < 2.0$ nm, type II-VI semiconductor quantum dots (QD). We demonstrate that the photoluminescence (PL) properties of these QDs can be controlled by their interfacial chemistry coupled with age-dependent surface reconstruction. We demonstrate a decoupling of the absorbing states determined by quantum confinement, (the band-edge), from the emission states which are determined primarily by the interfacial states. This decoupling allows PL emission from a single size QD to be tuned throughout the visible range by surface chemistry, while eliminating the problem of self-absorbance of the emitted light since the absorption onset remains fixed in the NUV. We demonstrate for the first time efficient, white light emission from a single material type, monodisperse nanosize phosphor. This discovery enables applications such as white LEDs based upon near-UV LEDs. The scientific principles governing the optical properties of these new phosphors should extend to other nanosize semiconductors like Si or Ge and thus these new nanomaterials have great potential as white phosphors for both solid-state and fluorescent illumination. Time permitting, results of doping of these type IV nanosize semiconductors with luminescent ions like Mn or Sb will be described.

Acknowledgement: This work was supported by the Division of Materials Sciences, Office of Basic Energy Research, US Department of Energy under contract DE-AC04-94AL8500. Sandia is a multiprogram laboratory operated by Sandia Corporation, a Lockheed-Martin Company, for the US Department of Energy.

Photonic Crystals and Negative Index Materials

C. M. Soukoulis

Department of Physics and Ames Laboratory, Iowa State University, Ames, Iowa, 50011

Photonic Band Gap (PBG) materials are artificial, periodic, dielectrics that enable engineering of the most fundamental properties of electromagnetic waves. These properties include the laws of refraction, diffraction, and spontaneous emission of light. Unlike traditional semiconductors that rely on the propagation of electrons through an atomic lattice, PBG materials execute their novel functions through selective trapping or “localization of light” using engineered defects within the dielectric lattice. This is of great practical importance for all-optical communications and information processing. Three dimensional (3D) PBG materials offer a unique opportunity for simultaneously (i) synthesizing micron-scale 3D optical circuits that do not suffer from diffractive losses and (ii) engineering the electromagnetic vacuum density of states in this 3D photonic crystal. This combined capability opens a new frontier in integrated optics as well as the basic science of radiation-matter interactions. We will review recent approaches to micro-fabrication of photonic crystals with a large 3D PBG centered near 1.5 microns. These include direct laser-writing techniques and holographic lithography.

The possibility of negative refraction has brought about a reconsideration of many fundamental optical and electromagnetic phenomena. This new degree of freedom has provided a tremendous stimulus for the physics, optics and engineering communities to investigate how these new ideas can be utilized. Many interesting and potentially important effects not possible in positive refracting materials, such as near-field refocusing and sub-diffraction limited imaging, have been predicted to occur when the refractive index changes sign. In this talk, I will review our own work on negative refraction in metamaterials, and describe the possible impact of them as new types of optical elements. In particular, we will present theoretical and experimental results on engineered microstructures designed to have both ϵ and μ negative. Results for different polarizations and propagation directions will be presented. Recent results on microstructures operating at 100-200 THz will be also discussed.

Programming Function in Photonic Crystals

Paul V. Braun
pbraun@uiuc.edu

Frederick Seitz Materials Research Laboratory & Department of Materials Science and Engineering, University of Illinois at Urbana-Champaign, Urbana, IL 61801

Program Scope

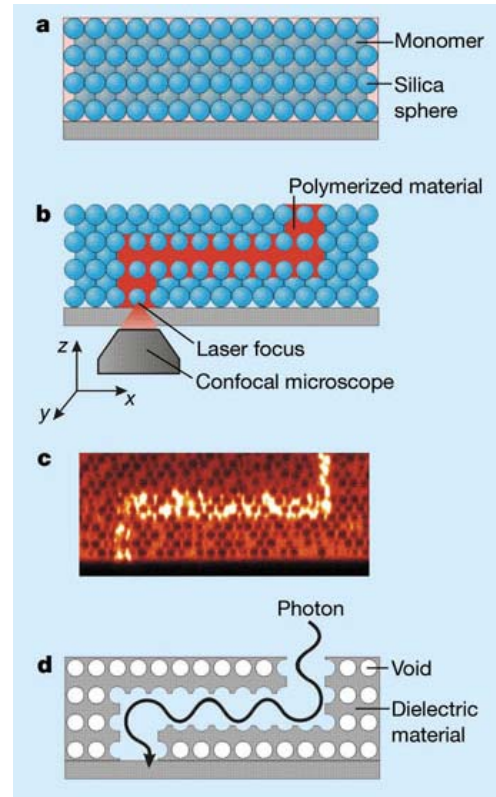
We are coupling our extensive understanding of self-assembly and three dimensional (3-D) fabrication chemistries with novel materials deposition routes to create 3-D photonic crystals. Though a coupled approach of template formation through colloidal self-assembly, holography, or direct writing and new materials chemistries, we have created 3-D structures from metallic, semiconducting, polymeric and ceramic materials which interact with light in defined, strong, and unique ways. As part of this, we are learning to program photonic materials with strong, nonlinear responsivities to light and other external stimuli. We are also learning how to form photonic band gap structures with embedded waveguides, which may find applications in the routing of light. Unique 3-D structures, formed through coupled template formation and materials growth strategies, which enhance the extraction or generation of light of specific frequencies are also being studied. Strong coupling between theory and experiment is assisting our understanding of the fundamental physical and optical properties of the photonic crystals and photonic band gap materials created in our group.

Important to our program are multiphoton and other direct write methodologies, which enable us to form otherwise inaccessible photonic structures. Multiphoton processes begin with the two-photon excitation of a dye molecule which then directly or indirectly initiates polymerization. Importantly, because multiphoton polymerization is non-linear with photon flux, it can be used for 3-D fabrication.[1] Essentially, the focal point of a laser is rastered through a polymerizable media, leaving behind a trace of the path of the focal point. This approach has enabled us to create complex structures within a self-assembled photonic crystal. In collaboration with Prof. Jennifer Lewis at UIUC, other ink based direct writing approaches are also utilized to create complex structures. The complex photonic structures we have created may find applications in solid state lighting, energy transduction, and other areas of importance to the Department of Energy.

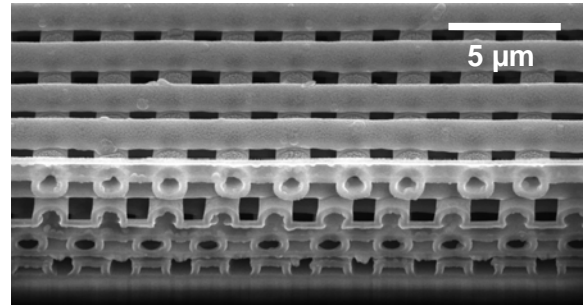
Recent Progress

Impressive developments in semiconductor micro-fabrication are enabling new applications in photonics, MEMS, and biotechnology. Yet conventional microfabrication techniques require expensive masks and time-consuming procedures, including multiple planarization or bonding steps, to generate 3-D structures. In contrast, direct-write approaches,[2] such as laser scanning[3,4] and ink deposition,[5,6] provide rapid flexible routes for fabricating 3D micro-periodic structures. However, conventionally these approaches are currently limited to polymeric structures that lack the high refractive index contrast and mechanical integrity required for many applications. To take full advantage of these rapid, flexible assembly techniques, one must develop a replication (or templating) scheme that enables their structural conversion within the temperature constraints imposed by both the organic and inorganic components of the system. We have now developed several novel routes for creating 3D structures of high refractive index semiconductors.

We have now demonstrated the creation of waveguide structures in 3-D self-assembled photonic crystals,[7] and very recently, their conversion into silicon structures. In this work, we demonstrated that waveguide structures and other optically active features could be created inside of a photonic crystal through multiphoton polymerization with a resolution of 100 nm, and subsequently converted into a high refractive index photonic band gap structure. This advance has enabled both new basic science and the creation of a wide range of optical devices inside of self-assembled materials. The graphic to the right outlines the general process as reported in a review of our early work in *Nature*. The structure of the waveguide/colloidal crystal is replicated into silicon through a combination of atomic layer deposition and chemical vapor deposition (CVD). The resulting inverse opal silicon structure exhibits a complete band gap, enabling the unique manipulation of light. These structures are not transparent in the visible, and so for solid state lighting applications, we are now working on forming high refractive index materials such as TiO_2 , that are transparent in the visible, into the necessary 3-D structures.



Along with colloidal templating, which can be rather limited in structural complexity because of the small number of crystal structures that can be formed by colloidal crystallization, in collaboration with Prof. Jennifer Lewis, we are now forming hollow-woodpile structures through a coupling of the direct-write assembly of concentrated polyelectrolyte inks[5,6] with a sequential low temperature silica/Si CVD process. The optical properties of the 3D micro-periodic woodpiles are characterized after each fabrication step and closely match theoretical spectra. These interconnected, hollow structures may find potential application as photonic materials, low-cost MEMS, microfluidic networks for heat dissipation, and biological devices. An example of a Si hollow woodpile structure we formed is shown to the right. Through a similar replication process, we are also creating optically active materials via a holographic route.



Very recently, we have shown that colloid crystal templated electrodeposition can be used to create 3D periodic metallic structures. These materials may have unique emissive properties due to the microperiodic structure, which, for example, may suppress the thermal emission of light over specific frequency ranges, effectively increasing the efficiency of a thermal photonic emitter created from such structures over the remaining frequency ranges where the emission is not suppressed. We have initial results demonstrating this effect from Ni and Au inverse opal metallic photonic crystals heated between 400 and 600 °C.

Future Plans

Three dimensional nano and microscale photonic structures have a number of interesting and unique optical properties. The majority of the interesting physics and most applications require a wide diversity of materials and structures which can not be formed through conventional top-down processing. A significant aspect of our future work will be to use techniques such as colloidal self-assembly, multibeam and phase mask holography, multiphoton polymerization, and direct ink writing, in concert with materials deposition routes such as electrodeposition, CVD, and ALD, which are effective in depositing high refractive index materials, to form 3D structures which may, for example, be useful for photoemissive, photovoltaic and other photonic applications. Through appropriate design it may be possible to form photonic crystal structures which serve to distribute light from, or concentration light into, small regions of space, which could lead to devices with enhanced photonic properties. In particular, concentration of light into high-Q cavities will be explored. The nonlinear optical properties of materials in high-Q cavities may result in new emissive and absorptive optical behaviors.

The electromagnetic energy distribution within photonic crystal structures is also interesting to explore. In these structures, the electric field intensity is very nonuniform, and highly wavelength dependent, which may open opportunities for new localized photonics. For example, if a photonic crystal is filled with quantum dots, the dots in the high field region will behave very differently than the dots in a low field region. With only very small changes in the incident radiation, the high and low field regions may switch, which will dramatically alter the emission of the quantum dots embedded in the structure.

Metallic photonic crystals have been of recent interest due in part to their emissive properties when heated to high temperature. We have now formed a few testbed structures, however have not fully explored the potential of these metallic photonic crystals. Over the next few years, we intend to carry out a coupled theory and experimental approach to the formation of emissive metallic photonic crystals with a focus on energy related applications.

References

- [1] J. H. Strickler, W. W. Webb, *Proc. SPIE* **1990**, 1398, 107.
- [2] J. A. Lewis, G. M. Gratson, *Mater. Today* **2004**, 7, 32.
- [3] B. H. Cumpston, S. P. Ananthavel, S. Barlow, D. L. Dyer, J. E. Ehrlich, L. L. Erskine, A. A. Heikal, S. M. Kuebler, I. Y. S. Lee, D. McCord-Maughon, J. Q. Qin, H. Rockel, M. Rumi, X. L. Wu, S. R. Marder, J. W. Perry, *Nature* **1999**, 398, 51.
- [4] M. Deubel, G. v. Freymann, M. Wegener, S. Pereira, K. Busch, C. Soukoulis, *Nature Mater.* **2004**, 3, 444.
- [5] G. M. Gratson, M. Xu, J. A. Lewis, *Nature* **2004**, 428, 386.
- [6] G. M. Gratson, J. A. Lewis, *Langmuir* **2005**, 21, 457.
- [7] W. Lee, S. A. Pruzinsky, P. V. Braun, *Adv. Mater.* **2002**, 14, 271.

DOE Sponsored Publications in 2003-2005

1. S. Jeon and P. V. Braun: Hydrothermal synthesis of Er-doped luminescent TiO₂ nanoparticles, *Chemistry of Materials* **15**, 1256-1263 (2003).
2. Y.-J. Lee and P. V. Braun: Tunable inverse opal hydrogel pH sensors, *Advanced Materials*, **15**, 563-566(2003).

3. H. Liang, T. E. Angelini, J. Ho, P. V. Braun and G. C. L. Wong: Molecular imprinting of biomaterialized CdS nanostructures: Crystallographic control using self-assembled DNA-membrane templates, *Journal of the American Chemical Society*, **125**, 11786-11787 (2003).
4. M. A. Meitl, T. M. Dellinger, and P. V. Braun: Bismuth-ceramic nanocomposites with unusual thermal stability via high-energy ball milling, *Advanced Functional Materials*, **13**, 795-799 (2003).
5. Y.-J. Lee, S. A. Pruzinsky and P. V. Braun: Glucose-sensitive inverse opal hydrogels: analysis of optical diffraction response, *Langmuir*, **20**, 3096-3106 (2004).
6. W. Lee, A. Chan, M. A. Bevan, J. A. Lewis and P. V. Braun: Nanoparticle-mediated epitaxial assembly of colloidal crystals on patterned substrates, *Langmuir*, **20**, 5262-5270 (2004).
7. T. M. Dellinger and P. V. Braun: Lyotropic liquid crystals as nanoreactors for nanoparticle synthesis, *Chem. Mater.*, **16**, 2201-2207 (2004).
8. R. G. Shimmin, A. B. Schoch and P. V. Braun: Polymer size and concentration effects on the size of gold nanoparticles capped by polymeric thiols, *Langmuir*, **20**, 5613-5620 (2004).
9. C. E. Heitzman, H. Tu, P. V. Braun: Two-dimensional diffusion of prodan on self-assembled monolayers studied by fluorescence recovery after photobleaching, *J. Phys. Chem. B.*, **108**, 13764-13770 (2004).
10. H. Tu, C. E. Heitzman, P. V. Braun: Patterned poly(N-isopropylacrylamide) brushes on silica surfaces by microcontact printing followed by surface-initiated polymerization, *Langmuir*, **20**, 8313-8320 (2004).
11. S. Jeon, J.-U. Park, R. Cirelli, S. Yang, C. E. Heitzman, P. V. Braun, P. J. A. Kenis, J. A. Rogers: Fabricating complex three-dimensional nanostructures with high-resolution conformable phase masks, *Proceedings of the National Academy of Sciences*, **101**, 12428-12433 (2004).
12. H. Liang, T. E. Angelini, P. V. Braun, and G. C. L. Wong: Roles of Anionic and Cationic Template Components in Biomaterialization of CdS Nanorods Using Self-Assembled DNA – Membrane Complexes, *J. Am. Chem. Soc.*, **126**, 14157-14165 (2004).
13. Z. Ge, D. G. Cahill, and P. V. Braun: AuPd Metal Nanoparticles as Probes of Nanoscale Thermal Transport in Aqueous Solution, *J. Phys. Chem. B*, **108**, 18870-18875 (2004).
14. Y.-J. Lee, S. A. Pruzinsky, and P. V. Braun: Diffraction Response of Colloidal Crystals: Effect of Numerical Aperture, *Optics Letters*, **30**, 153-155 (2005).
15. Z. Ge, Y. Kang, T. A. Taton, P. V. Braun, and D. G. Cahill: Thermal transport in Au-core polymer-shell nanoparticles, *Nano Letters*, **5**, 531-535 (2005).
16. F. Garcia-Santamaria, J. F. Galisteo-Lopez, P. V. Braun, and C. Lopez: Optical diffraction and high-energy features in three-dimensional photonic crystals, *Phys. Rev. B*, **71** (19), 195112 (2005).
17. A. Wolosiuk, O. Armagan, P. V. Braun: Double Direct Templating of Periodically Nanostructured ZnS Hollow Microspheres, *J. Am. Chem. Soc.*, **127**, 16356-16357 (2005).
18. S. A. Pruzinsky and P. V. Braun: Fabrication and Characterization of Two-Photon Polymerized Features in Colloidal Crystals, *Advanced Functional Materials*, **15**, 1995-2004 (2005).
19. G. M. Gratson, F. García-Santamaría, V. Lousse, M. Xu, S. Fan, J. A. Lewis, and P. V. Braun: Direct-Write Assembly of 3D Photonic Crystals: Conversion of Polymer Scaffolds to Silicon Hollow-Woodpile Structures, *Advanced Materials*, in press (2006).

Biased Self-Assemblies in Block Copolymers and Nanorods

T.P.Russell

Polymer Science and Engineering Department
University of Massachusetts
Amherst, MA 01003

Lighting based on field emission devices requires lateral positioning of anisotropic objects on patterned media. Top-down approaches use classic photolithographic processes to achieve the desired result. Bottom-up approaches, based on self-assembly processes, offer the possibilities of reducing the number of processing steps, obtaining unprecedented areal densities with nanoscopic conductors or semi-conductors, and utilizing flexible substrates. In one approach, the self-assembly of diblock copolymers, two chemically dissimilar polymers joined together at one end, will be described where, by using external fields, like electric fields or solvent fields, ordered arrays of cylindrical microdomains with diameters of 10-20 nm and aspect ratios of 100 or more, can be achieved. By selectively removing the minor component and backfilling with a conductor or semi-conductor or by phase-selective chemistries, high-density arrays of nanoscopic wires can be obtained that have field emission characteristics comparable to carbon nanotubes. In a second approach, the self-corralling self-assembly of CdSe nanorods, with aspect ratios of 20 or more, will be described where, by using an interfacial or line tension, ordered, hexagonally-packed arrays of nanorods can be produced in a straightforward manner. In both processes, selectively placing these arrays of nanowires or nanorods over a voltage source allows the fabrication of field emission devices that have promise for lighting applications.

Poster Sessions

Optical, Electrical and Magnetic Studies of Ordered π -Conjugated Systems

Z. Valy Vardeny

val@physics.utah.edu

Department of Physics, University of Utah, Salt Lake City, Utah 84112

Program Scope

Using a variety of optical, electrical and magnetic methods we study the primary photoexcitations and their dynamics in a variety of π -conjugated systems, in time ranging from 100 fs to minutes, and spectral range from 30 meV to 3.3 eV. The main method that we have used is transient and steady state photomodulation (PM) technique. In the fs time domain we follow the primary photoexcitations from their generation, to trapping and recombination. The main problem that we address is the branching ratio between excitons and polarons in pristine and C₆₀-doped polymer films. In the microsecond to millisecond time domain we follow the geminate polaron pairs as they recombine or dissociate into free polarons. In the seconds to minutes time domain we follow the photogeneration of metastable states in polymer films.

Spin injection into organic semiconductors can be achieved either by spin polarized injection from FM electrodes, or optically via spin dependent recombination with preference for spin parallel configuration. The former process is studied by the spin valve effect, whereas the later process is studied by the technique of optically detected magnetic resonance (ODMR). The various spin effects critically depend on the film morphology that can be changed by the solvent used, as well as by heat post treatment.

Recent Progress

(i) Polaron/exciton branching ratio in the ps time domain

Photogeneration of charge polaron excitations in organic semiconductor polymer films with various nanoscale morphologies is of interest because the traditional one-dimensional (1D) electronic properties of the π -conjugated polymer chains can be modified by the increased interchain coupling. In particular the quantum efficiency, η of ultrafast (primary) photogenerated polarons in pristine and fullerene-doped polymers is important for achieving more efficient organic solar cells that are the focus of intense interest nowadays; since the early process determines the charge separation efficiency in these devices. Yet there is no reliable method to determine the branching ratio, η between photogenerated polarons and excitons. Certainly η cannot be determined from cw spectroscopy, since polarons decay with a variety of time constants that are difficult to determine using phase sensitive techniques, and thus cw η -value estimates are too small. Measuring primary polaron photoexcitations in the sub-picosecond time domain is then the most accurate method to determine η ; alas, this is easy said than done. For example, in pristine films of poly(phenylene-vinylene) [PPV] derivatives four different methods of measuring η in the ps time domain were used thus far that yielded large variation $0.1\% < \eta < 10\%$ even in films casted from the same polymer. The reason for this is that each method focuses either on measuring polarons, or excitons, but not both; there is no method of *simultaneously* measuring these two kinds of photoexcitations. Picosecond

transient photoconductivity is sensitive only to charge carriers via mobility and η ; photoinduced infrared vibrations (IRAV) related to charges on the polymer chains is sensitive only to separated polaron pairs; photoinduced THz radiation is confined to a narrow spectral range; and in transient photomodulation (PM) in the visible range there are too many overlapping photoinduced absorption (PA) bands that does not allow an accurate determination of η . Similar to pristine polymers, the narrow spectral range of the photoinduced IRAV method used to study the photoinduced charge transfer (CT) dynamics in polymer/fullerene blends has not allow to simultaneously investigate the exciton dynamics; thus the existence of ‘an ultrafast photoinduced CT process’ in these films must be taken with a grain of salt.

In our recent work, we used the transient PM spectroscopy with 100 fs time resolution in an unprecedented broad spectral range from 0.15 to 2.7 eV, which, for the first time also included the polaron absorption band in the mid ir spectral range (~ 0.35 eV), to more accurately determine η , *since both excitons and polarons PA bands are well separated and simultaneously detected*. For obtaining η we used an intrinsic detection scheme, namely the ratio of the polaron/exciton PA bands in the mid ir range at low excitation intensities of less than 10^{16} cm⁻³. We used this method to obtain η in a variety of pristine and C₆₀-doped films of PPV derivatives having different morphologies on the nanometer scale. In MEH-PPV we found that η dramatically depends on the solvent used; $\eta \sim 10\%$ when the film is prepared from toluene solutions, but $\eta < 1\%$ if chloroform is used. Also η is much smaller in DOO-PPV compared to MEH-PPV and unsubstituted PPV, clearing up a controversy that exists in the field. Surprisingly, the primary polaron pairs in the pristine films set an upper limit for the photoinduced CT efficiency in C₆₀-doped MEH-PPV films; because mainly these species are separated onto the C₆₀ molecules. Rather than undergoing an ultrafast CT reaction with neutral C₆₀ molecules in the film, we found that the photogenerated excitons simply recombine at the polaron⁺/C₆₀⁻ complexes that are formed in the ps time domain from the primary polaron pairs.

(ii) CW studies

(a) CW measurements show that the emission quantum efficiency of distyryl-benzene [DSB] crystals is quite high (of the order of 70%) and therefore they may be excellent candidates for organic laser action. The PL emission band of these crystals contains several phonon side-bands with high and low phonon frequency series, which, however do not show up in the respective Raman spectrum. We have succeeded in analyzing the DSB PL emission spectrum with a model, dubbed ‘apparent mode’ model that takes into account the contribution of *all* phonon modes in the crystal weighted by their Huang Reiss factor. The weighting factors were directly taken from the experiment using the spectrum of resonant Raman scattering in DSB crystals.

(b) Using the PA and PADMR measurement techniques in which we have excelled during the previous funding periods, we discovered that the formation cross-section of singlet excitons is larger than that of triplet excitons in π -conjugated conjugated systems, and this is especially true in polymers rather than in short oligomers. During the present funding period we have extended our studies to also include Pt-containing polymers that were previously studied in Cambridge, using OLED with both PL and phosphorescence

(iii) Organic spintronics

We were the first group to report spin injection into organic semiconductors, and we would continue our efforts in this direction. (a) Firstly, we will explore the possibility to fabricate spin-valves that work at 300K. This is very important since otherwise application of organic spin-valves would be minimal. For this we plan to use an empirical technique, since a-priori we do not know what material would have the smallest spin lattice relaxation rate at 300K, which is needed for spin transport inside the organic layer. (b) We will also investigate the phenomenon of magnetic field effect (MFE) over the current and EL in non-magnetic OLED's. This phenomenon has been around for more than 4 years but no one has come up with a good explanation for it. We found that LSMO-based OLED's do not show this phenomenon, and this may be crucial in understanding the MFE.

DOE Sponsored Publications in 2004-2005

- (1) "Photoexcitation Dynamics and Laser Action in PPE-PPV Copolymers", M. Tong, C. X. Sheng, C. Yang, Z. V. Vardeny and Y. Pang, *Phys. Rev. B.* **69**, 155211 (2004).
- (2) "Confined and Delocalized Polarons in π -Conjugated Oligomers and Polymers; a Study of the Effective Conjugation Length", M. Wohlgenannt, X. M. Jiang, and Z. V. Vardeny, *Phys. Rev. B (Rapid Commun.)* **69**, 241204 (2004).
- (3) "Giant Magnetoresistance in Organic Spin-Valves", Z. H. Xiong, D. Wu, Z. V. Vardeny, and J. Shi, *Nature* **427**, 823 (2004).
- (4) "Studies of Single Molecule Resistance Using Self-Assembled-Monolayers", V. Burtman, A. S. Ndobé, and Z. V. Vardeny, *Jour. of Applied Phys.* **98**, 034314 (2005); Con-Mat/0502432(2005).
- (5) "Infrared Ultrafast Optical Probes of Photoexcitations in π -Conjugated Organic Semiconductors", C. X. Sheng and Z. V. Vardeny, Proceedings 27th International Conference on Semiconductor Physics, Flagstaff, Arizona July 2004, *AIP 0-7354-0257*, page 1081 (2005).
- (6) "Optical Studies of Spin Coherence in Organic semiconductors", C. Yang, C. Liu, and Z. V. Vardeny, Proceedings 27th International Conference on Semiconductor Physics, Flagstaff, Arizona July 2004, *AIP 0-7354-0257*, Page 1407 (2005).
- (7) "Spin-Dependent Exciton Formation Rates in π -Conjugated Semiconductors", C. Yang, Z. V. Vardeny, A Kohler, M. Wohlgenannt, M. K. Al-Suti and M. S. Khan, *Phys. Rev. B (Rapid Commun.)* **70**, 241202 (2004).
- (9) "Apparent Vibrational Side-Bands in π -Conjugated Systems; The Case of Distyrylbenzene", C. C. Wu, E. Ehrenfreund, J. J. Gutierrez, J. P. Ferraris, and Z. V. Vardeny, *Phys. Rev. B.* **71**, 081201 (2005).
- (10) "Efficiency Enhancement of an Organic Light Emitting Diode with a Cathode Forming 2D Metallic Photonic Crystal", C. Liu, V. Kamaev, and Z. V. Vardeny, *Appl. Phys. Lett.* **86**, 143501 (2005).
- (11) "Magnetic Field-Dependent Carrier Injection at $\text{La}_{2/3}\text{Sr}_{1/3}\text{MnO}_3$ /Organic Semiconductors Interfaces", D. Wu, Z. H. Xiong, X. G. Li, Z. V. Vardeny, and Jing Shi, *Phys. Rev. Lett.* **95**, 016802 (2005).

The Organic Chemistry of Conducting Polymers: From Molecular Wires to Photovoltaics

Laren M. Tolbert and Janusz Kowalik
School of Chemistry and Biochemistry, Georgia Institute of Technology
Atlanta, GA 30332-0400

laren.tolbert@chemistry.gatech.edu, janusz.kowalik@chemistry.gatech.edu

Program Scope.

The translation of molecular properties to materials and device properties represents a challenge to both molecular science (chemistry!) and materials science. The field of electroactive molecules and their extrapolation to conducting polymers and electronic devices presents a particularly daunting set of obstacles, not the least of which is that the properties of the material or device are often determined not by the molecular properties of the bulk, but rather by the properties of the interface, where impurities and oxidation can corrupt the interpretation of these results. The notion of "molecular wires" has been extant for a number of years, but only recently have the technology, the theoretical basis, and the synthetic tools evolved to the point that such applications, or at least an assessment of their possibilities, have entered the realm of the feasible. The approach used in this program views conducting polymers as a problem in mechanistic organic chemistry, examining the convergence to bulk properties of molecular properties. This approach has involved the synthesis of oligomers of defined length in which the charge carrier is an intrinsic part of the chain, for which the length scale can be controlled by the dimensions of nanoelectrodes or nanoparticles. In a separate but related effort, application of conducting polymers in dye-sensitized photovoltaic devices has emerged.

Recent Progress

We have proposed that the most efficient molecular "wires" are based upon the known structure of solitons in polyacetylene.¹ Since the highest occupied molecular orbital in ferrocene is a metal-centered orbital, an examination of the redox potentials in binuclear ferrocene complexes linked by linear unsaturated bridges has emerged as a compelling motif for studying properties of molecular "wires." For instance, Spangler reported on the intervalence electron transfer of bisferrocenylpolyenes,² while we have reported on a bisferrocene containing a solitonic (polymethine) charge transfer chain.³ However, the nature of the bridge in facilitating such communication is not a straightforward function of the oxidation potential of the bridge, but rather exhibits a more complex dependence on distance, oxidation potential, and orbital overlap. Since a number of chalcogens, heterocycles, and other moieties are proposed to intimately connect nanostructured materials electronically, an understanding of the nature of such communication is essential. Our approach is to place the redox mediator X

between two ferrocenylvinyl groups such that the steric effects are comparable in all cases (see Figure 1). We have uncovered some surprisingly effective linkers, as well as others which suppress communication in a counterintuitive fashion. Cyclic voltammetry of the sulfur-linked bisferrocene, for instance, exhibits two waves corresponding to oxidation of the first and second ferrocenes, indicating communication of oxidation state information from one metal to the other. At the same time, one electron oxidation of the molecule yields the spectrum of an intervalence charge-transfer complex, while double oxidation is consistent with formation of a bridge-centered radical cation. The competition between ferrocene and bridge oxidation offers the possibility of introducing “switches” which facilitate, or inhibit, communication between the two ferrocene moieties. The combination of electrochemistry and spectroscopy allows us to identify the nature of the charge carrier in each case. Attempts to measure the rate of charge transfer between oxidized and unoxidized ends are ongoing.

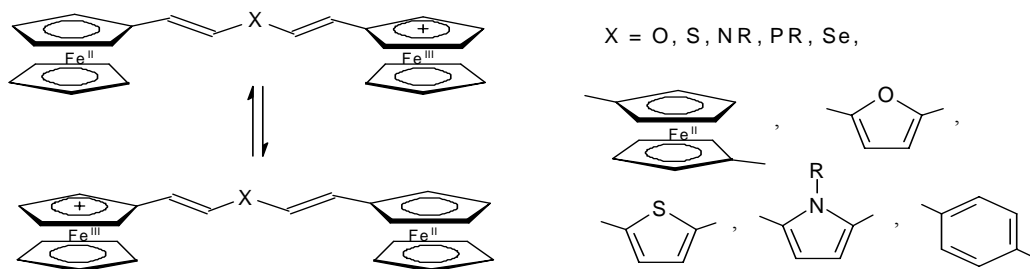


Figure 1. Examples of ferrocenes connected by various "wires".

We published some of the early work on the use of conducting polymers, particularly polythiophenes, to replace the liquid junction in the Grätzel dye-sensitized solar cell (DSSC).⁴ We have also discovered that the polymer itself can act as the light-harvesting dye. Such cells promise low cost fabrication without the leakage problems inherent in the DSSC. Success in this area, however, requires strategies for the development of high polymers with high carrier mobility. To date, high mobilities ($>1\text{-}10\text{ cm}^2/\text{V}\cdot\text{s}$) have only been achieved in single crystal materials.

Future Plans

We believe that a critical component of the construction of devices based upon organic materials will depend critically on the interface between organic and semiconductor or conductor surfaces. Such an interface can have two effects. First, it can facilitate charge transport between the dissimilar materials by avoiding charge traps. Second, the interface itself, if properly designed, may influence the long-range order in the polymer and thus affect the charge mobility. We have generated an organic field-effect transistor (OFET) platform that will allow rapid scanning of various surface treatments to ascertain their role on the

emissions. We found that the singlet excitons in these polymers have larger formation cross-section compared to triplet excitons, in perfect agreement with previous results.

(c) We have also studied the dependence of the lower polaron absorption band, namely P_1 in several polymers and oligomers as a function of their conjugation length (CL). We found that P_1 scales inversely with the CL. This is therefore a unique spectroscopy that may have important applications in the field of disordered organic semiconductors because it can yield the CL using a non-invasive method. We also found that planar polymers such as RR-P3HT, mLPPP and PFO deviate from the trend found and actually show even a lower P_1 . This was taken as an indication that these polymers have a quasi-2D structure, where the polarons may be delocalized in 2D.

(iii) Organic Spintronics

We routinely fabricate organic spin-valves based on FM electrodes such as the half-metal LSMO, or on more conventional FM electrodes such as Co and Fe. We also fabricate organic spin-valves based on SAM's of conducting molecules. With the fabricated organic spin-valves based on LSMO/Alq₃/Co we measured a giant magneto-resistance of 40% at 10K. This shows that FM electrodes can inject spin-polarized carriers into organic semiconductors, and this has tremendous promise for spintronics applications. This work has been published recently in the journal *Nature*.

In addition to the spin-valve related magneto-resistance (MR) we also found in LSMO-related OLED's a high field MR. This MR response is due to the change in the Fermi energy of the FM LSMO electrode with the applied magnetic field, which consequently changes its carrier-injection ability. This work was recently published in *Phys. Rev. Lett.*

Future Plans

(i) Ultrafast Spectroscopy

We will continue to make progress with the transient spectroscopy in the ir spectral range. (a) Firstly we plan to investigate primary photoexcitations in t-(CH)_x. It is true that this polymer is 'old hat' since it is non-luminescent. However interest in it has not diminished completely because of the peculiar excitations, namely 'solitons' that are unique for this degenerate-ground-state polymer. (b) In addition, we would also like to complete our investigation of pristine and C₆₀-doped MEH-PPV. This polymer was the center of controversy since the SB group claim electrons and holes as primary photoexcitations; whereas other groups insist that these are excitons. (c) In addition we also plan to complete the work on the commercially important polymer PFO. We will measure the spectrum of the two-photon-absorption and compare it with the transient PM and electro-absorption spectra.

(ii) CW investigations

We will continue to decipher the underlying mechanism of the ODMR. We will investigate the ODMR signal when nano-magnets are added to the polymer. Also we would investigate long time changes in polymers upon prolonged illumination. We found that prolonged illumination of MEH-PPV polymers give rise to a new phase in which polarons are generated more easily. We would study this metastable phase using the PM and PL techniques.

underlying organic polymer or single-crystal morphology.⁵

The basic strategy is to modify the metal or semiconductor surface using surface compatibilization groups. For instance (and unsurprisingly), attachment of sulfhydryl groups to the conducting polymer results in formation of robust bonds to gold surfaces. Similarly, use of phosphonate groups allows robust attachment of polymers to metal oxide surfaces, particularly titanium oxide. Alternatively, a self-assembled monolayer of a properly designed molecule can organize the phase of an overlying layer. For instance, we have discovered that a naphthalenethiol on gold will direct crystallization of aromatic molecules on the surface. We are particularly interested in the use of this strategy to organize materials, e.g., sexithiophenes, which are known to have high charge mobilities, in particular morphologies for use in OFETs. Similarly, we will attempt to organize our bisferrocenes in SAMs on electrode surfaces to measure the relative communication efficiency of each of our “wires.”

References

- ¹ (a) Tolbert, L. M. *Accs. Chem. Res.*, **1992**, 25, 561. (b) Tolbert, L. M.; Zhao, X. *Modular Chemistry, NATO Adv. Symp. Series*, Kluwer Acad. Publishers, **1997**; 123-134.
- ² Ribou, Anne-Cecile; Launay, Jean-Pierre; Sachtleben, Michelle L.; Li, Hu; Spangler, Charles W.. *Inor. Chem.* **35**(13), 3735 (1996).
- ³ L. M. Tolbert, X. Zhao, Y. Ding, L. A. Bottomley, *J. Am. Chem. Soc.*, **117**, 12891 (1995).
- ⁴ Spiekermann, S.; Smestad, G.; Kowalik, J.; Tolbert, L. M.; Gratzel, M. *Synth. Met.*, **2001**; *121*, 1603-1604.
- ⁵ Luke Roberson, Ph.D. thesis, Georgia Institute of Technology, 2005.

DOE Sponsored Publications in 2003-2005

Pentacene disproportionation during sublimation for field-effect transistors. Roberson, Luke B.; Kowalik, Janusz; Tolbert, Laren M.; Kloc, Christian; Zeis, Roswitha; Chi, Xiaoliu; Fleming, Richard; Wilkins, Charles. *J. Am. Chem. Soc.* **2005**, *127*, 3069-3075.

Patterning via surface monolayer initiated polymerization: A study of surface initiator photoreaction kinetics. McCoy, Kendra; Hess, Dennis W.; Henderson, Clifford L.; Tolbert, Laren M.. *J. Vac. Sci Tech.. B*, **2004**, *22*, 3503-3508.

Correlation of morphology and device performance in inorganic-organic TiO₂-polythiophene hybrid solid-state solar cells. Roberson, Luke B.; Poggi, Mark A.; Kowalik, Janusz; Smestad, Greg P.; Bottomley, Lawrence A.; Tolbert, Laren M.. *Coord. Chem. Rev.* **2004**, *248*, 1491-1499.

Patterning via surface monolayer initiated polymerization: A study of surface initiator photoreaction kinetics. McCoy, Kendra; Hess, Dennis W.; Henderson, Clifford L.; Tolbert, Laren M. *J. Vac. Sci Tech.. B*, **2004**, *22*, 3503-3508.

Highly aromatic polymer brushes: Toward “molecular masks.” Chen, X., Ruehe, Juergen; Tolbert, L. M.; Hess, D. W.; Henderson, C. *Polym. Preprints (Amer. Chem. Soc., Div. Polym. Chem.)*, **2003**, 44, 454.

Polymerization Of 3-Undecylbithiophene And Preparation Of Poly(3-Undecylbithiophene)/Polystyrene Composites In Supercritical Carbon Dioxide. Abbett, K. F.; Teja, A. S.; Kowalik, J.; Tolbert, L. M., *Macromolecules*, **2003**, 36, 3015-3019

Iodine Doping Of Poly (3-Undecylbithiophene) And Its Composites With Polystyrene Using Supercritical Carbon Dioxide. Abbett, K. F.; Teja, A. S.; Kowalik, J.; Tolbert, L. M., *J. Appl. Polym. Sci.*, **2003**, 90, 3876-3881.

Preparation Of Conducting Composites Of Polypyrrole Using Supercritical Carbon Dioxide. Abbett, K. F.; Teja, A. S.; Kowalik, J.; Tolbert, L. M., *J. Appl. Polym. Sci.*, **2003**, 90, 1113-1116

Optical and electrochemical characterization of poly(3-undecyl-2,2'-bithiophene) in thin film solid state TiO₂ photovoltaic solar cells. Grant, Christian D.; Schwartzberg, Adam M.; Smestad, Greg P.; Kowalik, Janusz; Tolbert, Laren M.; Zhang, Jin Z. *Synth. Metals* **2003**, 132, 197-204..

A technique to compare polythiophene solid-state dye sensitized TiO₂ solar cells to liquid junction devices. Smestad, G. P.; Spiekermann, S.; Kowalik, J.; Grant, C. D.; Schwartzberg, A. M.; Zhang, J.; Tolbert, L. M.; Moons, E. *Sol. En. Mat. Sol. Cells* **2003**, 76, 85-105.

Combinatorial Fabrication and Screening of Organic Light-Emitting Device Arrays

Joseph Shinar

*Ames Laboratory – USDOE and Department of Physics and Astronomy
Iowa State University, Ames, Iowa 50011*

shinar@ameslab.gov

Program Scope

The combinatorial approach for discovery and optimization of new materials has emerged as a powerful tool in diverse fields such as catalysis, optoelectronics, and luminescence.¹ The multiplicity of parameters that affect device performance renders combinatorial approaches an important tool for device development as well. Indeed, in recent years, such approaches have proven useful in fabricating, optimizing, and studying organic light-emitting devices (OLEDs) as well.²⁻¹⁰ Our program has included screening of 2-dimensional (2-d) UV/violet arrays, and 1-dimensional (1-d) arrays of blue-to-red OLEDs, intense white OLEDs, and arrays fabricated to study Förster energy transfer in guest-host OLEDs. It demonstrates that combinatorial fabrication of OLEDs has become a powerful tool for screening various OLED materials and configurations, and for studying their basic optoelectronic properties.

Recent progress

1. 2-d UV/violet OLED arrays. UV/violet OLEDs are highly desirable as, e.g., excitation sources for other red-to-blue fluorescent films and luminescent sensors. To this end, we fabricated and screened 2-d arrays of UV/violet ITO/[copper phthalocyanine (CuPc)]/[4,4'-bis(9-carbazolyl)biphenyl (CBP)]/[2-(4-biphenyl)-5-(4-*tert*-butylphenyl)-1,3,4-oxadiazole (Bu-PBD)]/CsF/Al OLEDs, as described by Zou et al.⁵ The emission, which peaks at ~380 nm, is due to CB. The OLEDs were fabricated combinatorially using a sliding shutter technique similar to that described by Schmitz et al.,^{2,3} to screen them for the optimal thicknesses of the CuPc hole injecting layer and the electron transport or hole blocking layer. The emission from these CBP-based OLEDs peaked at 380 - 390 nm and originated from the bulk of the CBP layer.

Similar 2-d combinatorial arrays of CBP OLEDs, but with the Bu-PBD replaced by the hole-blocking material 2,9-dimethyl-4,7-diphenyl 1,10-phenanthroline (BCP), are currently being studied by Zhou et al.¹¹ It is found that at any given bias higher than the turn-on voltage, the current through the CBP/BCP device is much higher than that through the CBP/Bu-PBD device. It is therefore suspected that the efficiency of CBP OLEDs with a BCP electron-transport layer (ETL) would be significantly higher than that of CBP devices with a Bu-PBD ETL.

2. 1-d Blue-to-red OLED arrays. Color modification in thermal vacuum evaporated small molecular OLEDs has attracted strong attention due to the applications of such OLEDs for full-color flat panel displays¹² and general lighting applications.¹³ One well-known method to modify the color is the guest-host (G-H) or molecular doping approach, where both the doping concentration^{12,14-16} and applied bias^{16,17} affect the emission spectrum. The guest emission spectra are shifted by the doping concentration,¹⁴⁻¹⁶ and the relative intensity of guest and host emission vary with applied bias.^{16,17} Yet control of the doping concentration is problematic due

to instabilities in the fabrication procedure. In contrast, color tuning via changes in the thickness of the doped layer may provide a facile fabrication process for vacuum evaporated devices. Our work demonstrated this approach by describing such 1-d combinatorial blue-to-red G-H OLEDs;⁷ The emission shifted from blue to red as the thickness of the doped layer increased from 0 to 35 Å.

The OLEDs' structure was ITO/[5 nm CuPc]/[38 nm N,N'-diphenyl-N,N'-bis(1-naphthylphenyl)-1,1'-biphenyl-4,4'-diamine (NPD)]/[t_d nm 5 ± 0.6 wt.% 2-methyl-6-[2-(2,3,6,7-tetrahydro-1H,5H-benzo[i,j]quinolizin-9-yl) ethenyl]-4H-pyran-4-ylidene] propane-dinitrile (DCM2)-doped NPD]/[4,4'-bis(2,2'-diphenyl-vinyl)-1,1'-biphenyl (DPVBi)]/[10 nm tris(8-hydroxy quinolinato) Al (Alq₃)]/[1 nm CsF]/[150 nm Al], where $t_d = 1, 2, 3, 4, 6, 10, 20,$ and 35 Å. For color tuning, DCM2 and NPD were co-deposited after the neat NPD layer; the ratio of their depositions rates corresponded to $c_d = 5 \pm 0.6$ wt.% DCM2 in NPD.

The t_d -dependence of both the peak emission wavelength and the efficiency of the OLEDs was found to be very similar to their doping concentration (c_d)-dependence described previously.^{12,14-16} Figure 1 shows an array of pixels with different t_d on a $2'' \times 2''$ substrate, at an applied bias of 8 V. In the first two columns $t_d = 0$, in the third column $t_d = 1$ Å, and beyond that column, t_d increased nonlinearly to 35 Å in the last columns. *Importantly, all the pixels are comparably bright at 8 V.* Hence, this approach is very promising for the development of red-green-blue (RGB) OLED arrays for multicolor applications.

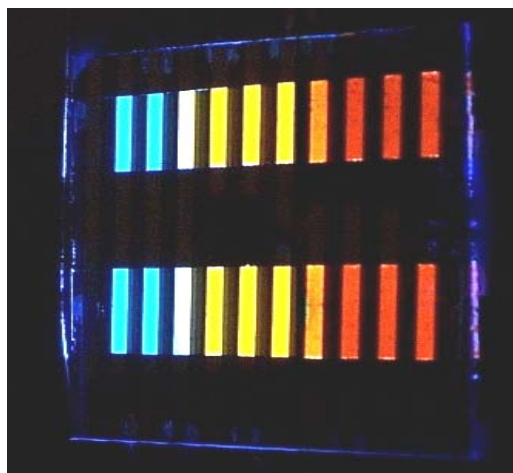


Fig. 1. Color evolution of OLEDs with varying DCM2-doped-layer thickness at $V_{app} = 8$ V.

3. 1-d Arrays of intense white OLEDs (WOLEDs). WOLEDs are drawing intense attention as general white solid-state light sources.^{13,16,18,19} For displays, the brightness $L \leq 300$ Cd/m² is sufficient, but lighting requires $L \sim 2000$ Cd/m². In addition, stability exceeding 10,000 hours and η_{power} superior to those of fluorescent tubes ($\eta_{power} \sim 50$ lm/W), both at $L \sim 2000$ Cd/m², must be achieved.

By lightly doping a host material with a dye, incomplete energy transfer from the host to the guest results in emission from both.^{18,19} In addition, since the emission spectra of organic molecules are usually broad, if the host is a blue emitter and the guest is a red or orange emitter, this single doped layer can yield white emission. This strategy previously yielded bright ($L = 42,000$ Cd/m²) and efficient ($\eta_{power} \sim 2.9$ lm/W) WOLEDs.¹⁹ Since the white emission is from one layer, the device shows relatively good color stability.^{18,19} Our recent study demonstrated very bright and efficient WOLEDs based on orange-emitting 2 - 10 nm-thick layers of 0.25 and 0.5 wt.% rubrene-doped DPVBi, with surprisingly stable color coordinates that barely changed from ~ 50 Cd/m² to 50,000 Cd/m².⁸ The maximal brightness achieved in pulsed operation was $> 74,000$ Cd/m².

4. 1-d Arrays fabricated to study Förster energy transfer in guest-host OLEDs.⁹ This study analyzed energy transfer in highly efficient doped DPVBi OLEDs. A region of the hole

transport layer (HTL) adjacent to the host DPVBi layer was doped with an efficient guest red dye. The host-to-guest energy transfer probability was determined by comparing the emission from the two fluorophores and its dependence on the applied field. It decreased with increasing field, probably due to an increasing fraction of positively charged dye molecules (i.e., molecules that trapped a hole). It was also estimated that at fields as low as 0.4 MV/cm, ~50% of the dye emission was due to trap emission rather than Förster energy transfer. The analysis yielded a Förster energy transfer radius $R_0 = 33.5 \pm 3.5 \text{ \AA}$.

Future Plans

The foregoing studies demonstrated the power of combinatorial screening for developing UV/violet, blue-to-red, and intense white small molecular OLEDs, and for studying the basic physical processes in such devices. However, they did not address the following issues:

1. Polymer OLEDs (PLEDs). The performance of PLEDs has consistently lagged that of small molecular devices, to the point where the efforts to develop them towards commercialization have been largely abandoned. This reduction in the efforts to develop them has occurred in spite of the clear cost and efficiency advantages of fabricating PLEDs by spin-coating or inkjet printing over the fabrication of small molecular OLEDs by thermal vacuum evaporation. Yet, it was recently shown that the quantum efficiency of poly(N-vinyl carbazole) (PVK)-based PLEDs, doped with an appropriate phosphorescent dye, rivals that of any small molecular OLED.²⁰ However, the stability of such PLEDs is all but unknown. Hence, the development of combinatorial libraries for screening the stability of high-efficiency PLEDs, especially at high brightness ($> 1000 \text{ Cd/m}^2$), could be extremely valuable for a definitive determination of their potential for solid state lighting applications.

2. The stability and the nature of the degradation processes in small molecular OLEDs at high brightness ($> 1000 \text{ Cd/m}^2$). While the degradation processes at low brightness ($< 300 \text{ Cd/m}^2$) have been studied extensively, relatively little attention has been focused on the processes that occur at high brightness. In general, it has been assumed that for all the degradation processes, the degradation level is approximately proportional to the total charge injected into the device. This assumption is the foundation for accelerated degradation measurements, which draw conclusions on the stability at low current based on the observed behavior at high current. It is obviously vitally important that this assumption be examined critically, and that the fundamental degradation processes at high current be elucidated.

References

1. T. X. Sun, *Biotech. Bioeng. (Combinatorial Chemistry)* **61**, 193 (1999).
2. C. Schmitz, M. Thelakkat, & H.-W. Schmidt, *Adv. Mat.* **11**, 821 (1999).
3. C. Schmitz, P. Pösch, M. Thelakkat, & H.-W. Schmidt, *Phys. Chem. Chem. Phys.* **1**, 1777 (1999).
4. M. Gross, D. C. Muller, H.-G. Nothofer, U. Scherf, D. Neher, C. Brauchle, & K. Meerholz, *Nature* **405**, 661 (2000).
5. L. Zou, V. Savvate'ev, J. Booher, C.-H. Kim, & J. Shinar, *Appl. Phys. Lett.* **79**, 2282 (2001).
6. X. Sun & G. E. Jabbour, *Mat. Res. Soc. Bull.* **27**, 309 (2002).
7. K. O. Cheon & J. Shinar, *Appl. Phys. Lett.* **83**, 2073 (2003).
8. G. Li & J. Shinar, *Appl. Phys. Lett.* **83**, 5359 (2003).

9. K. O. Cheon & J. Shinar, *Appl. Phys. Lett.* **84**, 1201 (2004).
10. M. Thelakkat, C. Schmitz, C. Neuber, & H-W Schmidt, *Macromol. Rapid. Comm.* **25**, 204-223 (2004).
11. Z. Zhou, R. Shinar, H. S. Wu, and J. Shinar, unpublished results.
12. V. Bulović, A. Shoustikov, M. A. Baldo, E. Bose, V.G. Kozlov, M. E. Thompson, & S. R. Forrest, *Chem. Phys. Lett.* **287**, 455 - 460 (1998).
13. A. R. Duggal, J. J. Shiang, C. M. Heller, & D. F. Foust, *Appl. Phys. Lett.* **80**, 3470 (2002).
14. M. A. Baldo, Z. G. Soos, & S. R. Forrest, *Chem. Phys. Lett.* **347**, 297 (2001).
15. G. Y. Zhong, J. He, S. T. Zhang, Z. Xu, Z. H. Xiong, H. Z. Shi, X. M. Ding, W. Huang, & X. Y. Hou, *Appl. Phys. Lett.* **80**, 4846 (2002).
16. K. O. Cheon & J. Shinar, *Appl. Phys. Lett.* **81**, 1738 (2002).
17. J. Kalinowski, P. Di Marco, V. Fattori, L. Giulietti, & M. Cocchi, *J. Appl. Phys.* **83**, 4242 (1998).
18. R. S. Deshpande, V. Bulovic, & S. R. Forrest, *Appl. Phys. Lett.* **75**, 888 (1999).
19. C. H. Chuen & Y. T. Tao, *Appl. Phys. Lett.* **81**, 4499 (2002).
20. S. A. Choulis, V.-E. Choong, M. K. Mathai, & F. So, *Appl. Phys. Lett.* **87**, 113503 (2005).

DOE-Sponsored Publications in this Area in 2003 – 2005

Combinatorial Fabrication and Study of Doped-Layer-Thickness Dependent Color Evolution in Bright Small Molecular Organic Light-Emitting Devices, K. O. Cheon & J. Shinar, *Appl. Phys. Lett.* **83**, 2073 (2003).

Combinatorial Fabrication and Studies of Bright White Organic Light-Emitting Devices Based on Emission from Rubrene-Doped 4,4'-bis(2,2'-diphenylvinyl)-1,1'-biphenyl, G. Li & J. Shinar, *Appl. Phys. Lett.* **83**, 5359 (2003).

Förster Energy Transfer in Combinatorial Arrays of Selective Doped Organic Light-Emitting Devices, K. O. Cheon & J. Shinar, *Appl. Phys. Lett.* **84**, 1201 (2004).

Electroluminescence Spikes, Turn-off Dynamics, and Charge Traps in Organic Light-Emitting Devices, K. O. Cheon and J. Shinar, *Phys. Rev. B (Rap. Comm.)* **69**, 201306 (R) (2004).

Combinatorial Fabrication and Screening of Organic Light-Emitting Device Arrays, J. Shinar, G. Li, K. O. Cheon, Z. Zhou, & R. Shinar, in *Combinatorial and High-Throughput Discovery and Optimization of Catalysts and Materials*, Edited by W. F. Maier and R. Potyrailo, CRC Press (invited) (in press).

Combinatorial Fabrication and Screening of Organic Light-Emitting Device Arrays, J. Shinar & R. Shinar, in *Combinatorial Methods and Informatics in Materials Science*, edited by Q. Wang, R. A. Potyrailo, M. Fasolka, T. Chikyow, U. S. Schubert, and A. Korkin, *Mat. Res. Soc. Symp. Proc.* **894**, xxx (Mat. Res. Soc., Pittsburgh, 2006) (invited).

Charge Injection and Transport in Polyfluorenes

Alexis Papadimitratos, Hon Hang Fong, and George G. Malliaras
[Department of Materials Science and Engineering, Cornell University, Ithaca, NY](#)
ap297@cornell.edu, hfh4@cornell.edu, ggm1@cornell.edu

Program Scope

Organic Light Emitting Diodes (OLEDs) represent an emerging technology for lighting applications [1]. Their compatibility with large-area, mechanically flexible substrates have the potential to lead to inexpensive and efficient new light sources with unique form factors. Poly(9,9-dicetylfluorene) and its copolymers are among the best performing polymers in OLEDs due to their high mobilities and fluorescence efficiency. However, the factors that determine the performance of polyfluorene-based OLEDs are currently not understood in detail. For example, the ohmicity of the contacts is known to determine the performance of organic light emitting diodes. This project attempts to provide a comprehensive understanding of charge injection and transport in model polyfluorene copolymers, which will help engineer more efficient polyfluorene-based OLEDs for applications in lighting.

Recent Progress

We developed a time-of-flight (TOF) experiment to measure the charge carrier drift mobility as a function of electric field and temperature. The experimental set-up involves a vacuum cryostat, where the sample can be held for the duration of the experiment without exposure to the ambient, and can control sample temperature with high accuracy. A nanosecond nitrogen laser is used as the photoexcitation source in the single pulse regime. A high voltage source-measure unit and a fast oscilloscope complete the setup. The sample geometry involves an indium tin oxide (ITO) covered glass slide, on which we deposit a layer of the conducting polymer poly(3,4-ethylene dioxythiophene) doped with poly(styrene sulfonic acid) (PEDOT:PSS). We then deposit a layer of the polyfluorene, which is several micrometers thick. The sample fabrication completes with the deposition of a semitransparent Al counter electrode.

Hole mobilities were measured by applying a bias across the sample (Al electrode positive), and photogenerating holes at the Al/polymer interface. The holes drift towards the ITO electrode, causing current flow at an external circuit, which is measured as a function of time. When the holes arrive at the ITO electrode the current drops to zero. The time it takes for the “average” hole to arrive at the ITO electrode is called the transit time and is inversely proportional to the mobility. The mobility was found to be temperature dependent and electric field dependent, as expected for transport in an amorphous material.

Knowledge of the mobility allows an estimation of the space charge limited hole current, the highest unipolar current that can flow through an organic semiconductor film. By reversing the bias (ITO electrode positive), it is possible to measure the injected hole current from PEDOT:PSS, and compare it to the space charge limited one. The ratio of the two gives the injection efficiency, a figure of merit for contact performance. An injection efficiency of one means that the contact is ohmic. We found injection efficiencies of the order of 10^{-5} , which mean that PEDOT:PSS is a poor hole injector in polyfluorenes. This means that the efficiency of OLEDs that utilize this contact can be improved considerably with the use of better anodes.

Future plans

We plan to work along three directions: The first one involves quantification of the above mentioned data. We will fit the electric field and temperature dependence of the mobilities to standard models to understand the mechanism of charge transport in polyfluorenes. We will also fit the injection efficiency data to injection models and extract the barrier height between the polyfluorenes and PEDOT:PSS. We will then compare the results with spectroscopy results from the group of Prof. Antoine Kahn at Princeton, who is working on the same contacts. This comparison will allow a deeper understanding of charge injection in these materials.

The second direction involves innovation in experimental techniques. We will set up a dark injection experiment [2] to measure the mobility and the charge injection efficiency

in a device relevant geometry. This will facilitate comparison with results from OLEDs and will help measure changes in mobility and injection during OLED degradation.

The third direction involves improving the hole injecting contact in polyfluorene devices. We will apply various surface treatments on ITO and repeat the injection efficiency measurements to quantify their influence on hole injection.

References

- 1) G.G. Malliaras and R.H. Friend, "An organic electronics primer," *Physics Today* **58**, 53 (2005).
- 2) J.C. Scott, S. Ramos, and G.G. Malliaras, "Transient space charge limited current measurements of mobility in a luminescent polymer," *J. Imag. Sci. Technol.* **43**, 234 (1999).

DOE sponsored publications in 2005

"Charge injection at the PEDOT:PSS/Polyfluorene contact," A. Papadimitratos, H.H. Fong, G.G. Malliaras, in preparation.

Spectroscopic study on sputtered PEDOT·PSS: role of surface PSS layer

Jaehyung Hwang, Fabrice Amy and Antoine Kahn

Dept. of Electrical Engineering, Princeton University, Princeton, NJ 08544, USA

The doped polymer poly(3,4-ethylenedioxythiophene)-poly(styrenesulfonate) (PEDOT·PSS) is known as an efficient hole injector in organic light emitting diode(OLED). Its work function is high (~ 5.2 eV) and it has relatively good transparency and high conductivity. Although its work function is similar to that of Au, PEDOT·PSS enables much lower hole injection barrier than the metal [1], which in turns gives much better device performance. Also surprising is the fact that direct and inverse photoemission spectroscopies performed on PEDOT·PSS films show that the Fermi level is situated deep in the gap of the surface material, in apparent contradiction with the notion of a heavily doped, conducting material. The purpose of this study is to investigate this apparent contradiction and identify the fundamental factor(s) that contribute to the far more advantageous hole injection barriers on PEDOT·PSS.

The structure of PEDOT·PSS is known to consists of an insulating PSS layer surrounding the PEDOT grains [2]. We perform here X-ray and ultraviolet photoelectron spectroscopy (XPS and UPS) on 40 nm thick films of PEDOT·PSS (Baytron P) spun ex-situ on ITO. The pristine films are investigated first, then lightly sputtered to identify the composition, electronic structure and role of the PSS layer. The pristine films show an extremely weak density of states near the Fermi level [2]. After sputtering, the film shows a significant increase in the PEDOT/PSS ratio (from 0.12 to 0.7) as well as a strong build up of the density of filled states close to the Fermi level, suggesting that the removal of the insulating PSS layer uncovers the bulk of the more conducting doped PEDOT·PSS mixture. The thickness of the PSS layer, calculated from the ratio between the XPS S 2p core-levels of PEDOT and PSS for the pristine PEDOT·PSS is estimated at 35 Å. Sputtering also reduces the PEDOT·PSS work function from 5.2 eV to 4.7 eV, close to that of highly doped PEDOT [3]. We investigate the effect of this change on the charge injection barrier at the interface with the hole-transport material N,N'-diphenyl-N,N'-bis(1-naphthyl)-1,1'-biphenyl-4,4'-diamine (α -NPD). The interface dipole (0.24 eV) and hole

injection barrier (0.97 eV) are found to be larger with sputtered PEDOT·PSS than with the as-loaded film (0.14 eV and 0.47 eV, respectively), suggesting a stronger interaction between two materials. We conclude that the insulating PSS layer formed at the interface increases the work function of the material and decouples the overlayer from the substrate. Both effects contribute to lowering the injection barrier for holes, improving the device performance.

1. N. Koch, et al., *Appl. Phys. Lett.*, **82**, 70 (2003)
2. G. Greczynski, et al., *Thin Sol. Films.*, **354**, 129 (1999)
3. X. Z. Xing, et al., *Synth. Met.*, **89**, 161 (1997)

White-light Emission from Ultra-small Cadmium Selenide Nanocrystals

Michael J. Bowers II; James R. McBride and Sandra J. Rosenthal
michael.j.bowers@vanderbilt.edu, james.r.mcbride@vanderbilt.edu,
sandra.j.rosenthal@vanderbilt.edu
Department of Chemistry Vanderbilt University, Nashville, TN 37235

Program Scope

Great emphasis has been placed on direct white-light emitting materials and the use of nanomaterials to manufacture efficient solid-state lighting devices. Semiconductor nanocrystals or quantum dots are an attractive material for applications in solid-state lighting for several reasons. Being inorganic, they are much more robust than organic molecules, the electronic and optical properties are easily modified without major changes to the synthetic methodologies and they have been shown to exhibit fluorescence quantum yields of near 100%. The specific goals of this research are to build and characterize light emitting devices that utilize ultra-small CdSe nanocrystals as the light emitting medium and to study the fundamental physics that produce the observed behavior of the ultra-small (< 2 nm) CdSe nanocrystals. Ultrafast spectroscopy, confocal fluorescence microscopy and Z-contrast scanning transmission electron microscopy will be used to further characterize the structure, optical and electronic properties of the ultra-small nanocrystals.

Recent Progress

We have pyrolytically synthesized magic-sized CdSe nanocrystals through a modified version of the methods of Peng *et al.*¹ These ultra-small nanocrystals exhibit broadband emission (420 - 710 nm) throughout most of the visible light spectrum while not suffering from self absorption. This is the direct result of the extremely narrow size distribution and an unusually large (30-40 nm) Stokes shift (Figure 1). The first absorption feature is at 414 nm which has been assigned as a thermodynamically determined 'magic size', on the order of 15 Å, for CdSe.^{2,3} The emission spectrum shows a band edge emission followed by two features attributed to emission from energetically different midgap states. The fluorescence quantum yield for this material thus far is on the order of 2 to 3% with a calculated extinction coefficient of 22311 per mole of nanocrystals.⁴ Additionally, this material has demonstrated good photostability. Thin films of magic-sized CdSe (neat on a glass slide) were able to maintain their optical properties after ten days of exposure to intense UV light from a 1000 μ W, 370 nm LED (LEDtronics) under ambient conditions (air at room temperature).

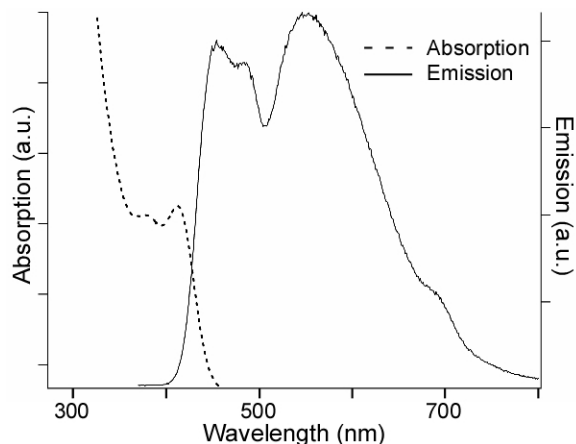


Figure 1. Absorption and emission spectra of magic-sized CdSe. Static absorption and emission spectra were obtained using a Cary Bio 50 UV-Visible spectrometer and an ISS photon counting fluorescence spectrometer ($\lambda_{\text{ex}} = 367$ nm), respectively.

Our pyrolytically grown magic-sized nanocrystals do not typically exhibit the strong band edge emission feature that is observed in CdSe nanocrystals, but do exhibit strong band edge absorption features indicative of high quality CdSe nanocrystals. We attribute the broad emission to charge recombination from surface midgap states that arise from the presence of non-coordinated surface selenium sites.⁵ While band edge emission occurs by direct recombination of the electron and hole within the nanocrystal, deep trap emission occurs when a photogenerated hole, trapped in a midgap state, encounters an electron before it can relax non-radiatively to the ground state.⁶

This phenomenon of hole trapping to the selenium surface sites has been studied by ultrafast fluorescence upconversion spectroscopy.⁶ These studies indicate that as nanocrystal size decreases, the amount of hole trapping increases. This is due not only to the reduced physical distance the hole must travel to reach the surface, but also to an increased surface-to-volume ratio resulting in more available surface sites. It is not unreasonable to infer that as the nanocrystal size continues to decrease, an even larger population of photoexcited excitons would be funneled toward the hole-trapping decay pathway, ultimately making it the dominant mode of radiative relaxation. Magic-sized nanocrystals are so small that the electron wave function has significant overlap with the selenium surface sites.^{7,8} Therefore any hole trapped on the surface would likely encounter the electron before non-radiatively relaxing to the ground state.⁶ Compounding this situation, the nanocrystal growth time is so short (10-20 seconds normally) that surface reconstruction and high temperature annealing have little time to occur. This results in a surface that is likely defect-ridden. Furthermore, unlike larger nanocrystals, the diameter of the magic-sized nanocrystal and the length of the ligand are quite comparable. Coupling of vibrational modes of the ligand to surface atoms, as well as collisional relaxation, could provide other avenues for energy dissipation, providing more effective trap sites and potentially contributing to the broad lognormal emission line shape.

While deep trap emission is quite common in small (<30 Å) nanocrystals, it is usually accompanied by a large band edge emission feature.^{9,10} The presence of a strong band edge feature would bias the white-light emission toward a particular color, reducing the quality of the white light produced. The band edge emission feature of our material is greatly diminished, providing a more balanced white-light emission with chromaticity coordinates of 0.322, 0.365, which fall well within the white region of the 1931 CIE diagram.¹¹ Examples of the white-light emission are shown in Figure 2.

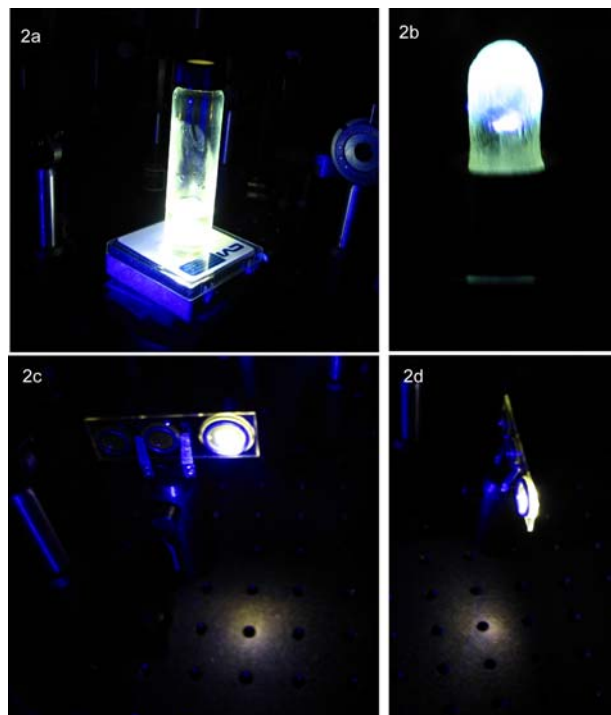


Figure 2. Light emission from magic-sized CdSe nanocrystals. Nanocrystals in solution 2a, and in polyurethane films (c and d) illuminated by a frequency doubled titanium:sapphire laser (400 nm). 2b is UV LED coated with a polyurethane-magic-sized nanocrystals film.

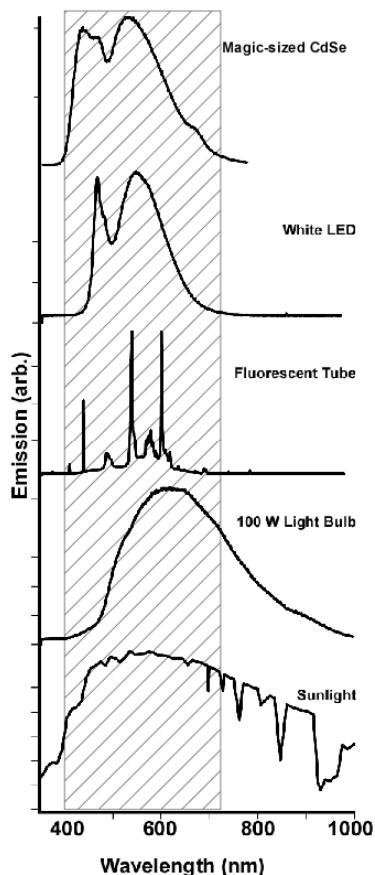


Figure 3. Comparison of conventional tungsten and fluorescent lighting emission spectra with the AM 1.5 solar spectrum, a commercial white LED and magic-sized CdSe nanocrystals. The magic-sized CdSe nanocrystals exhibit a broad emission covering most of the visible spectrum. Unlike conventional tungsten sources no energy is wasted producing wavelengths beyond the visible spectrum.

Future Plans

Further studies of the reaction conditions for the pyrolysis reaction will be undertaken in an attempt to understand why the bottom up pyrolysis reaction leads to a product with these unique optical properties. Surface passivation will be investigated as a means of increasing the modest quantum yield of roughly 3-5%.¹²

Characterization of the nanocrystal size and morphology will be carried out using Z-contrast scanning transmission electron microscopy. This technique offers the ability to probe the structure of these ultra-small nanocrystals where traditional electron microscopy lacks the required resolution. Confocal fluorescence microscopy studies will be undertaken to determine if the broad emission is an ensemble phenomenon or if in fact all nanocrystals produce the broad spectrum light.

Ultrafast fluorescence upconversion spectroscopy and ultrafast transient absorption spectroscopy will be used to attempt to elucidate the relaxation mechanisms leading to the broad emission from the ultra-small CdSe nanocrystals. Examining the time evolution of the emission

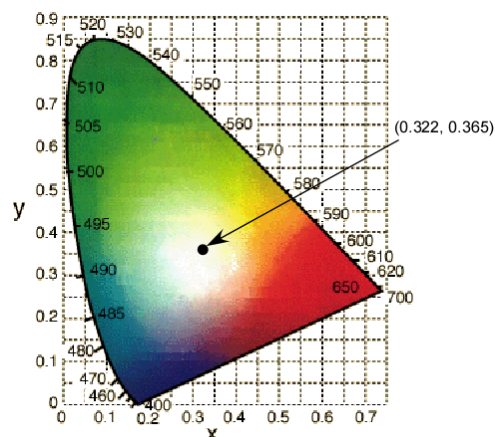


Figure 4. C. I. E. 1931 chromaticity diagram. The chromaticity diagram illustrates all of the colors of the visible spectrum corrected for the response of the human eye. The dot indicates the chromaticity coordinates of our magic-sized CdSe nanocrystals. This figure illustrates that our nanocrystals produce a slightly warm white light that is comparable to that of a tungsten light bulb.

*Chromaticity diagram from:
<http://hyperphysics.phy-astr.gsu.edu/hbase/vision/cie.html>

and bleaching of the excited states should afford insight into the nature of the relaxation mechanisms involved.

Finally, light emitting devices utilizing ultra-small CdSe nanocrystals as the emitting material will be constructed. Device designs utilizing the nanocrystals in both frequency conversion and electroluminescence roles will be investigated and characterized with respect to spectral quality, conversion efficiency, and luminous efficacy.

References

- (1) Peng, Z. A.; Peng, X. *J. Am. Chem. Soc.* **2001**, *123*, 183-184.
- (2) Qu, L.; Yu, W. W.; Peng, X. *Nano Lett.* **2004**, *4*, 465-469.
- (3) Landes, C.; Braun, M.; Burda, C.; El-Sayed, M. A. *Nano Lett.* **2001**, *1*, 667-670.
- (4) Yu, W. W.; Qu, L.; Guo, W.; Peng, X. *Chem. Mater.* **2003**, *15*, 2854-2860.
- (5) Hill, N. A.; Whaley, K. B. *J. Chem. Phys.* **1994**, *100*, 2831-2837.
- (6) Underwood, D. F.; Kippeny, T. C.; Rosenthal, S. J. *Journal of Physical Chemistry B* **2001**, *105*, 436-443.
- (7) Brus, L. E. *J. Chem. Phys.* **1984**, *80*.
- (8) Brus, L. *J. Phys. Chem.* **1986**, *90*, 2555-2560.
- (9) Landes, C. F.; Braun, M.; El-Sayed, M. A. *J. Phys. Chem. B* **2001**, *105*, 10554-10558.
- (10) Murray, C. B.; Norris, D. J.; Bawendi, M. G. *J. Am. Chem. Soc.* **1993**, *115*, 8706-8715.
- (11) <http://hyperphysics.phy-astr.gsu.edu/hbase/vision/cie.html#c2>.
- (12) Bowers, M. J., II; McBride, J. R.; Rosenthal, S. J. *J. Am. Chem. Soc.* **2005** *127*, 15378-15379.

DOE Sponsored Publications in 2004-2006

White-Light Emission from Magic-Sized Cadmium Selenide Nanocrystals, Bowers, M. J., II; McBride, J. R.; Rosenthal, S. J., *J. Am. Chem. Soc.* **2005** *127*, 15378-15379.

Aberration-corrected Z-Contrast Scanning Transmission Electron Microscopy of CdSe Nanocrystals, McBride, J. R.; Kippeny, T. C.; Pennycook, S. J.; Rosenthal, S. J., *Nano Lett.* **2004** *4* 1279-1283.

Growth, structure, and functionality of nanocrystals through Z-contrast microscopy and theory, Pennycook, S. J.; Lupini, A. R.; Kadavanich, A.; McBride, J. R.; Rosenthal, S. J.; Puetter, R. C.; Yahil, A.; Krivanek, O. L.; Delby, N.; Nellist, P.; Duscher, G.; Wang, L. G. and Pantelides, S. T., *Proceedings of the Materials Research Society* In Press

Spherical Aberration Corrected Z-STEM Characterization of CdSe and CdSe/ZnS Nanocrystals. McBride, J. R.; Kippeny, T. C.; Pennycook, S. J.; Rosenthal, S. J., *Proceedings of the Materials Research Society* **2005** M815.1-15.6.

Spectroscopy of Single- and Double-Wall Carbon Nanotubes in Different Environments, Hertel, T.; Hagen, A.; Talalae, V.; Arnold, K.; Hennrich, F.; Kappes, M.; Rosenthal, S. J.; McBride, J.; Ulbricht, J. H.; Flahaut, E., *Nano Lett.* **2005** *5* 511-514.

Enhanced Light Emission from Lu₂SiO₅ Induced by Ion Irradiation

Luiz G. Jacobsohn, Ross E. Muenchausen and D. Wayne Cooke
lgjacob@lanl.gov, rossm@lanl.gov, cooke@lanl.gov
Materials Science & Technology Division, Los Alamos National Laboratory,
Los Alamos, NM 87545

Program Scope

This abstract corresponds to a subtask of the BES Program titled “*Nanophosphors: Fundamental Science of Insulators in the Nanoscale Regime*” started last April. There, among other ideas, Ce implantation into Lu₂SiO₅ (LSO) crystals to achieve enhanced light output was proposed. LSO doped with Ce is extensively used as a radiation detector because it exhibits high mass density (7.4 g/cm³), fast emission (40 ns), and excellent light output. For optical efficiency Ce must be in the 3+ valence state and must substitute for Lu in the monoclinic crystal structure. However, because of the low Ce segregation coefficient in LSO, 0.22, light output is limited by the Ce solid solubility of ~0.05 at.% with respect to Lu.¹ By using ion implantation, a technique that is capable of obtaining stable materials in conditions far from thermodynamic equilibrium, we suggested that this limit could be extended to higher concentrations and presumably achieve enhanced light output. Moreover, relative to the high temperatures required for Czochralski growth of LSO (~2150°C), ion implantation and post-implantation annealing offer an attractive alternative for synthesizing this technologically important material. While photoluminescence measurements of LSO crystals implanted with 132 keV Ce⁺ up to 4.84x10¹⁴ atoms/cm² followed by 1h annealing at 1000 °C in vacuum showed no improvement in the light output, other ion implantations into LSO revealed interesting results.

In LSO:Ce-based radiation detectors, efficient energy transfer from the ionization track to the Ce sites, a process in which electronic defects play a major role, is necessary to achieve good light output. On the other hand, the presence of defects caused by the incoming radiation may provide radiationless pathways that ultimately reduce the total light output. For these reasons we carried out H⁺ and He⁺ irradiations of LSO at room temperature and monitored the effects on light emission from self-trapped defects (STDs) as a function of the temperature to gain insight into the effects of ion irradiation on undoped LSO.

Recent Progress

Irradiation of LSO with 40 keV H⁺ and 53 keV He⁺ ions were carried out with doses of 2 and 1 x10¹⁶ atoms/cm² at room temperature, respectively. The ion energies were chosen to achieve the same projected range, calculated to be ~240 nm using the Stopping Power and Range of Ions in Matter (SRIM 2003) code.² As a consequence, defect production is close to the surface and within similar volumes in all samples. Pristine and irradiated samples were investigated by radioluminescence (RL) measurements carried out in vacuum from room temperature to liquid He, using a Mo-

target x-ray source operated at 50 kV and 40 mA. The effective x-ray energy was ~25 keV and the dose rate at the sample was 1.75 Gy/s (measured in air).

Two emission bands centered at 256 and 315 nm were observed in the pristine and the irradiated samples. They were assigned to self-trapped excitons (STEs) and self-trapped holes (STHs), respectively,³ following the observation that STE bands with maximum around 250 nm, and STH bands with maximum around 300 nm, occur in all yttrium- and lutetium-based compounds investigated to date.⁴⁻⁵ Since the intensity of these bands obtained by H⁺ and He⁺ irradiations was found to be controlled by radiation-induced ballistic damage, with no indication of chemical effects arising from the chemical nature of the implanted species, as observed in other materials, we focused our research on the H⁺ results.

The thermal behavior of the two bands, before and after ion irradiation, is summarized in Fig. 1. The STE curve for the irradiated sample is shifted to lower temperatures relative to the unirradiated one, has an inflection point at $T^* \sim 75$ K, and exhibits two-fold increase in emission intensity. In contrast, following ion irradiation the STH band shifts to higher temperatures with no change in emission intensity and no evidence for an inflection point. The shifts of the curves are associated with changes in the thermal stability of the defects. After irradiation, STEs are less thermally stable with a three-fold decrease in the thermal activation energy as determined by applying the two-level Mott-Seitz equation, $I(T) = I_0/(1 + Ce^{-E/kT})$, where T is the temperature, C is a constant related to the probabilities of radiative and nonradiative decay modes, E is the thermal activation energy, and k is Boltzmann's constant.⁶ On the other hand, STHs present a two-fold increase in the activation energy after irradiation. Strikingly is the fact that ion irradiation, which is confined to a shallow region close to the surface (~240 nm depth), has such pronounced effect on radioluminescence intensity. Similar results have been reported in ion irradiated SrTiO₃.⁷

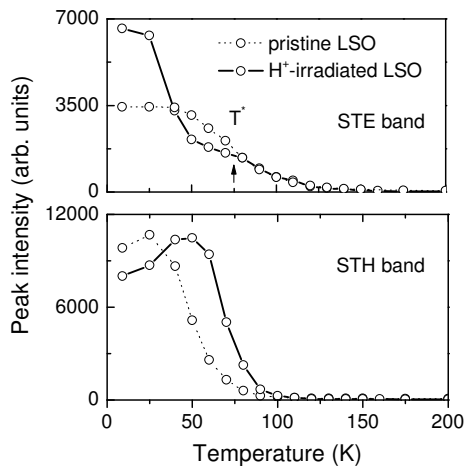


Figure 1 - Peak intensity of the STE and STH bands at 256 and 315 nm, respectively, before and after H⁺ irradiation as a function of temperature. The arrow marks the inflection point.

Future Plans

We now outline a qualitative model to explain the RL results that is presently in development by our group. It incorporates the structural damage induced by H⁺ irradiation, oxygen ions and vacancies as the STH and STE luminescence centers, and a

surface dead layer. Monte Carlo simulations of 40 keV H^+ irradiation of LSO using the SRIM 2003 code showed that the number of oxygen vacancies comprises nearly 50% of the total number of vacancies, which is of the order of 10^{21} vacancies/cm³, corresponding to atomic fractions of a few atomic percent. Even if one assumes that the original concentration of oxygen vacancies in the pristine material is high, of the order of 10^{18} vacancies/cm³, irradiation promotes a huge increase in the overall concentration. Conversely, the reduction of the number of oxygen ions in the crystalline network due to interstitial production is less than 10%. Although self-healing of the structure is expected to occur, a significant fraction of these defects will be retained in the structure. Moreover, STDs are not stable at room temperature and, therefore, we conclude that the major effect of H^+ irradiation at room temperature is to produce a large concentration of oxygen vacancies in LSO.

Because the x-ray flux utilized in the RL experiment is constant and only produces electron-hole pairs, the observed increase in the STE luminescence intensity is attributed to an increase in concentration of recombination centers, *i.e.*, of the number of oxygen vacancies. On the other hand, since the number of oxygen ions in the crystalline network is only slightly changed by the ion irradiation, no significant changes in the STH emission intensity are expected, consistent with observation (*cf.* Fig. 1). The presence of an inflection point at $T^* \sim 75$ K in the temperature-dependent STE emission intensity is attributed to the superposition of two thermal quenching curves originating from two very similar STEs. These defects correspond to STEs, and to STEs perturbed by a nearby structural defect that is most probably an oxygen vacancy. The full-width at half-maximum of the STE band is ~ 0.6 eV, which is large enough to accommodate two unresolved emission bands. Perturbed STEs, usually associated with impurities, have been reported before in other materials.⁸ In the alkali halides they are responsible for luminescence at temperatures where STE emission is quenched,⁹ supporting our view that the observed changes in the thermal stability of the STDs are related to ion-induced structural damage.

While the above model qualitatively describes the effects of ion irradiation on the behavior of STD emission in LSO, the fact that a shallow modified region ~ 240 nm thick is capable of doubling the STE light output when excited by ~ 25 keV x-rays is quite remarkable. The penetration depth of the x-rays is of the order of a few mm, which is $\sim 10^4$ times the range of H^+ ions. Thus, RL is probing a very large volume relative to the volume affected by ion irradiation. The explanation to this observation is related to presence of a surface dead layer from which no luminescence is emitted. The existence of this layer in phosphor materials has been extensively reported in the literature, particularly for semiconductor materials, and many mechanisms have been proposed to explain its existence: (i) surface space-charges causing electric fields that separate electron-hole pairs, thus reducing the rate of radiative recombination; (ii) lattice defects and imperfections in the surface region, including oxidation; (iii) changes in composition (segregation); and (iv) changes in the crystallographic phase causing a decrease in the luminescence efficiency. The decrease in efficiency has been attributed to enhanced scattering and thus lower carrier mobility, creation of electronic states within the gap (surface states) that provide a pathway for radiationless de-excitation, and changes in the rate of radiative recombination.¹⁰ Our results suggest that structural damage created by

the ion irradiation, particularly oxygen vacancies, was enough to compensate the dead layer effect thus allowing emission from this region of the crystal.

Future perspectives for this work are to use electron spin resonance spectroscopy to identify the defects created by the ion irradiation and to extend the investigation to other materials to check for the generality of the proposed model.

References

- (1) C.L. Melcher and J.S. Schweitzer, *IEEE Trans. Nuc. Sci.*, **1992**, 39, 502-505.
- (2) The SRIM 2003 code can be found at <http://www.srim.org/SRIM/SRIM2003.htm>.
- (3) D. W. Cooke, B. L. Bennett, R. E. Muenchausen, J.- K. Lee, and M. Nastasi, *J. Lumin.*, **2004**, 106, 125-132.
- (4) M. V. Korzhik and W. P. Trower, *Appl. Phys. Lett.*, **1995**, 66, 2327-2328.
- (5) P. Lecoq and M. Korzhik, *IEEE Trans. Nuc. Sci.*, **2002**, 49, 1651-1654.
- (6) *Luminescence in Solids*, C.C. Klick and J.H. Schulman, in "Solid State Physics vol. 5", edited by F. Seitz and D. Turnbull, Academic Press **1957**, pp 97.
- (7) B. Yang, P.D. Townsend and R. Fromknecht, *Nuc. Instrum. Meth. Phys. Res. B* **2004**, 217, 60-64.
- (8) D. S. McClure and C. Pedrini, *Phys. Rev. B*, **1985**, 32, 8465-8468.
- (9) N. Itoh, T. Shimizu-Iwayama and T. Fujita, *J. Non-cryst. Solids*, **1994**, 194-201.
- (10) B.L. Abrams and P.H. Holloway, *Chem. Rev.*, **2004**, 104, 5783-5801.

DOE Sponsored Publications in 2005-2006

Effects of ion beam irradiation on self-trapped defects in single-crystal Lu₂SiO₅, L. G. Jacobsohn, J.- K. Lee, B. L. Bennett, R. E. Muenchausen, M. Nastasi and D. W. Cooke, *J. Lumin.* (to be published).

The central role of oxygen on H⁺ irradiated Lu₂SiO₅ luminescence, L. G. Jacobsohn, B. L. Bennett, J.- K. Lee, R. E. Muenchausen, J. F. Smith, B. P. Uberuaga and D. W. Cooke, *J. Lumin.* (submitted).

Ion irradiation of porous silicon: the role of surface states, L.G. Jacobsohn, B.L. Bennett, D.W. Cooke, R.E. Muenchausen and M. Nastasi, *Nuc. Instrum. Methods Phys. Res. B*, **2006**, 242, 164-166.

The role of the chemical nature of implanted species on quenching and recovery of photoluminescence in ion irradiated porous silicon, L.G. Jacobsohn, D.W. Cooke, B.L. Bennett, R.E. Muenchausen and M. Nastasi, *J. Appl. Phys.*, **2005**, 98, 076108-1 to 3.

The effects of ion irradiation on porous silicon photoluminescence, L.G. Jacobsohn, B.L. Bennett, D.W. Cooke, R.E. Muenchausen and M. Nastasi, *J. Appl. Phys.*, **2005**, 97, 033528-1 to 5.

Nanophosphors

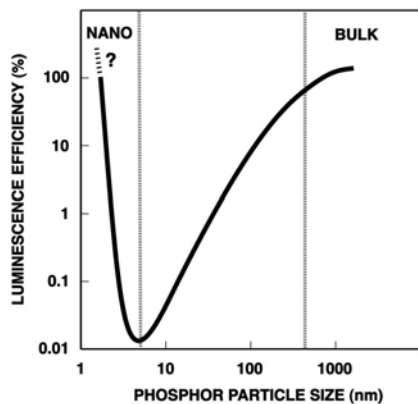
Ross E. Muenchausen, Luiz. G. Jacobsohn, and D. Wayne. Cooke

rossm@lanl.gov, lgjacob@lanl.gov, cooke@lanl.gov

Materials Science & Technology Division, Los Alamos National Laboratory,
Los Alamos, NM 87545

Program Scope

Within the last few years nanotechnology has rapidly progressed from scientific curiosity to a bona fide realm of intellectual inquiry. Discovery, development, and fundamental understanding of materials confined to nanometer dimensions dominates the scientific horizon in many disciplines and offers vast potential for improved technological devices. Driven by applications, much of the research has focused on novel properties of quantum-confined semiconductors.¹ Recently, however, nanoscale research has broadened to include inorganic insulators that exhibit unique optical properties resulting from reduced dimensionality.² These “nanophosphors” are typically derived from bulk phosphors that exhibit excellent luminescence efficiency; thus, a large class of interesting phosphors is those doped with rare earth ions, e.g., $\text{Ln}_2\text{SiO}_5:\text{Ce}$ ($\text{Ln} = \text{Y}, \text{Lu}$) and $\text{Y}_2\text{O}_3:\text{Tb}$, with well known optical properties.³ Nanophosphors of these materials are expected to exhibit novel optical behavior owing to reduced dimensionality. The goal of our work is to synthesize nanophosphors of this class, characterize their optical properties, and compare results with their bulk counterparts to gain fundamental understanding of the role of reduced dimensionality on these materials. An important aspect of this research is fabrication of nanophosphors wherein the particle size can be controlled and the dopant ion concentration can be varied.



It is well known that luminescence efficiency decreases as the particle size becomes smaller than nominally a few microns, as illustrated in the accompanying graph. This is typically attributed to the increased role of surface states (defects, dangling bonds, etc.) that act as nonradiative luminescence centers. In striking contrast, luminescence efficiency increases for nanophosphor particles smaller than several nanometers, presumably due to quantum effects. Unlike semiconductor quantum dots, where delocalized, spatially extended electronic states are quantum confined, rare-earth-ion electronic states are

spatially localized to dimensions smaller than the nanoparticle. However, vibrational states are spatially extended and are therefore strongly affected by confinement. Thus, the phonon density of states is modified in nanophosphors and the resulting electron-phonon interaction is quite different from that observed in bulk specimens. Because the low-frequency acoustic phonons contribute strongly to nonradiative relaxation of luminescence in nanophosphors, and because these modes are cut off due to spatial confinement, optical properties of nanophosphors will vary from bulk phosphors.⁴ Of course other factors affect optical properties of nanophosphors: crystal structure variation

with size reduction, i.e., polymorphism, and the role of surface states in the overall luminescence mechanism. Because nanophosphors of interest usually contain rare-earth ions, concomitant crystal-field and spin-orbit effects add additional complexity to the task of analyzing and interpreting nanophosphor data.

Although driven by scientific inquiry, the possibility for enhanced light output and reduced emission lifetime, as recently reported for nanophosphor $\text{Y}_2\text{SiO}_5:\text{Eu}$,⁵ offers possibilities for improved radiation detectors and lighting sources that support the mission of the Department of Energy.

Recent Progress

Nanophosphors of $\text{Y}_2\text{SiO}_5:\text{Ce}$ (YSO), $\text{Lu}_2\text{SiO}_5:\text{Ce}$ and $\text{Y}_2\text{O}_3:\text{Tb}$ have been prepared by hydrothermal and solution-combustion synthesis methods and characterized by optical and microstructural techniques. As an example of recent progress we highlight our results on YSO. TEM data show nanophosphor YSO particle size to be in the range 25 – 100 nm, and XRD results indicate that it consists primarily of the monoclinic phase with space group $\text{P}2_1/\text{c}$. The usual structure of bulk YSO is monoclinic with space group $\text{B}2/\text{b}$.⁶ Each of these structures have two inequivalent rare earth sites coordinated with either 6 and 7 oxygens ($\text{B}2/\text{b}$) or with 7 and 9 oxygens ($\text{P}2_1/\text{c}$). The nanophosphor photoluminescence (PL) spectrum exhibits a well-defined maximum at 431 nm ($\lambda_{\text{ex}} = 366$ nm) along with a knee near 470 nm, and is red shifted relative to the bulk spectrum, which is characterized by emission peaks at 395 and 420 nm ($\lambda_{\text{ex}} = 356$ nm). The latter peaks are attributed to the well-known emission from the spin-orbit split ground state of the Ce^{3+} 4f electron manifold. Overlap of the excitation and emission bands is greater in the bulk material than in nanophosphor, thus yielding increased self-absorption (reduced Stokes shift), which implies reduced emission relative to the nanophosphor. Variations in PL and PL excitation spectra of bulk and nanophosphor YSO are attributed to crystal symmetry rather than reduced dimensionality.

However, reduced dimensionality effects are manifested in the emission lifetime data. Ambient optical excitation of the main bands in bulk and nanophosphor YSO powder yields fitted lifetime ($1/e$) values of 39 and 55 ns, respectively. When measured in various media the nanophosphor lifetime was found to be dependent on the medium in which it was immersed whereas the bulk YSO was independent of the medium. Measured lifetimes of the nanophosphor varied from 35 to 55 ns. Now, cerium emission is dominated by parity-allowed electric dipole transitions and the reciprocal lifetime is proportional to the transition oscillator strength and local electric field correction in terms of the materials' refractive index. In bulk YSO most Ce ions are far from the surface and their dielectric interaction with the embedding medium is negligible; the index of refraction is just that of the host lattice. Conversely, nanoscale YSO has a much larger surface-to-volume ratio with most of the dopant Ce ions residing near the surface. These ions now experience a local electric field induced by the surrounding medium, which is different from the average field of bulk YSO. Consequently, nanophosphor YSO lifetimes vary according to the medium in which they are immersed. Thus, tunability of the emission lifetime is a reality in this material and, presumably, in other nanophosphors as well. A direct measurement of the radiative lifetime as a function of refractive index allows extraction of the optical transition oscillator strength. This is a unique and

straightforward method for obtaining this important parameter. The obtained oscillator strength in nanophosphor YSO is 0.013, which is higher than the bulk value, 0.009.⁷

Additional reduced-dimension behavior is associated with enhanced light output of nanophosphor YSO. Upon x-ray excitation the nanophosphor light yield is ca. three times that of bulk powder when the data are normalized to mass. This large increase cannot be solely explained by the different bulk and nanophosphor structures with their intrinsically different luminescent efficiencies, nor can it be explained by photon scattering as a function of particle size. Although we do not understand the origin of this enhancement, it underscores the novel behavior of nanophosphors and provides ample motivation for further research.

Future Plans

This project began in mid-FY05 and we have already demonstrated novel structural and optical behavior of select rare-earth nanophosphors, but, although intriguing, the paucity of present experimental data allows only sample-specific conclusions to be drawn. We will utilize additional methods to synthesize several rare-earth nanophosphors with a primary goal of reducing (and controlling) particle size as well as dopant concentration. An important issue to be resolved is the putative enhanced luminescence efficiency via particle size reduction, as suggested by the earlier graphic and supported by limited experimental data. Knowledge of luminescence quenching as a function of dopant concentration as well as particle size distribution are required to address this issue. Additional experiments designed to flesh out the role of the local electric field perturbation on nanophosphor radiative lifetime will be pursued by employing nanophosphor embedding media that cover a broad range of refractive indices, and also by investigating the effect in different nanophosphors.

In addition to our present suite of microstructural and optical techniques, we will add electron paramagnetic resonance and Fourier-transform infrared spectroscopy to assist in detecting the presence and identification of surface states. Theoretical work aimed at understanding formation of polymorphic phases in YSO will also be initiated.

References

- (1) H. Chandar, *Mater. Sci. Engr. R*, 2005, 49, 113-155.
- (2) R. S. Meltzer, in Spectroscopic Properties of Rare Earths in Optical Materials, edited by G. Liu and B. Jacquier (Springer, New York, 2005), pp. 251-256.
- (3) G. Blasse and B. C. Grabmaier, in Luminescent Materials (Springer-Verlag, Berlin, 1994), pp. 40-49.
- (4) G. Liu, X. Chen, H. Zhuang, S. Li and R. Niedbala, *J. Sol. State Chem.*, 2003, 171, 123-132.
- (5) W. Zhang, P. Xie, C. Duan, K. Yan, M. Lin, L. Lou, S. Xia and J.-C. Krupa, *Chem. Phys. Lett.*, 1998, 292, 133-136.
- (6) C. Cannas, M. Mainas, A. Musinu, G. Piccaluga, A. Speghini and M. Bettinelli, *Opt. Mater.*, 2005, 27, 1506-1510.
- (7) D. W. Cooke, B. L. Bennett, K. J. McClellan, J. M. Roper, M. T. Whittaker and A. M. Portis, *Phys. Rev. B.*, 2000, 61, 11973-11978.

DOE Sponsored Publications in 2005-2006

Spectral Emission of Rare-Earth Doped Lu₂SiO₅ Single Crystals, D. W. Cooke, R. E. Muenchausen, K. J. McClellan, and B. L. Bennett, *Opt. Mater.* 2005, 27, 1781-6.

Effects of Thermal Annealing and Aging on Porous Silicon Photoluminescence, L. G. Jacobsohn, D. W. Cooke, B. L. Bennett, R. E. Muenchausen, and M. Nastasi, *Phil. Mag.* 2005, 85, 2611-20.

The Role of the Chemical Nature of Implanted Species on Quenching and Recovery of Photoluminescence in Ion Irradiated Porous Silicon, L. G. Jacobsohn, D. W. Cooke, B. L. Bennett, R. E. Muenchausen, and M. Nastasi, *J. Appl. Phys.* 2005, 98, 76108-10.

Luminescent Properties and Reduced Dimensional Behavior of Hydrothermally Prepared Y₂SiO₅:Ce Nanophosphors, D. W. Cooke, J.-K. Lee, B. L. Bennett, et al., *Appl. Phys. Lett.* Submitted.

Effects of Ion Beam Irradiation on Self-Trapped Defects in Single Crystal Lu₂SiO₅, L. G. Jacobsohn, J.-K. Lee, B. L. Bennett, R. E. Muenchausen, M. Nastasi, and D. W. Cooke, *J. Lumin.* To be published.

The Central Role of Oxygen on H⁺ Irradiated Lu₂SiO₅ Luminescence, L. G. Jacobsohn, B. L. Bennett, J.-K. Lee, R. E. Muenchausen, J. F. Smith, B. P. Uberuaga, and D. W. Cooke, *J. Lumin.* Submitted.

Patents

Method for Preparation of Rare-Earth Oxyorthosilicate Phosphor Films, R. E. Muenchausen, D. W. Cooke, J.-K. Lee, M. Nastasi, and Q. Jia, S-104-811. Patent Pending.

Nanocomposite Scintillator and Detector, D. W. Cooke, E. A. McKigney, R. E. Muenchausen, and B. L. Bennett, S-104-966. Patent Pending.

In-Situ Synchrotron X-ray Studies of Metal Organic Chemical Vapor Deposition of $\text{In}_x\text{Ga}_{1-x}\text{N}$

G. Brian Stephenson^{1,2}, Fan Jiang¹, Stephen K. Streiffer^{1,2}, Anneli Munkholm^{3*}
stephenson@anl.gov, fjiang@anl.gov, streiffer@anl.gov, anneli.munkholm@lumileds.com

¹ Materials Science Division, Argonne National Laboratory, Argonne, Illinois 60439

² Center for Nanoscale Materials, Argonne National Laboratory, Argonne, Illinois 60439

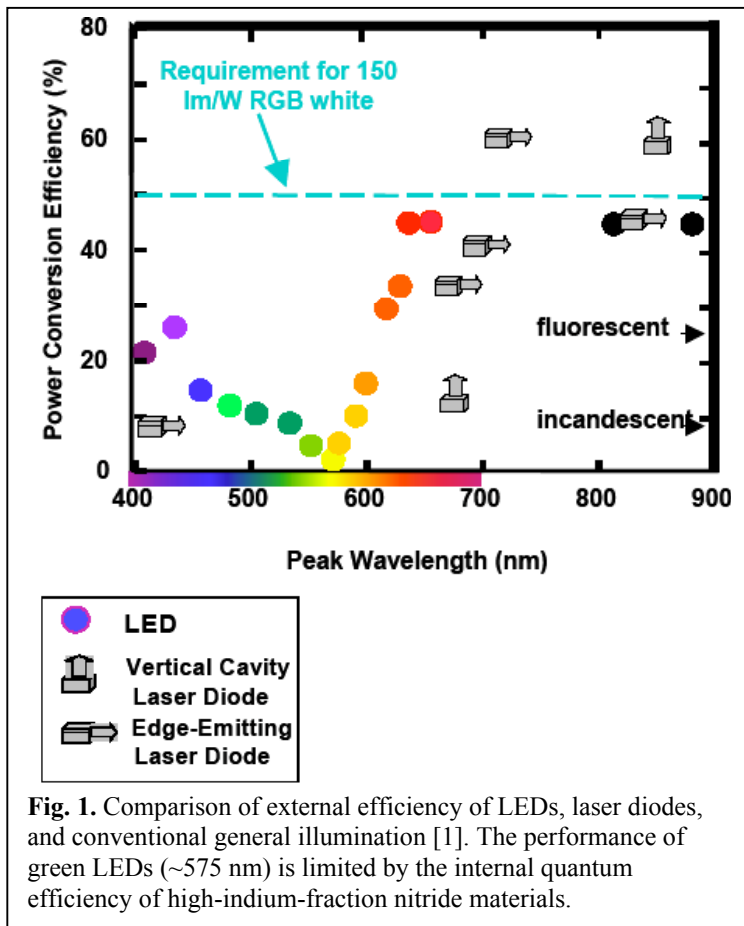
³ Lumileds Lighting, San Jose, California 95131

Program Scope

Understanding the incorporation of indium during synthesis of $\text{In}_x\text{Ga}_{1-x}\text{N}$ materials by metal organic chemical vapor deposition (MOCVD) is a fundamental materials problem that is key to continued improvement in the performance of light-emitting diodes. The scientific issues include the kinetically-controlled growth of a supersaturated alloy compound, its atomic-scale growth modes, and the potential formation of compositionally-segregated regions. We have previously developed a unique capability for *in situ* studies of MOCVD growth that is ideally suited to investigate these processes, using synchrotron x-ray beams from the Advanced Photon Source (APS). We have initiated an exploratory project to carry out real-time grazing-incidence x-ray scattering and fluorescence studies of surface and film structure during growth of $\text{In}_x\text{Ga}_{1-x}\text{N}$, in order to provide the fundamental understanding of the underlying science and for rational design of MOCVD processes for

improved materials.

For white light or RGB applications, nitride LEDs with appropriate wavelength emission are used in the blue and green portions of the spectrum. While improvements in device design and packaging have increased light extraction in LEDs, *it is the internal quantum efficiency that provides the most room for further significant improvements in nitride LED performance.* The light emitting layer(s) in nitride LEDs consist of thin $\text{In}_x\text{Ga}_{1-x}\text{N}$ quantum wells ($\sim 30\text{\AA}$), where the indium fraction x in the well determines the emission wavelength. While UV and blue LEDs have a composition $x = 0.10$ to 0.12 , green nitride LEDs require at least $x = 0.20$. The internal quantum efficiency (IQE) of LEDs with $x = 0.10$ is estimated at $\sim 35\%$, but at $x = 0.20$ the IQE falls to only $\sim 5\%$.



This decay in IQE with higher indium fraction x is not presently understood. Thus, as discussed in the technology roadmap "Light Emitting Diodes for General Illumination" [1], one of the key scientific issues for improving nitride LED materials is to understand and control the incorporation and spatial distribution of indium during growth of $\text{In}_x\text{Ga}_{1-x}\text{N}$ films, such that light emission is enhanced. With this goal in mind, the focus of this project is to understand indium incorporation during the synthesis of $\text{In}_x\text{Ga}_{1-x}\text{N}$ by MOCVD.

Although MOCVD is the best deposition process for production of nitride LED devices, the MOCVD growth process for $\text{In}_x\text{Ga}_{1-x}\text{N}$ displays complex behavior. Growth rates are typically less than the desired transport-limited growth rate, and much more temperature dependent than expected. Indium fraction x is also very sensitive to processing conditions, being highly temperature and growth rate dependent, and not a simple function of gas-phase composition. The $\text{In}_x\text{Ga}_{1-x}\text{N}$ quantum wells must be grown at much lower temperatures than other layers in the device structure so as to achieve reasonable indium incorporation. In addition, while the rest of the device is typically grown in an H_2 ambient, the $\text{In}_x\text{Ga}_{1-x}\text{N}$ must be grown in N_2 , because it is very difficult to incorporate indium into the film in an H_2 ambient [2]. The mechanisms underlying these empirically determined behaviors have not yet been determined. The use of such growth conditions (lower temperatures and N_2 carrier gas) is known to produce lower crystal quality, higher impurity levels, and rougher surfaces in GaN growth. These effects could be responsible for the lower IQE of high x $\text{In}_x\text{Ga}_{1-x}\text{N}$ quantum wells. Additionally, the strain state of the growing layers is expected to have strong impact on the spatial distribution of indium incorporation. Indium segregation, driven either by spinodal decomposition or by the so-called composition-pulling effect, is poorly understood. There are several reports that InN may form clusters or nano-regions in the quantum well [3], and that this effect is enhanced for high indium fraction. This phase separation has been cited as a significant factor determining IQE [1], but a quantitative understanding and control is lacking.

Clearly, a better characterization, understanding, and optimization of $\text{In}_x\text{Ga}_{1-x}\text{N}$ growth conditions could be key to improving device performance. Most knowledge about the MOCVD process is obtained by post-growth analysis of deposited films, because of the difficulty in characterizing the growing film surface directly in the near-atmospheric-pressure, reactive MOCVD environment. The need for improved *in-situ* diagnostics has been recognized [1]. X-ray techniques offer one of the only possibilities for *in-situ* measurements of atomic-scale structure in the MOCVD environment. We have pioneered the use of synchrotron x-ray scattering to observe surface structure and growth modes during MOCVD growth of materials such as GaN and PbTiO_3 . Our unique facility employs high brilliance x-rays to penetrate the quartz walls of a MOCVD chamber, allowing the observation of atomic-scale surface structure during growth in real time. A schematic of the MOCVD/x-ray chamber is shown in Fig. 2. Examples of results achieved from *in-situ* studies of GaN growth are determination of the equilibrium surface structure [4], mapping of the homoepitaxial growth mode as a function temperature and growth rate [5], and observing the effect of silicon on the growth mode [6]. In this project we are expanding the capabilities of this facility by adding the apparatus needed for MOCVD of $\text{In}_x\text{Ga}_{1-x}\text{N}$ alloys, and for additional x-ray measurements such as grazing-incidence fluorescence and specular reflectivity to monitor surface and film composition and strain. We will explore the first application of *in situ* x-ray techniques to the problem of $\text{In}_x\text{Ga}_{1-x}\text{N}$ alloy growth.

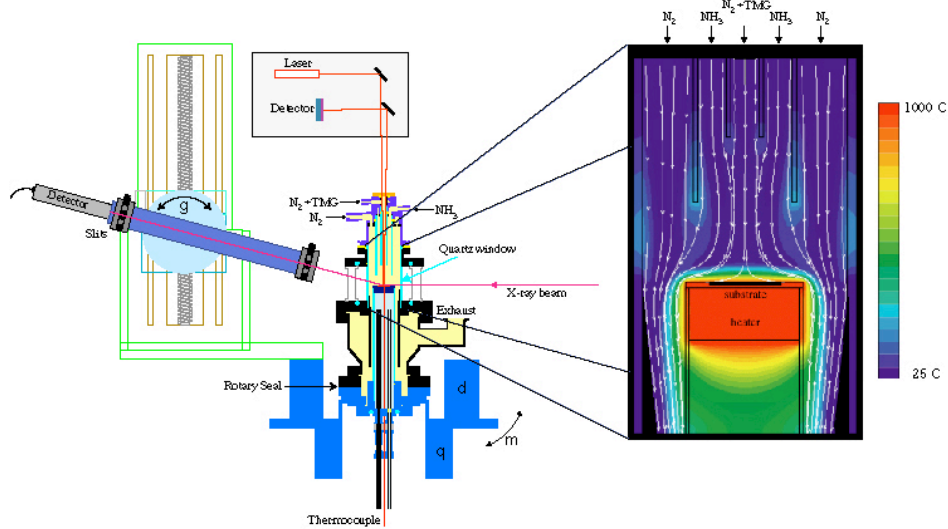


Fig. 2: Schematic of vertical flow nitride MOCVD chamber mounted on a diffractometer for *in-situ* synchrotron studies at beamline 12-ID-D of the Advanced Photon Source.

Recent Progress

This project is currently in an exploratory phase. In the past few months we have successfully grown high-quality $\text{In}_x\text{Ga}_{1-x}\text{N}$ films in the *in situ* x-ray facility, and have performed initial x-ray studies of surface structure and composition using x-ray reflectivity and fluorescence.

Some of our initial studies have focused on simply dosing the GaN surface with indium. Because InN is relatively volatile in the MOCVD environment, growth does not occur when Ga is not supplied. We have found that we can conveniently determine the effective indium vapor pressure at the surface by observing the point at which elemental indium begins to condense, as indium precursor (TMI) flow is increased. Indium condensation produces a continuing increase in the In Ka x-ray fluorescence signal. The change is reversible when TMI flow is reduced, indicating that the liquid indium evaporates. We have mapped the condensation boundary as a function of vapor flows, vapor composition, and substrate temperature. We have also found that both x-ray fluorescence and reflectivity are sensitive to sub-monolayer coverages of indium on the surface. This has allowed us to map the indium surface coverage at precursor flows below the condensation boundary, as a function of vapor composition and substrate temperature. Both the condensation boundary and surface coverage depend sensitively on the hydrogen content of the vapor. Analysis of these effects is underway.

These initial results give us confidence that *in-situ* x-ray techniques can provide key insights into the atomic scale mechanisms of $\text{In}_x\text{Ga}_{1-x}\text{N}$ synthesis by MOCVD.

Future Plans

Indium incorporation: A key issue is to understand the detailed mechanisms by which In incorporates into a growing films, and synthesize this knowledge to establish an optimum MOCVD process window for the growth of high-quality, high x $\text{In}_x\text{Ga}_{1-x}\text{N}$ films. Indium incorporation efficiency into the film is typically very low, requiring vapor phase In/Ga

ratios much larger than the deposited film composition. By investigating the dependence of film composition on growth conditions, we will be able to understand the factors limiting indium incorporation and potentially design more optimal growth conditions or procedures.

Surface structure and morphology: Knowledge of the surface structure is critical to understanding thin film growth. We will be able to use x-ray scattering to determine if a reconstruction or a wetting layer is present, to determine step structure *in situ* during growth, and to explore the effects of high indium fraction.

Growth mode and surface kinetics: By observing surface scattering in real time during growth, we can determine the growth mode (e.g. step flow, island nucleation and coalescence, or 3-dimensional). Indium may be acting as a surfactant during growth since smooth layers often can be achieved by flowing the indium precursor into the chamber. Real-time studies of island coalescence and surface reconstruction formation following growth will give key insight to the surface mobility and kinetics.

Vapor phase: Even very small amounts of H₂ (e.g. 2% of the carrier gas) are known to severely limit the indium fraction that can be achieved [2]. This is very puzzling, since even without H₂ carrier gas, the chemistry of the MOCVD process inherently creates significant atomic hydrogen through the decomposition of both organo-metallics and ammonia. We can determine the origin of this phenomenon by observing the effects of H₂ on the surface structure and growth modes.

Composition inhomogeneities: Indium-rich clusters have been cited as a significant factor determining IQE, and considerable effort has been made to study this important issue. Evidence of nanocluster-induced luminescence in In_xGa_{1-x}N films has been observed [3,7,8]. X-ray diffraction studies have shown multiple peaks indicating regions of different lattice parameter consistent with different compositions [9-11]. TEM and AFM images have revealed In-rich regions having dimensions of 3-100 nm [7,8,12,13]. However, it has also been shown that electron-beam damage can be responsible for the formation of these regions in TEM studies [14]. *In-situ* scattering studies with x-rays, which are not expected to affect indium segregation, can clarify whether indium-rich nano-regions are present in as-grown quantum wells.

References:

* Lumileds Lighting is an industrial collaborator on this project.

- [1] "Light Emitting Diodes for General Illumination, a Technology Roadmap (Update 2002), J. Y. Tsao, editor, (<http://www.netl.doe.gov/ssl>).
- [2] E.L. Piner *et al.*, Appl. Phys. Lett. **70**, 461 (1997).
- [3] S. Chichibu *et al.*, Appl. Phys. Lett. **71**, 2346 (1997).
- [4] A. Munkholm *et al.*, Phys. Rev. Lett. **83**, 741 (1999).
- [5] G. B. Stephenson *et al.*, Appl. Phys. Lett. **74**, 3326 (1999).
- [6] A. Munkholm *et al.*, Appl. Phys. Lett. **77**, 1629 (2000).
- [7] L. Nistor *et al.*, Appl. Phys. Lett. **77**, 507 (2000).
- [8] H. J. Chang *et al.*, Appl. Phys. Lett. **86**, 021911 (2005).
- [9] S.W. Feng *et al.*, Appl. Phys. Lett. **83**, 3906 (2003).
- [10] N.A. El-Masry *et al.*, Appl. Phys. Lett. **72**, 40 (1998).
- [11] D. Doppalapudi *et al.*, J. Appl. Phys. **84**, 1389 (1998).
- [12] M.D. McCluskey *et al.*, Appl. Phys. Lett. **72**, 1730 (1998).
- [13] T. Sugahara *et al.*, Jpn. J. Appl. Phys. **37**, L1195 (1998).
- [14] T.M. Smeeton, *et al.*, Appl. Phys. Lett. **83**, 5419 (2003).

Luminescence, Structure, and Growth of Wide-Bandgap InGaN Semiconductors

S. R. Lee, D. D. Koleske, S. R. Kurtz, R. J. Kaplar, M. H. Crawford, D. M. Follstaedt, and A. J. Fischer
Email contact: srlee@sandia.gov

Sandia National Laboratories, Albuquerque, NM 87185-0601

Program Scope

Wurtzite-structure III-nitride alloys of InN, GaN, and AlN exhibit unusual optoelectronic and structural properties unlike those of well-known cubic-structure alloys such as SiGe, InGaAs, and InGaP. For example, the InGaN alloys span an unprecedented range of direct bandgaps that reach from the infrared (InN), to the visible (InGaN), upwards into the ultraviolet (AlN). These wide-bandgap alloys enable diverse new technologies important to solid-state lighting, remote sensing, and perhaps even quantum computing. Yet, the high lattice mismatch, the immiscibility, and the widely varying thermal stability of the III-nitride alloys make their synthesis almost as challenging as their promise.

Consequently, as-grown III-nitride materials often contain extended defects like dislocations or V-defects, as well as various point defects or impurity complexes, not to mention possible carrier-localizing compositional inhomogeneities -- the resulting complex microstructure alters the underlying intrinsic properties of these materials. These intrinsic properties are in themselves distinctive. For example, the wurtzite structure of the III-nitrides produces enormous piezoelectric fields that fundamentally alter bandstructure via the quantum-confined Stark effect (QCSE). Compared to cubic alloys, the wurtzite structure of the III-nitrides also alters both the elastic properties and the dislocation slip systems available for strain relaxation.

Against this remarkable backdrop, we seek improved understanding of the luminescence mechanisms that operate in InGaN alloys. Our approach combines complementary optical and structural characterization studies with unique experimental designs based on novel heterostructures and tailored materials growth. This approach attempts to isolate specific processes, structures, or defects in order to improve our understanding of the mechanisms that link epitaxial growth, materials microstructure, and luminescence pathways in these alloys. These studies help to provide the fundamental knowledge needed to make energy-efficient solid-state white lighting a practical reality. Such a reality could ultimately reduce American energy expenditures for lighting by as much as \$30 billion/year.

Recent Progress

Quantum-Confined Stark Effect

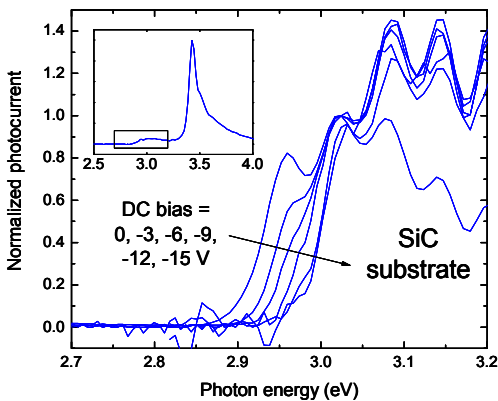


Figure 1. Photocurrent spectra in the vicinity of the SQW absorption edge measured versus p-n junction bias voltage. Note the blue-shift that occurs as negative bias lowers the QCSE.

In several previous works, the measured Stark shifts due to the QCSE in InGaN single quantum wells (SQWs) grown on the basal plane of GaN have been found to be smaller than the theoretical values expected for coherently strained QWs; subsequently inferred InGaN/GaN QW polarization fields are consequently too small as well. In this study, we measure the QCSE in modulation-doped, InGaN/GaN SQW LEDs. The well-behaved capacitance-voltage characteristics of these devices allow us to unambiguously and independently determine the applied field with bias. With this analysis, we can completely decouple the Stark shift measurements from the QW polarization field measurements. In contrast with previous work where these effects are not independently characterized, we find that the applied field needed to cancel the opposing QW polarization field at near-flatband

conditions approaches the theoretically expected value; nevertheless, the separately measured Stark shift remains much too small as in previous work. These new results lead us to propose a localized-hole picture of the InGaN QW that reconciles the anomalously reduced Stark shift seen in the presence of the theoretically expected QW polarization field.

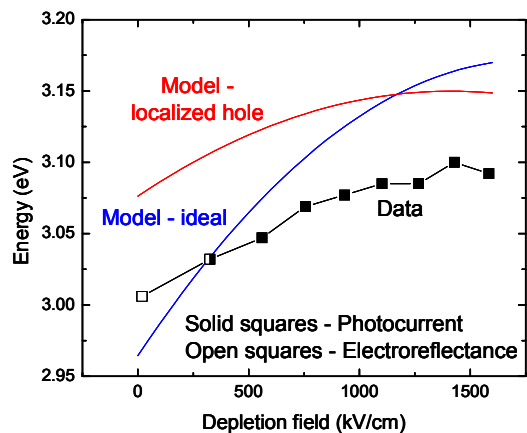


Figure 2. Energy of the absorption edge versus the diode depletion field at the SQW. Solid and open squares indicate experimental points obtained from photocurrent and contacted electroreflectance, respectively. Smooth curves indicate the expected Stark-shift calculated using Schrödinger-Poisson modeling techniques.

Stark-shifts were $\approx 50\%$ less than predicted by theory. To reconcile these results, we modeled the proposed localized-hole picture for InGaN QWs. As shown in Fig. 2, hole localization is consistent with the reduced blue-shift that we measure; moreover, hole localization does not alter the QW polarization field or the applied field required to achieve flatband. The success of this model indicates that electron-hole wave-function overlap in InGaN QWs may be larger than previously thought; thus, improvements in brightness for InGaN QWs grown on non-polar substrates may be less than expected.

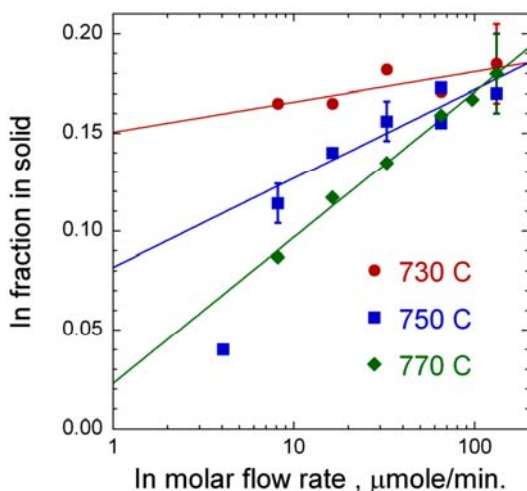


Figure 3. Solid-phase InGaN composition vs. TMIn flow rate. The gas-phase composition is held constant at $\text{In}/(\text{In}+\text{Ga})=0.4$.

In these experiments, $\text{In}_x\text{Ga}_{1-x}\text{N}$ SQWs are embedded in the n-side of GaN p^+n junctions that were grown by metal-organic chemical vapor deposition on sapphire ($x \approx 0.11$) and SiC ($x \approx 0.14$) substrates. In addition, we use a Si modulation doping layer that is well removed (25 nm) from the SQW. Capacitance-voltage (C-V) measurements of the electron density profile in these structures reveal a sharp peak associated with charge storage in the SQW, with a total QW charge consistent with calculated values. The applied depletion-layer field at the SQW was determined by integrating the C-V charge profile. Low-temperature (77 K) photocurrent and electroreflectance spectra were measured versus the applied electric field. As seen in Fig. 1, SQW features were well resolved and displayed a blue-shift in reverse-bias due to the QCSE.

Using a Schrödinger-Poisson model, the theoretical QCSE and screened polarization field were calculated for comparison with experiments. In the more robust sample on sapphire, where the calculated polarization field at flatband was 1.9 MV/cm, a reverse-bias applied field of 1.6 MV/cm was measured. Although the applied field approached the calculated flatband value, the observed

InGaN Materials Growth and Characterization

Initial materials growth work has focused on the successful installation of a new Veeco D-125 MOCVD reactor and subsequent optimization of this reactor to grow state-of-the-art InGaN/GaN heterostructures in support of fundamental studies of luminescence. Optimization studies have examined the influence of growth parameters such as temperature, pressure, growth rate, precursor flow, and carrier-gas flow on both indium incorporation and attendant materials defects. Optical and structural characterization of these epitaxial layers was performed using photoluminescence spectroscopy (PL), electroluminescence quick tests, x-ray diffraction (XRD), atomic-force microscopy, and transmission electron microscopy (TEM). These studies have led to Sandia's first multi-milliwatt blue LEDs and Sandia's first green LEDs emitting at 525 nm.

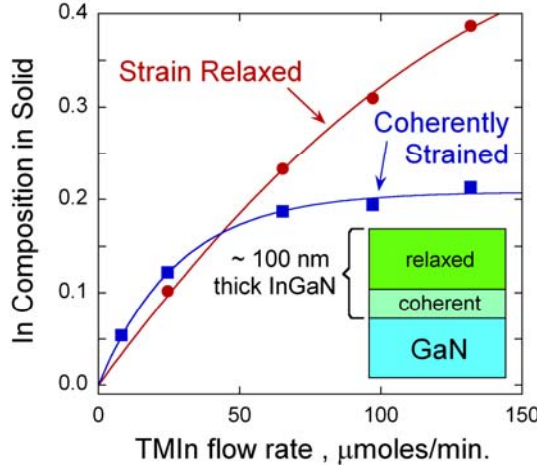


Figure 4. XRD measurements of the composition of 100-nm-thick InGaN films grown on GaN at 760 °C. Initially coherent $\text{In}_x\text{Ga}_{1-x}\text{N}$ films are limited to $x=0.20$. Strain relaxation occurs as the film grows thicker yielding a second layer with higher In content.

flow increases. As previously seen in Fig. 3, the solid-phase composition of thin, coherent InGaN layers is again limited to $x \approx 0.2$; however, when these layers are grown much thicker so that strain relaxation occurs, the composition almost doubles to $x \approx 0.4$. Clearly, the coherency strain fundamentally limits indium incorporation when InGaN alloys grow pseudomorphically on GaN.

Initial cross-sectional TEM images of thin InGaN MQWs grown on GaN show coherent quantum wells that are laterally uniform in thickness. Imaging with $g = (0004)$ or (0002) diffraction vectors often produces contrast that varies from one side of the image to the other, indicating that contrast is very sensitive to the exact specimen orientation. High magnification imaging shows nanometer-scale contrast variations along the quantum wells; however, material outside the quantum wells shows variations as well, apparently due to specimen roughness. Thus the surface roughness of our present specimens obscures any similar variations in contrast due to fluctuations in In content within the quantum wells.

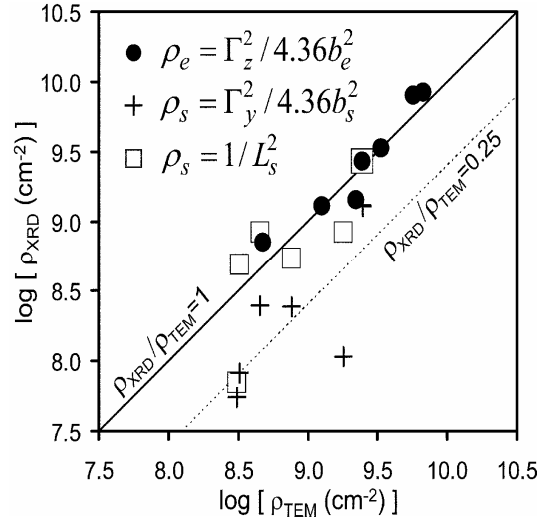


Figure 5. Comparison of threading-dislocation densities measured by XRD (ρ_{XRD}) to those measured by TEM (ρ_{TEM}). Various GaN, AlGaIn, and AlN epilayers are compared.

These growth studies confirm that temperature, growth rate, and coherency strain strongly influence the composition attained during InGaN epitaxy on GaN. For example, Fig. 3 shows the $\text{In}_x\text{Ga}_{1-x}\text{N}$ alloy composition vs the trimethylindium (TMIn) flow rate for a fixed gas-phase composition of 0.4. Since the growth rate is approximately proportion to the TMIn flow rate when the gas-phase composition is held constant, the figure in effect shows that the solid-phase composition increases with growth rate. This growth-rate dependence weakens at lower growth temperatures; moreover, lower temperatures also produce higher indium compositions. In all cases shown, the solid-phase composition is limited to $x < 0.2$, which is well below the gas-phase composition.

Additional experiments show that this $x \approx 0.2$ composition limit for $\text{In}_x\text{Ga}_{1-x}\text{N}$ growth on GaN arises from coherency strain. Figure 4 again shows $\text{In}_x\text{Ga}_{1-x}\text{N}$ composition vs TMIn flow, but now the trimethylgallium flow is held constant such that a range of gas-phase compositions (from 0.08 to 0.58) are probed as the TMIn

XRD Studies of Threading-Dislocation Density

We have also developed a new reciprocal-space model describing the (hkl) -dependence of the broadened Bragg peakwidths produced by x-ray diffraction from a dislocated epilayer. Comparisons of this model to experiments show that it accurately describes the peakwidths of 16 different Bragg reflections in the $[010]$ zone of both GaN and AlN heterolayers. Using lattice-distortion parameters determined by fitting the model to selected reflections, we estimate threading-dislocation densities for seven different GaN and AlGaIn samples and find improved agreement with transmission electron microscopy measurements. As seen in Fig. 5, the accuracy of this approach depends on both the dislocation type and the formulation used to extract the dislocation density from the fitted lattice distortions. Rapid, nondestructive feedback provided by this XRD analysis method has allowed us to efficiently develop GaN pseudo-

substrates with controlled threading-dislocation densities spanning a wide range from 4×10^8 to 1×10^{11} cm^{-2} . These tailored substrates will be used in future studies of the impact of threading dislocations.

Future Plans

The focus of selected near-term plans are summarized below; further details, as well as our longer-term research plans, will appear in our upcoming FWP submission to DOE/BES.

The influence of growth temperature on the optoelectronic properties of InGaN remains poorly understood because the composition of these alloys is strongly temperature dependent. Resulting temperature-induced composition changes alter key luminescence mechanisms (the QCSE and localization, for instance) thereby masking other important growth-temperature-dependent effects like the incorporation of point-defects and impurities. We will probe these latter effects by developing growth techniques that hold the InGaN/GaN heterostructure design constant even as the growth temperature varies. Similar heterostructures thus grown over a wide range of temperatures will then be optically and structurally characterized in order to isolate the changes in luminescence that specifically result from temperature-dependent defect formation.

The addition of even small concentrations of indium produces a large increase in the luminescence efficiency of GaN. A seemingly related effect occurs when a single heterolayer of relatively dilute $\text{In}_x\text{Ga}_{1-x}\text{N}$ ($x \sim 0.02-0.06$, thickness ~ 100 nm) is inserted between a GaN pseudo-substrate and an overlying InGaN/GaN MQW. In preliminary experiments, we find that the MQW PL intensity increases by up to 8X when this dilute InGaN underlayer is added, even though the basic structure of the MQW remains unchanged. These PL-efficiency enhancements have been variously attributed to indium-induced carrier-localization and defect reduction, but in fact, remain poorly understood. We have begun optical studies of the effects produced by varying the design and the growth conditions of these InGaN underlayers. These will be followed by structural studies that will seek the physical mechanisms responsible for this intriguing improvement in luminescence efficiency.

Finally, while strain relaxation greatly increases indium incorporation into InGaN alloys, we find that defects introduced during relaxation profoundly reduce the resulting InGaN luminescence -- this contrasts with the widespread notion that dislocations are relatively benign in typical wurtzite-structure III-V semiconductors such as InGaN. These divergent observations motivate us to pursue further studies of strain-relaxation processes in InGaN materials with emphasis on complementary optical studies that evaluate the impact of relaxation on luminescence pathways.

DOE Sponsored Publications in 2004-2005

- [1] *Optical and electrical step-recovery study of minority-carrier transport in an InGaN/GaN quantum-well light-emitting diode grown on sapphire*, R. J. Kaplar, S. R. Kurtz, and D. D. Koleske, Appl. Phys. Lett. **85**, 5436 (2004).
- [2] *Characterization of minority-carrier hole transport in nitride-based light-emitting diodes with optical and electrical time-resolved techniques*, R. J. Kaplar, S. R. Kurtz, D. D. Koleske, A. A. Allerman, A. J. Fischer, and M. H. Crawford, Mater. Res. Soc. Symp. Proc. Vol. **831**, E10.9 (2005).
- [3] *Novel optical probes of InGaN/GaN light-emitting diodes: 1. Electroreflectance Stark spectroscopy, and 2. Time-resolved emission*, R. J. Kaplar, S. R. Kurtz, and D. D. Koleske, Phys. Stat. Sol. (c) **2**, 2866 (2005).
- [4] *Effect of threading dislocations on the Bragg peakwidths of GaN, AlGaIn, and AlN heterolayers*, S. R. Lee, A. M. West, A. A. Allerman, K. E. Waldrip, D. M. Follstaedt, P. P. Provencio, D. D. Koleske, and C. R. Abernathy, Appl. Phys. Lett. **86**, 241904 (2005).
- [5] *Analysis of the Quantum-Confined Stark Effect in InGaN Single Quantum Wells*, R. J. Kaplar, S. R. Kurtz, and D. D. Koleske, Appl. Phys. Lett. (submitted 2005).
- [6] *Quantum-Confined Stark Effect and Polarization Field in Single Quantum Well InGaN/GaN LEDs*, R. J. Kaplar, S. R. Kurtz, and D. D. Koleske, Mater. Res. Soc. Symp. Proc., FF32.1 (submitted 2005).

Overcoming Doping Bottlenecks in Semiconductors and Wide-gap Materials

Shengbai Zhang and Su-Huai Wei
National Renewable Energy Laboratory, Golden, CO 80401
shengbai_zhang@nrel.gov

Program Scope

Doping semiconductor is a necessary step in controlling its conduction type and free-carrier concentration. Yet, there often exist strong doping bottlenecks that could severely restrict potential applications of semiconductors, especially the wide-band-gap ones where bipolar doping is almost universally difficult. Recent rapid progress in semiconductor researches has reached a point where these doping limitations can be, and have to be, overcome in order to tune their properties for desirable new functionalities. We have developed an initial theoretical underpinning toward overcome such doping bottlenecks in several important prototypical semiconductors such as p-type zinc oxide, n-type diamond, bipolarly dopable transparent conducting oxides, ultra-highly doped silicon, and isovalent dilute nitride alloys. Doping semiconductors is essential for applications in clean affordable energy generation and in improved energy efficiency, which is vital to our nation's long-term energy security and sustainability, and is hence of significance to the mission of the Department of Energy.

Recent Progress

Silicon is the most studied semiconductor. Yet, ultrahigh doping of silicon is poorly understood. As part of the efforts of developing a systematic non-equilibrium doping theory for semiconductors, we recently examined some recent work on very high hole-concentration in boron-doped silicon.¹ Our study revealed that the ultrahigh solubility of boron in silicon is a result of epitaxial growth. We predicted that by adequately passivating the silicon surfaces during growth, up to atomic % of boron could be incorporated into bulk silicon. We also analyzed the boron ionization processes, finding good agreement with experiment. Ultrahigh doping could enable a number of new applications such as ultrafast switches and ultra-dense device arrays.

Among the wide-gap semiconductors, diamond is special not only because it can sustain extremely harsh conditions but also because diamond can be doped only p-type, in sharp contrast to others where p-type is the doping bottleneck. We have studied codoping of diamond by nitrogen with impurities isovalent to carbon. By a careful design of four silicon atoms plus the nitrogen, we showed that the electron ionization energy of the complex (a tenth of an eV) could be significantly lower than that of isolated nitrogen (more than an eV). This is perhaps the first time that a shallow donor was theoretically demonstrated for diamond.

In recent years, zinc oxide has attracted much attention as an alternative direct wide-gap material after gallium nitride for blue and UV lasers and LEDs, and potentially solid-state lighting. The big hurdle with zinc oxide, however, is that it is very difficult to be doped p-type. Recently, some very puzzling experimental results emerge where it was shown that large group-V atoms such as phosphorous, arsenic, and antimony could be

used as the dopants for p-type conductivity,² potentially better than the size-matched group-V nitrogen. Our study showed that these group-V impurities do not substitute the next column, group-VI oxygen, but rather substituting the group-III zinc as triple donors. The prediction was recently confirmed by emission channeling experiment.³ Interestingly, we predicted that in such samples zinc vacancy acceptors should be spontaneously created, leading to net p-type conductivity. While recent positron experiment is indicative of the correlation between the zinc vacancy and group-V impurities, our work has already spurred a great deal of interests in the research community to understand the deeper physics of doping in highly ionic semiconductors.

Besides the “traditional” bulk materials, more attentions are also paid to the doping and defect physics of nanostructures. Recently, we studied the electronic properties and doping of carbon nanotubes supported on flat semiconductor surfaces. To our surprise, no extrinsic dopant is necessary in order to dope the carbon nanotubes. By using a polar substrate with different crystal orientations, one can engineer either p- or n-type conductivity of the nanotubes with desirable free carrier concentration. The elimination of impurities could greatly simplify the process of fabricating devices out of such nanostructures, as their doping is not always easy. The underlying mechanism, which should enable coherent carrier transport, is also general for other one-dimension systems beyond just the carbon nanotubes.

In another “nano” example, we studied the stability of the DX center in GaAs quantum dots. The formation of the DX centers from shallow donors is an important mechanism for the self-compensation of intended dopants. It was found that the formation energy of the shallow donor increases noticeably with size reduction, whereas that of the DX center does not. As a result, it is energetically more likely for the donor to go through a shallow-to-deep transition, accompanied by a large local lattice distortion. This study reveals one of the challenges that we are facing in terms of doping nanostructures that is how to stabilize the dopants structurally to avoid such shallow-to-deep transitions.

Not only defect and impurity doping can alter the electronic properties of a nanostructure, but also at the nanometer size scale certain defects (stacking faults, in particular) can spontaneously form, leading to new nanostructures never envisioned before. Recently, we predicted that several hundreds or even thousands of silicon atoms would form a novel 20-sided polyhedron with icosahedral symmetry to minimize its free energy. The polyhedrons or dots have optimal *quantized* band structures that are drastically different from those of conventional silicon quantum dots. A subsequent literature search revealed direct relevance of these dots to experiment.⁴ Moreover, a very recent theoretical study⁵ showed that a nano drop of silicon liquid would spontaneously condense into the icosahedral phase that we have predicted instead of the bulk phase.

Future Plans

Non-equilibrium doping for higher carrier concentration will be a focus of our future plan. This requires a comprehensive study of epitaxial growth and associated surface physics in the presence of dopants, the formation of native defects and their interplay with extrinsic impurities, and the finite-temperature effects such as diffusion barriers and the kinetics of cooling. More emphasis will also be placed on nanostructures

and organic semiconductors, as the theory of doping in such systems is at best just starting to emerge.

We will continue our quest of p-type zinc oxide. It is now experimentally established that the incorporation of dopants during epitaxy depends critically on the face of the crystal,⁶ so does the electrical behavior of the doped ZnO films.⁷ Despite of the observations, so far little is known about the atomic structure of the ZnO surfaces. The best STM images for the polar (0001) surfaces are still lack of atomic resolution.⁸ It is difficult to even obtain unipolar films (namely, either Zn- or O-polar, but not multigrains with both polarities).⁹ On the other hand, zinc oxide is one of the few semiconductors with a great flexibility to form rich nanostructures, ranging from simple nanobelts to more complex nanocombs, flowers, tetrapods, and to the recently discovered double helices. Available theory on all of the above (nanostructures) appears naive, simply making use of classic electrostatics.¹⁰ Clearly, our first-principles quantum mechanical study can play a central role in both areas. As we enter the realm of non-equilibrium doping, it is also important to understand kinetic factors other than those associated with the growth front. For instance, several recent studies^{11,12} attributed certain defect complex formation to the effect of thermal cooling when at least one of the defects has small diffusion barrier. These observations offer a new handle to maneuver the dopant concentration and their electrical behaviors beyond the thermodynamic limits.

We will study the interaction between defects and dopants under illumination, which is also important for solid-state lighting. Even in semiconductors as benign as silicon, photoinduced diffusion and subsequent generation of complexes involving dopant can have detrimental effects on the device performance as in the case of solar cells.¹³ Currently, we are investigating such an effect in boron doped silicon. In non-equilibrium doped materials, not surprisingly, photoinduced carrier-type conversion from *p* to *n* is more commonly seen. In p-type zinc oxide, the observed type-conversion usually subsides after the light source is removed. All these observations raise critical issues concerning photoresponse and stability of non-equilibrium doped semiconductors.

In the context of doping nanostructures, there emerges a novel surface transfer doping mechanism, which does not require any impurity inside the host material. A recent example involves surface p-type conductivity of diamond, which has made important technological advances such as field-effect transistors (FTE). The concept is new, and, in our view, could have implications also to other semiconductor nanoparticles. For example, surface doping of carbon nanotubes can also be viewed as a transfer doping. We plan to understand the microscopic origin of the transfer doping in diamond and to establish the concept over a wide range of semiconductor nanostructures. In cases where extrinsic impurities are indeed required, one needs to know how the impurity interacts with surfaces, and to what extent surface segregation will take place. Experimentally, it has been shown that impurity solubility can increase significantly in a nanostructure, for example, copper-doped CdSe could have a Cu concentration as high as 10%,¹⁴ to be many orders of magnitude higher than that of the bulk. It was also observed that doping could alter the crystal structure of a quantum dot to be distinctly different from that of the bulk,¹⁴ just like the stacking faults did to the silicon dots.

References

- (1) J. E. Greene, MRS Bulletin **26**, 777 (2001).
- (2) D. C. Look, Semi. Sci. Technol. **20**, S55 (2005).
- (3) U. Wahl, et al., Phys. Rev. Lett. **95**, 215503 (2005).
- (4) M. Takeguchi, et al., Surf. Sci. **493**, 414 (2001).
- (5) K. Nishio, et al., Phys. Rev. B **72**, 245321 (2005).
- (6) M. Sumiya, et al., Appl. Surf. Sci. **223**, 206 (2004).
- (7) O. Schmidt, et al., Jap. J. Appl. Phys. **44**, 7271 (2005).
- (8) O. Dulub, U. Diebold, and G. Kresse, Phys. Rev. Lett. **90**, 016102 (2003).
- (9) Y. Wang, et al., Appl. Phys. Lett. **87**, 051901 (2005).
- (10) Z. L. Wang, et al., Adv. Funct. Mater. **14**, 943 (2004).
- (11) T. Miyazaki and S. Yamasaki, Appl. Phys. Lett. **86**, 261910 (2005).
- (12) C. G. Van de Walle and J. Neugebauer, J. Appl. Phys. **95**, 3851 (2004).
- (13) J. Schmidt and K. Bothe, Phys. Rev. B **69**, 024107 (2004).
- (14) R. W. Meulenbergh, et al., Nano Lett. **4**, 2277 (2004).

DOE Sponsored Publications in 2003-2005 (A Partial List)

Understanding Ultrahigh Doping: The Case of Boron in Silicon, X. Luo, S. B. Zhang, and S.-H. Wei, Phys. Rev. Lett. **90**, 026103 (2003).

Design of Shallow Donor Levels in Diamond by Isovalent-Donor Coupling, D. Segev and Su-Huai Wei, Phys. Rev. Lett. **91**, 126406 (2003).

Doping by Large Size-Mismatched Impurities: The Microscopic Origin for Arsenic- or Antimony-Doped p-Type Zinc Oxide, S. Limpijumnong, S. B. Zhang, S.-H. Wei, and C. H. Park, Phys. Rev. Lett. **92**, 155504 (2004).

Nanotube Wires on Commensurate InAs Surfaces: Binding Energies, Band Alignments, and Bipolar Doping by the Surfaces, Y.-H. Kim, M. J. Heben, and S. B. Zhang, Phys. Rev. Lett. **92**, 176102 (2004).

First-Principles Prediction of Icosahedral Quantum Dots for Tetravalent Semiconductors, Y. Zhao, Y.-H. Kim, M.-H. Du, and S. B. Zhang, Phys. Rev. Lett. **93**, 015502 (2004).

Hole-Mediated Stabilization of Cubic GaN, G. M. Dalpian and S.-H. Wei, Phys. Rev. Lett. **93**, 216401 (2004).

Stability of the DX-Center in GaAs Quantum Dots, J. B. Li, S. H. Wei, and L. W. Wang, Phys. Rev. Lett. **94**, 185501 (2005).

Evidence for Native-Defect Donors in n-Type ZnO, D. C. Look, G. C. Farlow, P. Reunchan, S. Limpijumnong, S. B. Zhang, K. Nordlund, Phys. Rev. Lett. **95**, 225502 (2005).

Theoretical and Experimental Study of Solid Composition and Ordering in III/V Systems

G.B. Stringfellow, F. Liu, A. Howard, and J. Zhu

Department of Materials Science and Engineering, University of Utah, Salt Lake City,
Utah 84112

Program Scope

The solid composition and microstructure of semiconductor alloys is complex and of great importance for devices such as high efficiency light emitting diodes (LEDs) and cascade solar cells. The most important single alloy for these two applications is the AlGaInP system, grown by organometallic vapor phase epitaxy (OMVPE). Previous work on this DOE-supported project has shown that the addition of surfactants isoelectronic with P (namely Sb and Bi) can be used during epitaxial growth to control the microstructure, in particular ordering and phase separation, and dopant incorporation.

The incorporation of dopants, particularly acceptors, in high bandgap materials has been a major technological hurdle retarding the development of materials, particularly for yellow, green, and blue LEDs. This is believed to be due to the high energy cost of moving the Fermi Level to a position near the valence band edge in high bandgap semiconductors. This leads to compensation. In III/V semiconductor alloys grown by OMVPE, this occurs most commonly by the introduction of hydrogen, forming neutral acceptor-hydrogen complexes.

The use of surfactants to control dopant incorporation in GaInP has major technological implications for LEDs and solar cells. In addition, this research provides insights into the “last frontier” of fundamental understanding of OMVPE, namely the understanding and control of the surface during growth in order to enhance materials properties. Thus, the results of this research will be of direct relevance to the other major alloy system for LED applications, namely AlGaInN.

Recent Progress

Dramatic changes in the incorporation of both dopant and background impurities during the OMVPE growth of GaAs, GaInP, and GaP has been demonstrated by the use of the surfactants Sb and Bi. Since these surfactants are isoelectronic with P, they produce no independent doping. In addition, both are much larger than P; thus, they incorporate very little into the epitaxial layer. Their low vapor pressures enhances their usefulness as surfactants.

Our initial studies indicated that incorporation of the acceptor Zn into GaAs could be increased by a factor of 3 using the surfactant Sb, added as TMSb during OMVPE growth[1]. In the last year the scope of the study has been increased to include the higher bandgap materials GaInP and GaP. This has given a clearer idea of the mechanism responsible for the increased doping.

In GaInP both Sb and Bi were observed to increase Zn doping[2]. In this case, SIMS profiles of 3 layer structures, with surfactant present only during growth of the middle layer, clearly showed an increase in the H incorporation induced by the surfactant. Repeating the earlier GaAs experiments showed that no H was detected either with or without Sb or Bi in the system.

Experiments in the GaP system were more dramatic. For growth at 650 C, the presence of Sb gave a 10-fold increase in Zn doping to 10^{20} cm^{-3} , the highest Zn doping ever reported for GaP[3]. Unfortunately, not all of the Zn is electrically active, indicating that some Zn is incorporated onto interstitial sites at these high Zn doping levels. The H concentration was also clearly observed to increase when either Sb or Bi was added during growth. The H:Zn ratios were typically on the order of 1:5.

The mechanism responsible for the increased Zn incorporation induced by surfactant Sb or Bi was explored by the use of first principles calculations. One possible mechanism for the increase in Zn incorporation induced by addition of surfactant to the system is related to the observed increase in H incorporation. If Zn is incorporated as a neutral Zn-H complex, the solubility will be much higher, for thermodynamic reasons: it requires a large amount of energy to push the Fermi Level down to a position near the valence band edge in high bandgap materials[4]. LDA calculations of the total energy performed using the VASP code with ultrasoft pseudo-potentials, indicated that the concentration of H on the reconstructed surface is actually reduced when the normal (for OMVPE growth) surface termination is replaced by Sb. This is simply due to the much weaker Sb-H (as compared to P-H) bonds. Thus, unless the H concentration is increased at the step edge, where Zn incorporation occurs, it appears unlikely that increased incorporation of Zn-H complexes accounts for the surfactant effect on Zn incorporation. A second set of calculations compared the incorporation of Zn from the vapor onto a Ga site just below the surface for surfaces terminated by P dimers with a surface terminated by Sb dimers. The result was a remarkable 1000 meV reduction in the energy of the Zn atom beneath an Sb terminated surface. This would give a large thermodynamic advantage for Zn incorporation provided by the surfactant Sb, even at the growth temperature.

For growth at 775 C, the same favorable effect of Sb on Zn incorporation was observed. In addition, a huge (>100 X) reduction in the concentration of the background acceptor carbon was observed. A similar decrease was observed for Bi. This is a second beneficial effect of surfactant Sb and Bi, since C is a potentially harmful background impurity. The mechanism for the decreased C incorporation is likely to be a simple result of the decrease in the binding energy of CH_3 radicals to the Sb (or Bi) terminated surface.

The residual impurities S and Si, due to autodoping from the substrates, were also detected by SIMS analysis of the GaP structures. The concentrations of both of these impurities were also significantly decreased when either Sb or Bi was added to the system during growth. Perhaps more significantly, the concentration of residual oxygen in GaInP was observed to decrease when either Sb or Bi was added to the system. This is an additional beneficial effect of the addition of one of these surfactants to the system during OMVPE growth.

Future Plans

In the immediate future the incorporation of two other acceptor dopants, Mg and Cd, will be studied, in particular the effects of Sb and Bi on the distribution coefficients. These two acceptors were chosen because Mg, Zn, and Cd are all from the same column of the periodic table and Mg is smaller than Zn while Cd is larger. It is believed that the advantage in Zn incorporation energy provided by Sb and Bi is related to strain energy considerations. Thus, the surfactant effects would be expected to be significantly different for Mg and Cd. Furthermore, Mg is the commonly used acceptor in LED applications for both AlGaInP and AlGaInN. The Mg and Cd incorporation will be studied experimentally, using the established technique of SIMS analysis of 3 layer structures. In addition the total energy calculations will be performed for both Mg and Cd.

Further calculations will be used in additional efforts to probe the effects of surfactant Sb on Zn incorporation: 1) The effect of temperature (entropy) on the concentration of H on the surface and 2) The effect of removing surface dimers by hydrogen “passivation” of the surface. These calculations will be necessary in order to validate the proposed mechanism for the surfactant effect on acceptor incorporation. Both calculations require a major effort.

The experimental and theoretical methodologies established for the acceptor impurities will be expanded to include donor impurities.

A more ambitious goal of the computational part of the project will be the addition of surface steps. Of course, dopant incorporation during growth is expected to occur at surface steps. To date, we have not addressed the configuration and bonding of the atoms at the step edge. Such problems produce formidable obstacles for first principles calculations, because they are computationally very demanding. Although it is not practical to carry out extensive first-principles step calculations, we plan to perform trial calculations aided by an educated guess of the possible step configurations. Our goal is to obtain the typical values of energy difference between H adsorption at a step and on the singular surface for given surfactants. This information can then be used as input into phenomenological models and Monte-Carlo simulations to investigate the role of surface steps. The goal of these calculations will be the determination of the effect of the surfactants Sb and Bi on the concentration of H adsorbed at both A and B type steps during OMVPE growth.

References

1. J.K. Shurtleff, S.W. Jun, and G.B. Stringfellow, *Appl. Phys. Lett.* 78, 3038 (2001).
2. D.C. Chapman, A.D. Howard, and G.B. Stringfellow, *J. Crystal Growth* (in press).
3. A.D. Howard, D.C. Chapman, and G.B. Stringfellow, *J. Appl. Phys.* (submitted).

4. W. Shockley and J.L. Moll, Phys. Rev. 119, 1480 (1960).

DOE Sponsored Publications in 2004-2005

Effects of surfactants Sb and Bi on the incorporation of Zinc and Carbon in III/V materials grown by Organometallic Vapor Phase Epitaxy, (with A.D. Howard and D.C. Chapman), J. Appl. Phys. (submitted)

Zn enhancement during surfactant mediated growth of GaInP and GaP (with D.C. Chapman and A.D. Howard), J. Crystal Growth (in press).

Nitrogen surfactant effects in GaInP (with D.C. Chapman, A. Bell, F. Ponce, J. Lee, T. Seong, S. Shibakawa, and A. Sasaki), J. Appl. Phys. 96, 7229 (2004).

Te surfactant effects on the morphology of patterned (001) GaAs homoepitaxy, (with R.R. Wixom and L.W. Rieth), J. Crystal Growth 269,276 (2004).

Thermodynamics of Modern Epitaxial Growth Processes, in Crystal Growth – From Fundamentals to Technology, ed. G. Muller, J.J. Metois, and P. Rudolph (Elsevier, Amsterdam, 2004) pp. 1-26.

Effects of Surfactants N and Br on Ordering in GaInP (with D.C. Chapman, A.D. Howard, L. Rieth, R.R. Wixom, and G.B. Stringfellow), Materials Research Society Proceedings Vol. 794, p. 291 (2004).

Sb surfactant effects on homeo-epitaxy of GaAs (001) patterned substrates (with R.R. Wixom and L.W. Rieth), J. Crystal Growth 265, 367 (2004).

The Use of Nitrogen to disorder GaInP (with D.C. Chapman, L.W. Rieth, J.W. Lee, and T.Y. Seong), J. Appl. Phys. 95, 6145 (2004).

Effects of Br and Cl on Organometallic Vapor Phase Epitaxial Growth and Ordering in GaInP (with A.D. Howard, L. Rieth, D.C. Chapman, R.R. Wixom, B.J. Kim, and T.Y. Seong) J. Appl. Phys. 95, 2319 (2004).

Development and Current Status of OMVPE, J. Crystal Growth 264, 620 (2004).

Many Body Effects in Nanotube Fluorescence Spectroscopy

E.J. Mele and C.L. Kane
mele@physics.upenn.edu

Department of Physics, University of Pennsylvania, Philadelphia PA 19104

Program Scope

Fluorescence excitation spectroscopy from suspensions of single wall carbon nanotube probes their intrinsic electronic excitations with unprecedented resolution, focusing attention on the fundamental role of electron electron interactions in the excited state properties. Prior to this work, the most widely accepted theoretical models for carbon nanotubes posited that their electronic properties are controlled mainly by the periodicity of their wrapped lattice structures. Experimental work now provides a database of the fundamental first and second subband excitations for over thirty different wrapped semiconducting tube structures and challenges this point of view. The band theoretic description of the excitations of these systems fails quantitatively and in some cases even qualitatively. The goals of our work are: (a) to use the existing experimental database to extract the rules governing the dependence of optical excitation energies on tube structure, radius, chirality, strain and (b) to extend the theoretical models to include interaction effects and account for these rules.

Progress

By examining the scaling of the observed first and second subband transition energies with tube radius and chirality, we find that the breakdown of the independent particle model is manifest by the failure of three of its fundamental scaling predictions. These are referred to as (a) the “ratio problem”, (b) the “blue shift problem” and (c) the “deviations problem.” The most important of these is the “blue shift” problem, namely the observed excitation energies are systematically shifted to the blue with respect to the analogous interband transitions in graphene, and remarkably these energies exhibit a nonlinear dependence on inverse tube radius that persists into the large tube-radius limit. This implies that the quasiparticle dispersion relation remains nonlinear in the large wavelength limit, contradicting the assumption that the effective dispersion relation is described by the linear solid state “Dirac cone” in graphene.

We discovered that these difficulties could be largely accounted for by extending the theory to include the interactions through the exchange self energy which are anomalous in two dimensional graphene because of its gapless excitation spectrum. Indeed we find that the quasiparticle exchange self energy inherits a nonanalytic term, varying with momentum according to $E(q) = \hbar v_F q (1 + (g/4) \log(\Lambda/q))$ instead of as proportional to q as one might have naively expected. This signals a marginal breakdown of the Fermi liquid description of the quasiparticle dispersion relation.

Remarkably, we find that this nonanalytic self energy provides an extremely good description of the scaling of the observed excitation energies with inverse tube radius.

The success of this model is problematic because since it neglects the excitonic binding of the electron to the hole in the optically excited states. This effect is expected to be large because of the low dimensionality of the nanotube. Precisely because it is a one dimensional structure, the long distance attractive electron-hole interaction is ineffectively screened and the exciton binding energy is expected to be large. Indeed most theoretical estimates (including ours) suggest that the excitonic binding energy remains a substantial fraction, perhaps one-third, of the quasiparticle bandgap.

We found that large effects of the electron hole binding energy are largely offset by a correspondingly large positive band gap renormalization from the Coulomb interaction. Thus the strongest effect of the Coulomb interaction enter with opposite signs, and nearly cancel. This cancellation provides access to the finite momentum structure of the quasiparticle self energy. These ideas were refined and quantified by a solution of the Bethe Salpeter equation for the particle hole excitation spectrum in the static screening approximation.

Future Plans

The existence of strong effects of the electronic excitations has important implications for the photophysics of carbon nanotubes. Indeed the fluorescence yields for nanotubes are known to be very small (of order 10^{-4}), a situation which may be controlled by the thermalization of photoexcitations into intrinsic optically forbidden excitonic states. The graphene derived nanotubes are particularly susceptible to this since: (a) intervalley scattering provides a spectrum of optically forbidden low energy singlet states and (b) the strong interactions suggest that the long lived excited states may be triplet states populated by intersystem conversion following a pump in to the optically allowed band.

Theoretical work exploring these possibilities is at a primitive stage of development. The goal of our work is to develop controlled theoretical models that will provide access to the many body excitations, allowing us to understand their dependence on tube radius, chirality, applied static electric and magnetic fields, and possibly also on doping density.

Publications

“Topological Order and the Quantum Spin Hall Effect” Physical Review Letters 95, 146802 (2005) (with C.L. Kane)

“Quantum Spin Hall Effect in Graphene” Physical Review Letters 95, 226801 (2005) (with C.L. Kane)

“Continuum Theory for Nanotube Piezoelectricity” Physical Review Letters 95, 116803 (2005) (with P.J. Michalski and Na Sai)

“Many Body Effects in Carbon Nanotube Fluorescence Spectroscopy” Solid State Communications 135, 527 (2005) (with C.L. Kane)

“Electron Interactions and Scaling Relations for Optical Excitations in Carbon Nanotubes” Physical Review Letters 93, 197402 (2004) (with C.L. Kane)

“Electron Interactions, Excitons and Carbon Nanotube Fluorescence Spectroscopy” Proceedings of the XVIII-th Winterschool on the Electronic Properties of Novel Materials (IWEPNM)” AIP Proceedings 723, 402 (2004)

“Microscopic Theory for Nanotube Piezoelectricity” Physical Review B 241405 (2003) (Rapid Communications) (with Na Sai)

“Ratio Problem in Carbon Nanotube Fluorescence Spectroscopy” Physical Review Letters 90, 207401 (2003)

“Probing the Electronic Structure of Nanotube Peapods with Scanning Tunneling Spectroscopy” Applied Physics A 76, 469 (2003)

“Excitons in Nanotube Fluorescence Spectroscopy” in Proceedings of the XVII-th Winterschool on the Electronic Properties of Novel Materials (IWEPNM)” AIP Proceedings Volume 685 (J. Fink, H. Kuzmany, M. Mehring and S. Roth, editors) p 460-464 (2003)

“Theory of Scanning Tunneling Spectroscopy of Fullerene Peapods” Physical Review B 66, 235423 (2002) (with C.L. Kane, A.T. Johnson, D.E. Luzzi, B.W. Smith, D.J. Hornbaker and A. Yazdani)

“Electric Polarization of Heteropolar Nanotubes as a Geometric Phase” Physical Review Letters 88, 056803 (2002) (with P. Kral)

“Mapping the Electronic States of Fullerene Peapods” Science 295, 828-831 (2002) (with D.J. Hornbaker, S.-J. Kahng, S. Misra, B.W. Smith, A.T. Johnson, D.E. Luzzi and A. Yazdani) (Cover Story in Science Magazine, February 4, 2002)

Solid-State MAS NMR Studies of Supramolecular Zinc Chelates and ZnO Nanorods

Linda Sapochak, Li-Qiong Wang, Kim Ferris, Chunhua Yao, Greg Exarhos

Program Scope

The ability to assemble materials with well-defined structure (i.e., pore/channel size, geometry, dimensionality), function (i.e., sensing, catalysis, charge transporting), and/or property (i.e., magnetic, optical) has been the impetus behind development of new nanostructured materials and synthetic strategies. This program uses a combination of unique material synthetic approaches, characterization techniques (solid-state NMR techniques) and theoretical modeling to establish an understanding of structure and structure evolution of advanced functional materials. The targeted goals of the project are to ultimately control and manipulate self assembly of nanostructured materials with tuneable properties. Some of the current materials systems under investigation include organic electroluminescent metal chelates and inorganic metal oxide nanostructures. A key component of the program is in the detailed structural characterization leading to a more fundamental understanding of bulk properties.

Recent Progress

We previously investigated the oligomeric purity and stability of the organic electroluminescent metal chelate, zinc (8-quinolinolato) (Znq_2). X-ray diffraction studies showed that the metal chelate formed a tetrameric structure composed of a chain of three Zn_2O_2 four-membered rings via oxo-bridging of the 8-quinolinolato ligand.^{1,2} Methylated derivatives of Znq_2 showed enhanced organic light-emitting device (OLED) properties,³ but material structure characterization had been elusive. Through a combination of theoretical modeling of the oligomerization energetics leading to supramolecular structures and experimental size exclusion chromatography we showed that all methylated derivatives likely form supramolecular structures.⁴ However, solid state characterization of these structures was still lacking.

A combination of ^{13}C CP MAS solid state NMR and DGAIO-SCFF calculations was then used to characterize the Zn(II) (8-quinolinolato) tetrameric solid state structure.⁵ Crystallographic splitting of the carbon resonances in the solid state were correlated to different ligand environments defined by how the phenolato oxygens were bonded (bridging vs. nonbridging) to the two crystallographically distinct Zn ions in the tetrameric structure. These assignments were supported by the ^{13}C spectral simulation for the known Znq_2 tetrameric structure (see Fig. 1). Structural information was unavailable for the methylated Znq_2 derivatives, so ab initio Hartree-Fock computations (GIAO) were performed for the series of methylated ligands and proposed Zn tetrameric structures. By focusing on ^{13}C chemical shifts and their statistical correlations, we were able to extend the utility of these methods to larger sized systems, even without invoking molecular symmetry. As the eventual tetrameric target structures are considerably sized for extensive basis set Hartree-Fock methods, smaller basis set results were explored for correlation for the ligand chemical shifts. Comparisons of the simulated spectra of the

individual ligands with experimental results gave strong linear correlation coefficients (>0.99). Similar strong linear correlation coefficients (>0.96) were obtained for the methylated Znq_2 tetrameric derivatives using gas phase optimized tetrameric structures and allowed us to: 1) differentiate between the size of the oligomeric structures, and 2) be predictive on the ligand effects on the local and extended structure.

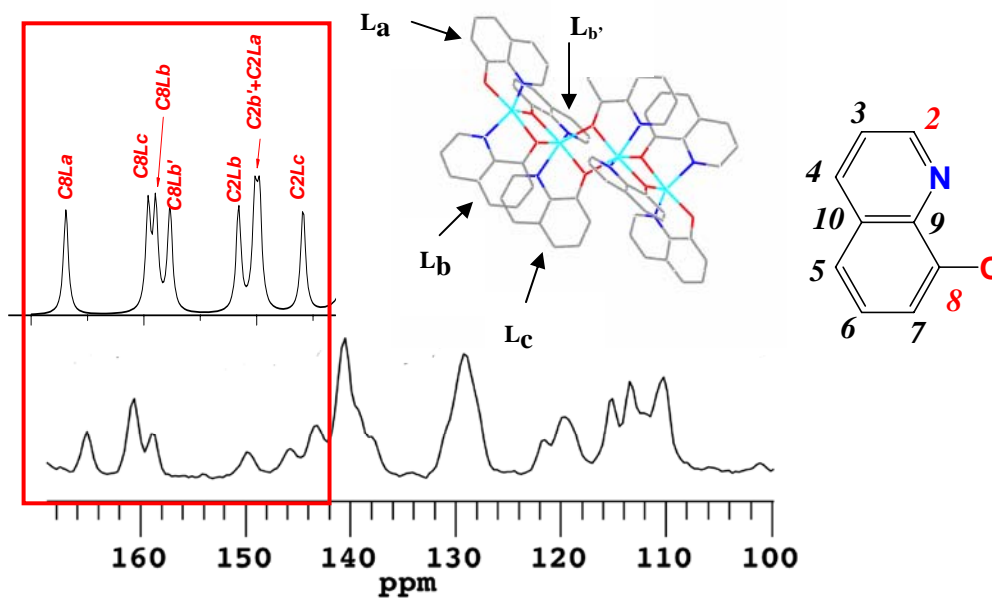


Figure 1. Solid state ^{13}C CP-MAS NMR spectrum for $Zn(II)(8\text{-quinolinolato})$ tetramer showing C8 and C2 resonances are different depending on the mode and environment of ligand chelation. (Inset: Simulated spectrum showing C8 and C2 resonances from DGAIO-SCFF calculations).

Another material system of great interest is ZnO , because nanorods and/or nanowires made from this material have shown extremely interesting catalytic and optoelectronic properties. However, achieving large quantities of well-dispersed and uniform ZnO structures for fine-tuning these properties has been a challenge. We have developed a new low-temperature reflux method to form large quantities of uniform ZnO nanorods ~ 200 nm in diameter.⁷ Different surfactants were used to control the nanostructure morphologies. Since structural defects can impart significant influence over the physical and chemical properties of ZnO nanostructures, it is vital to characterize these defects. We show that temperature dependent high resolution 1H MAS NMR studies of ZnO nanorods allows determination of the adsorption and desorption of protons from different sites on the nanorods providing a unique structural probe which differentiates ZnO nanorods prepared by different synthetic methodologies. In contrast to commercially available ZnO nanorods, our uniform nanorods show a surprisingly sharp 1H NMR resonance that appears after heating to 175 °C and is sustained upon heating to

500 °C (see Fig. 2). This suggests that some unusually stable OH species exist, most likely due to the lattice defects in ZnO nanorods. These new NMR results will be used to better understand and establish structure / function properties of ZnO materials related to its photoluminescent, catalytic and proton conductivity properties.

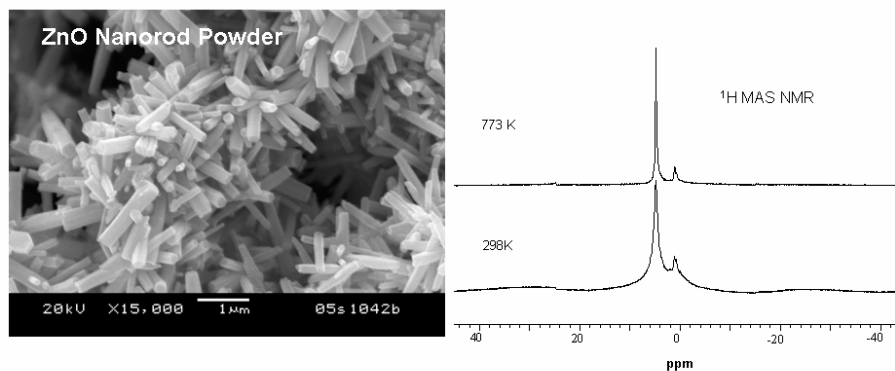


Figure 2. ZnO nanorods grown uniformly by a new low-temperature reflux method and corresponding temperature-dependent ^1H MAS NMR spectrum.

Future Plans

While controlling the orientation and reactivity of specific chemical building blocks remains a considerable challenge, computational methodologies offer a means for systematic investigation of the controlling influences through structure-property relationships. In the case of zinc quinolate chelate materials, the topology and the critical energetic balance between inorganic-coordination and oligomerization are key elements to the evolution of the three dimensional supramolecular structure. Critical phenomena, such as aspects affecting the reactivity of specific building blocks needs to be accessed prior to developing a synthetic method for forming such supramolecular structures in a controlled fashion. As evidenced by recent computational studies, thermodynamic and spectroscopic quantities for the formation of inorganic-organic building blocks and the structure of the resulting supramolecular structures are achievable. We hope to apply computational modeling techniques, such as eigenvector following⁷ and intrinsic reaction coordinate (IRC) analysis,⁸ which have proven invaluable for assessing the viability of new materials through examination of the enthalpies and entropies of candidate reaction pathways. In addition, we plan to extend our solid state NMR studies to new organic phosphine oxide materials developed for organic light emitting devices and novel metal oxide nanostructures developed in our laboratory.

References

1. Kai, Y.; Moraita, M.; Yasuka, N.; Kasai, N. *Bull. Chem. Soc. Jpn.* **1985**, *58*, 1631.
2. Sapochak, L.S.; Benincasa, F.D.; Schofield, R.; Baker, J.; Riccio, K.; Fogarty, D.; Kohlmann, H.; Ferris, K.; Burrows, P.E. *J. Am. Chem. Soc.* **2002**, *124*, 6119.

3. Schofield, R. M.S. in *Electrical and Computing Engineering*, Univ. Nevada, Las Vegas, 2003.
4. Sapochak, L.S.; Falkowitz, A.; Ferris, K.F.; Steinberg, S; and Burrows, P.E., "Supramolecular molecular structures of Zn(II) (8-quinolinolato) chelates," *J. Phys. Chem. B* **2004**, *108*, 8558.
5. Sapochak, L.S.; Ferris, K.F.; Wang, L.-C., "Experimental and Theoretical Structure Characterization of Supramolecular Zinc (II) (n-Methyl-8-Quinolinolato) Chelates by ^{13}C CP-MAS Solid-State NMR Spectroscopy and DGAIO-SCFF Calculations," in preparation.
6. Yao, C.; Wang, L.-Q.; Zhou, X.; Windisch, Jr., C.F.; Exarhos, G., paper in preparation for *Chem. Comm.*
7. Jensen, F. *J. Chem. Phys.* **1995**, *102*, 6706.
8. Baldrige, K.K.; Gordon, M.S.; Steckler, R.; Truhlar, D.G. *J. Phys. Chem.* **1989**, *93*, 5107.

Related DOE Sponsored Publications 2004-2006

Nuclear Magnetic Resonance Studies of Aluminosilicate Gels prepared in High-Alkaline and Salt-Concentrated Solutions, L. -Q. Wang, S. V. Mattigod, K.E. Parker, D.T. Hobbs, D. E. McCready, *J. Non-Crystalline Solids*, **2005**, *351*, 3435.

Nuclear Magnetic Resonance Studies of Resorcinol-Formaldehyde Aerogels, I.L. Moudrakovski, L. -Q. Wang, G. J. Exarhos, V. V. Terskikh, C. I. Ratcliffe, J. A. Ripmeester, *J. Phys. Chem. B* **2005**, *109*, 11215.

Supramolecular Structures of Zinc (II) (8-Quinolinolato) Chelates, L.S. Sapochak, A. Falkowitz, K.F. Ferris, S. Steinberg, P.E. Burrows, *J. Phys. Chem. B* **2004**, *108*, 8558.

Structure and Three-Dimensional Crystal Packing Preferences for mer-Tris(8-quinolinolato) Indium (III) Vapor Phase Grown Crystals, L.S. Sapochak, A. Rasasinghe, H. Kohlmann, K.F. Ferris, P.E. Burrows, *Chem. Mater.* **2004**, *16*, 401.

Nuclear Magnetic Resonance Investigation of Organic Aerogels, I. L. Moudrakovski, L. -Q. Wang, G. J. Exarhos, V. V. Terskikh, C. I. Ratcliffe, J. A. Ripmeester, *J. Am. Chem. Soc. Commun.* **2004**, *126*, 5052.

Theoretical Investigations of Nanoscale Structures and Semiconductor Surfaces

J. Bernholc and C. Roland

bernholc@ncsu.edu, roland@gatubela.physics.ncsu.edu

Center for High Performance Simulation and Department of Physics
North Carolina State University, Raleigh, NC 27695-7518

Program Scope

This proposal addresses fundamental issues in nanoscale science and technology, namely the design of nanostructured materials and processes with desired, novel characteristics. The research projects focus on several broad areas: (i) nanotube-based structures for high-specificity sensors, multi-terminal electronic components and capacitance probes, (ii) the formation of organic/Si interfaces for integration of biomolecules with Si technology, (iii) properties of magnetic semiconductors for spintronic applications, and (iv) optical signatures of complex materials for structural identification and feedback-controlled layer-by-layer growth. These projects build on the work accomplished during the prior proposal period, which included several investigations of electronic properties and quantum transport in nanotube structures, and of complex adatom and molecular structures at Si surfaces. We have also made substantial methodological gains and can now study quantum transport from first-principles using accurate real-space methods that scale essentially linearly with the number of atoms N , and we have refined the methodology for computing optical signatures of surface structures, aiding in the identification and classification of complex adsorbate-induced surface configurations. Our technical approach relies on proven, large-scale electronic structure methods implemented on the latest state-of-the-art parallel computers. The calculations use recently developed real-space multigrid techniques, which provide for automatic preconditioning and convergence acceleration on all length scales.

Recent Progress

Using large scale $O(N)$ real-space-based *ab initio* calculations, we carried out a theoretical study of novel carbon nanotube-cluster composites as prototype systems for molecular sensing at the nanoscale. Dramatic changes in the electrical conductance of the composite are predicted when gas molecules are adsorbed onto the metal clusters. The effects of different adsorbing gases at different coverage have been investigated for systems based on either metallic or semiconducting nanotubes. The observed sensitivity and selectivity of the change in the electrical resistance upon gas adsorption suggests new avenues for the design and production of nanotube-based molecular sensors.

Although it has long been known that classical notions of capacitance needs modification at the nanoscale, in order to account for quantum effects, very few first-principles investigations of these properties exist for any real material systems. We have investigated the capacitance properties of prototypical carbon nanotube systems with a recently developed real-space nonequilibrium Green's function method, with special attention paid to the treatment of the bound states present in the system. Specific systems investigated include two and three-nested nanotube shells, the insertion of a capped nanotube into another, a connected (12,0)/(6,6)

nanotube junction, and the properties of a nanotube acting as a probe over a flat aluminum surface. First principles estimates of the capacitance matrix coefficients for these systems have been determined, along with the origin of the quantum corrections. For the case of the nanotube junction, the numerical value of the capacitance is sufficiently high as to be useful for future device applications.

We investigated (Ga,Mn)As, which is the most widely studied diluted magnetic semiconductor (DMS). It is widely regarded as a testing ground for understanding DMS properties. Our calculations explain well the experimentally observed substantial increase of the ferromagnetic transition temperature in GaMnAs upon low temperature annealing. We show that this is due to out-diffusion of compensating Mn interstitials towards the surface. Our calculated diffusion barrier is in very good agreement with the experimental data, and our calculations highlight the complex interplay between the substitutional and interstitial Mn configurations. Our key conclusions (diffusion and surface-accumulation of interstitial Mn; formation of p-n junctions to inhibit diffusion into bulk) will have important implications for many previously published experimental works. The low temperature annealing effect, the reported thickness dependence of T_c , and the effect of capping layers are some examples. Mn diffusion will also have to be a consideration when designing (Ga,Mn)As-based heterostructures or examining previously published heterostructure studies. In particular, for Mn in (Ga,Mn)As, the nature of the diffusion is richer and more complex than in more 'traditional' cases (e.g., interstitial Li in GaAs) due to the percolation character of the diffusion and distribution of energy barriers, Mn-Mn interactions, and spin-dependence of the barriers. These effects had to be fully accounted for in order to explain the experimental data.

As a new area for us, we investigated many-body effects in the optical spectrum of water. This spectrum provides an important signature for its detection and a measure of its properties, yet it is poorly understood despite decades of effort. Usually, when individual molecules condense into a liquid or a solid, the first absorption peak shifts to lower energies, because of broadening of their energy levels. For water the opposite occurs and this puzzle remained unexplained. Our supercomputer calculations, which use newly developed theoretical methods (GW and Bethe-Salpeter in a real-space basis), show that hydrogen bonds between neighboring molecules enable optically excited electrons to move farther away from their origin, thus lowering the binding energy of the electron-hole pair. In fact, the pair "sees" the first and even the second neighbors of the excited molecule. The optical shift, which is fully reproduced by the calculations, can be used to measure microscopic aspects of intermolecular interactions in water.

Understanding the time evolution of modulated systems has been a problem of long-lasting interest and importance. Recently, there has been a resurgence of interest in this issue brought about by the advent of nanotechnology. It has become clear that future molecular electronic, biomedical and photonic systems will require the self-assembly of the associated device elements into a functional unit. One way to achieve this is to make use of patterns that are produced by modulated systems, which can act as lithographic templates. In particular, spectacular long-range ordering on suitable length scales has been achieved with soft-condensed matter systems such as block copolymers and related surface systems. To date, the current patterns for templates are for the most part based on "stripes" and "bubble" patterns. We have analyzed the domains and instabilities that form in modulated systems and have shown that a very much larger variety of

patterns -- based on long-lived metastable and glassy states -- may be formed as a compromise between the required equilibrium modulation period and the strain present in the system. The strain is the result of topological constraints, which effectively preclude the system from reaching its equilibrium configuration. Ultimately, it is hoped that many of the new patterns will be identified experimentally, and find their application as nanolithographic templates, thereby enriching the choice of patterns in current use.

Future Plans

A considerable effort is currently devoted to the search of semiconductors with ferromagnetism controlled by band carriers for potential spintronic applications. (Ga,Mn)N attracts a particular attention because the predicted Curie temperatures T_C exceed the room temperature. However, ferromagnetic spin alignment in (Ga,Mn)N has proven highly elusive, with typically only a small fraction of about 1-10% of Mn spins participating in ferromagnetism and coexistence of ferro- and paramagnetism. Several of these observations are not compatible with the assumption of FM mediated by free carriers in samples with a random distribution of Mn ions. We are thus investigating the possibility of the formation of MnN inclusions in (Ga,Mn)N. Turning to organics-on-Si structures, we are examining the electron transport properties of cyclopentene on Si(001). We have previously determined its precise adsorption geometry through a comparison of the computed and measured reflectance anisotropy spectra, which are extremely sensitive to surface and adsorbate structure.

Currently, the transport characteristics of two different semiconducting nanotubes (carbon and boron nitride) coupled to metallic Al leads are under investigation with the combined nonequilibrium Green's function/density functional theory formalism. The characteristics of such a device are determined by Schottky barrier, Fermi-level pinning and band-bending phenomena, which we are probing. Specifically, there is evidence for a modest Schottky barrier of about 0.46 eV for the carbon nanotube system, which is subject to Fermi level pinning because of the metal-induced gap states (MIGS).

DOE-sponsored publications for 2004-2005

1. "Mn Interstitial Diffusion in GaMnAs," K.W. Edmonds, P. Bogusławski, B.L. Gallagher, R.P. Campion, K.Y. Wang, N.R.S. Farley, C.T. Foxon, M. Sawicki, T. Dietl, M. Buongiorno Nardelli, J. Bernholc, *Phys. Rev. Lett.* **92**, 037201 (2004).
2. "Calculation of surface optical properties: From qualitative understanding to quantitative predictions," W. G. Schmidt, K. Seino, P. H. Hahn, F. Bechstedt, W. Lu, S. Wang, and J. Bernholc, *Thin Solid Films* **455/456**, 764 (2004).
3. "Atomic Indium nanowires on Si(111): The (4x1)-(8x2)-phase transition studied with Reflectance Anisotropy Spectroscopy," K. Fleischer, S. Chandola, N. Esser, W. Richter, J. F. McGilp, F. Bechstedt, S. Wang, W. Lu, W.G. Schmidt, J. Bernholc, *Appl. Surf. Sci.* **234**, 302 (2004).
4. "Simulations of nanotube-based structures and devices," J. Bernholc, M. Buongiorno Nardelli, W. Lu, V. Meunier, S. Nakhmanson and Q. Zhao, *Proc. Conf. on Foundations of Nanoscience: Self-assembled Architectures and Devices*, Science Technica, 367 (2004).

5. "Calculation of surface optical properties: from qualitative understanding to quantitative predictions," W. G. Schmidt, K. Seino, P.H. Hahn, F. Bechstedt, W. Lu, S. Wang, and J. Bernholc, *Thin Solid Films* **455/456**, 764 (2004).
6. "Large-scale quantum-mechanical simulations of nanoscale devices and new materials," J. Bernholc, M. Buongiorno Nardelli, W. Lu, V. Meunier, S. M. Nakhmanson, and Q. Zhao, *Proceedings of DoD 2004 Users Group Conference*, IEEE Computer Society, 34 (2004).
7. "Oxidation- and organic-molecule-induced changes of the Si surface optical anisotropy: ab initio predictions, W. G. Schmidt, F. Fuchs, A. Hermann, K. Seino, F. Bechstedt, R. Passmann, M. Wahl, M. Gensch, K. Hinrichs, N. Esser, S. Wang, W. Lu and J. Bernholc, *J. Phys.: Condens. Matter* **16**, S4323 (2004).
8. "Capacitance, induced charges, and bound states of biased carbon nanotube systems", P. Pomorski, L. Pastewka, C. Roland, H. Guo and J. Wang, *Phys. Rev. B* **69**, 115418 (2004).
9. "Quantum transport through short semiconducting nanotubes: a complex band structure analysis", P. Pomorski, C. Roland and H. Guo, *Phys. Rev. B* **70**, 115408 (2004).
10. "Theory of Electronic Structure and Magnetic Interactions in (Ga,Mn)N and (Ga,Mn)As," P. Bogusławski, and J. Bernholc, *AIP Conf. Proc.* **772**, 1331 (2005).
11. "Optical Absorption of Water: Coulomb Effects versus Hydrogen Bonding," P. H. Hahn, W. G. Schmidt, K. Seino, M. Preuss, F. Bechstedt, and J. Bernholc, *Phys. Rev. Lett.* **94**, 037404 (2005), listed also in *Virtual Journal of Biological Physics Research*, February 1 (2005).
12. "Carbon nanotube-metal cluster composites: a new road to chemical sensors?" Q. Zhao, M. Buongiorno Nardelli, W. Lu and J. Bernholc, *Nano Letters* **5**, 847 (2005).
13. "Non-equilibrium quantum transport properties of organic molecules on silicon," W. Lu, V. Meunier, and J. Bernholc, *Phys. Rev. Lett.* **95**, 206805 (2005).
14. "Fermi level effects on the electronic structure and magnetic couplings in (Ga,Mn)N," P. Bogusławski and J. Bernholc, *Phys. Rev. B* **72**, 115208 (2005).
15. "Properties of wurtzite w -MnN and of w -MnN inclusions in (Ga,Mn)N," P. Bogusławski and J. Bernholc, *Phys. Rev. B* **72**, 115208 (2005).
16. "Electron transport in molecular systems," V. Meunier, W. Lu, J. Bernholc, and B. G. Sumpter, *Journal of Physics: Conference Series* **16**, 283 (2005).
17. "Mn Interstitial Diffusion in GaMnAs – Reply," K.W. Edmonds, P. Bogusławski, B.L. Gallagher, R.P. Campion, K.Y. Wang, N.R.S. Farley, C.T. Foxon, M. Sawicki, T. Dietl, M. Buongiorno Nardelli, J. Bernholc, *Phys. Rev. Lett.* **94**, 139702 (2005).
18. "Multiscale simulations of quantum structures," J. Bernholc, W. Lu, S. M. Nakhmanson, V. Meunier, and M. Buongiorno Nardelli, *Proceedings of DoD 2005 Users Group Conference*, IEEE Conference Proceedings (2005).
19. "Hydrogenation effects on the structural transition of C60," J.-Y. Yi and J. Bernholc, *Chem. Phys. Lett.* **403**, 359 (2005).
20. "Quantum calculations of carbon nanotube charging and capacitance", P. Pomorski, L. Pastewka, C. Roland, H. Guo, and J. Wang, *Mater. Res. Soc. Symp. Proc.* **789**, N3.6 (2004).
21. "New and exotic self-organized patterns for modulated nanoscale systems", C. Sagui, E. Asciutto, and C. Roland, *Nano Letters* **5**, 389 (2005).
22. "Self-assembled patterns and strain induced instabilities for modulated systems", E. Asciutto, C. Roland and C. Sagui, *Phys. Rev. E* **72**, 021504 (2005).

Theory of Surface and Interface Properties of Correlated Electron Materials

Andrew Millis and Satoshi Okamoto

millis@phys.columbia.edu, okapon@phys.columbia.edu

Department of Physics, Columbia University
538 West 120th Street, New York, New York 10027

Program Scope

One of the exciting developments in materials science has been the discovery that a wide class of transition metal oxide materials can exhibit exotic (and possibly useful) electronic properties, including “half metallicity” (metallic ferromagnetism with complete spin polarization) and high temperature superconductivity. A key scientific obstacle to practical applications of these materials is a lack of understanding of the surface and interface physics; in particular, proximity to a surface or interface seems to change the interesting electronic behavior in ways we do not yet fully understand. Our research aims to fill this gap.

We investigate theoretically the effects of proximity to a surface or interface on “correlated electron” phenomena such as magnetism and superconductivity. The issue is important in its own right as a fundamental scientific question, is crucial for the interpretation of wide classes of experiment and is necessary background information for the development of devices. The research is fundamental and exploratory in nature: the basic physics and materials science of the systems is not at present understood. The problem is difficult because the phenomena of interest (high-spin-polarization magnetism, high temperature superconductivity) occur in transition metal oxide materials characterized by strong electron-electron interaction effects and a strong coupling of the electronic behavior to the lattice and local structure.

Our approach is to identify the relevant physical, structural and chemical changes (“control parameters”) occurring near surfaces/interfaces, develop a theoretical understanding of the effects of each control parameter separately, and then produce a picture of the combined effects. A crucial aspect of the study of the individual control parameters is the identification of systems which express a particular control parameter strongly and can be fabricated and studied experimentally, so that the theory can be compared to data. The theoretical work requires development of new methods, capable of treating strongly interacting systems with strong spatial inhomogeneity. Our current focus is on “heterostructures”: multicomponent systems containing atomically thin layers of one or more materials with important magnetic or electrical properties.

Recent Progress

Two crucial issues are the development of appropriate theoretical and computational methods, and the validation of these methods by comparison to appropriate experimental control systems. We are interested in electronic properties such as magnetism which arise from the correlations induced in the quantum mechanical wave function by electron-electron-interactions. Study of these phenomena is difficult, and the difficulty is increased by the spatial symmetry breaking occurring at surfaces and interfaces. For this reason the established techniques of many body physics are inadequate. We have developed and tested for accuracy a new “semiclassical” computational method (see publication[2] below) which is more than two orders of magnitude faster than the standard approaches, and have also found a new way to test for electronic phase separation (publication[3] below). We have applied our results to gain insight into theoretical model systems which capture important parts of the physics of heterostructures, including the competition between different possible magnetic orderings (publication[4]) and the

interplay between charge confinement and magnetic order (publication [5]).

Recently, experimental groups have succeeded in fabricating two classes of heterostructures: SrTiO₃/LaTiO₃ (studied by the group of H.Y. Hwang at the University of Tokyo and by scientists at the Max-Planck institute in Stuttgart) and “Colossal Magnetoresistance” (LaMnO₃/SrMnO₃) (studied by the group of J. Eckstein at the University of Illinois at Urbana-Champaign). For the SrTiO₃/LaTiO₃ we have combined band-theoretic and many-body physics methods to produce predictions for the phase diagram, transport and optical properties which can be fruitfully compared to experiment. We predict large lattice distortions and a novel form of XY orbital order, as well as ferromagnetism (in systems which are antiferromagnetic in bulk (publication [6]). We are presently engaged in the computations which will allow us to make analogous predictions for the manganite-based materials.

In addition, two review articles summarizing the present status and future prospects of the field were prepared and are in press (manuscripts [1] and [7] below).

Future Plans

We are continuing the development of theoretical methods. We have begun a collaboration with a group at Ecole Polytechnique (France), who are developing a new computational method which may be suitable for the problems of interest to us. We are also continuing to develop the techniques and ideas needed to combine the band-theoretic and many-body physics calculational tools, to allow accurate study of the effects of strain and lattice relaxation. Of particular importance is the development of techniques which can capture the behavior of systems with partially filled *d*-shells (where the high degree of orbital degeneracy leads to a multiplicity of interactions and a great richness of behavior). An approach involving expressing the interactions in terms of the rotational invariants of the system and applying continuous Hubbard-Stratonovich transformation techniques is presently being developed.

Concerning experimental systems, we plan to extend our techniques to a wider variety of heterostructures, in particular to systems with components involving different transition metals. Another crucial open question concerns surfaces. Because most of the surfaces of materials of interest are polar, significant lattice reconstructions are expected to occur and to couple strongly to the many-body physics. In collaboration with experimental groups at Brookhaven, Oak Ridge and elsewhere, we will develop an understanding of how to “passivate” or otherwise control the surface of a transition metal oxide.

DOE Sponsored Publications

- 1 *Electronic Reconstruction at Surfaces and Interfaces of Correlated Electron Materials*, A.J. Millis, chapter in *Oxide Thin Films*, S. Ogale, ed. Springer Verlag (in press, 2005).
- 2 *Benchmarking a semiclassical impurity solver for dynamical-mean-field theory: self-energies and magnetic transitions of the single-orbital Hubbard model*, S. Okamoto, A. Fuhrmann, A. Comanac and A. J. Millis, Phys. Rev B 71, 235113 (2005).
- 3 *Implications of the low-temperature instability of dynamical mean-field theory for double-exchange systems*, C. Lin and A. J. Millis, Phys. Rev. B72, 245112 (2005).
- 4 *Interface ordering and phase competition in a model Mott-insulator-band-insulator heterostructure*, S. Okamoto and A. J. Millis, Phys. Rev. B72, 235108 (2005).
- 5 *Dynamical Mean Field Study of Model Double-Exchange Superlattices*, C. Lin, S. Okamoto, A. J. Millis, cond-mat/0512061.
- 6 *Lattice relaxation, electronic screening, and spin and orbital phase diagram of LaTiO₃/SrTiO₃ superlattices*, S. Okamoto, A. J. Millis, N. A. Spaldin, cond-mat/060108.

7. *Electrostatic Tuning of Novel Materials*, C.H. Ahn, A. Bhattacharya, M. DiVentra, J. N. Eckstein, C. Dan Frisbie, M. E. Gershenson, A. M. Goldman, I.H. Inoue, J.Mannhart, A. J.Millis, A.Morpurgo, D. Natelsonand J. M. Triscone (submitted to Rev. Mod. Phys).
8. *Electronic reconstruction in correlated electron heterostructures*, S. Okamoto and A.J. Millis, Proc. SPIE Int. Soc. Opt. Eng. 5932, 593218 (2005).

Metal-Insulator-Semiconductor Photonic Crystal Fibers: A New Paradigm for Optoelectronics

Y. Fink and J. D. Joannopoulos

Research Laboratory of Electronics

Massachusetts Institute of Technology, Cambridge MA, 01239

Abstract

The demonstrated ability of photonic crystals to control light in truly unique ways makes them extremely attractive candidates for addressing problems in the general areas of radiation conversion, conservation, and control. Guiding radiation through air-waveguides without losses, radiation insulation inside and outside homes, heat-retaining lightweight clothing, and energy-generating thermal or solar collectors, are obvious examples where photonic crystal materials could play a very important role. By the same token, the ability to work within a fiber-processing platform, as in the optical or textile fiber industries, provides the intrinsic possibility for very low cost production and for very large area coverings. Unfortunately, virtually all electronic and optoelectronic devices are made of conductors, semiconductors, and insulators in well-defined geometries and prescribed length scales. Clearly, it would be an enormous benefit if there were some way to combine the advantages of all three *without* a corresponding sacrifice in performance. Recently, we succeeded in taking the first steps along this direction by demonstrating that cylindrical, *omnidirectionally reflecting* multilayer film photonic crystal fibers can be drawn with exquisite precision and exceptional optical properties. We also demonstrated that such fibers can be co-drawn with *metal, insulator, and semiconductor* (M-I-S) components leading to new fiber functionalities for the simultaneous guiding of both electrons and photons, and for creation of optoelectronic fiber devices. Current efforts are being focused on exploring the feasibility of designing and producing extended lengths of efficient and flexible *power-generating* M-I-S containing fibers for use in *Photovoltaic* (PV) and *Thermoelectric* (TE) applications.

Three-Dimensional Photonic Crystals by Soft Lithographic Technique

Jae-Hwang Lee^{1,2}, Yong-Sung Kim^{1,2}, Joong-Mok Park^{1,2}, Wai-Y. Leung^{1,2}, Chang-Hwan Kim^{1,2}, Ping Kuang^{1,3}, Rana Biswas^{1,2}, Kristen Constant^{1,3}, Kai-Ming Ho^{1,2}
kmh@ameslab.gov

¹Ames Laboratory-USDOE, Ames

²Dept of Physics and Astronomy, Iowa State University, Ames, IA 50011

³Dept of Materials Science and Engineering, Iowa State University, Ames, IA 50011

Program Scope

There is increasing interest in three-dimensional (3D) crystals which can confine light in all directions. This will lead to efficient light emission by controlling transition probabilities of excited atoms or molecules. However, most research has been limited to 2D photonic crystals mainly because of difficulties in 3D micro-fabrication. The program we are developing uses a non-photolithographic process, called two-polymer microtransfer molding (2P- μ TM), and is expected to realize low cost and tailorable 3D structures. Polymer templates fabricated by 2P- μ TM were successfully converted to both dielectric and metallic 3D photonic crystals. With this expertise in 3D microfabrication, the program aims to extend 2P- μ TM to photonic crystals applicable at near-infrared or visible frequencies, and to explore novel photonics applications of 3D periodic polymer microstructures. We are developing a 2D holographic lithography tool to generate smaller master patterns for 2P- μ TM and to develop a 2nd generation scheme of our alignment method using fluorescence-based moiré fringes. As this program progresses, we believe that our techniques for fabrication of dielectric, metallic and polymeric microstructures will improve the performance of a variety of solid lighting devices, especially organic light emitting devices and miniaturized lasers.

Recent Progress

Photonic crystals were first proposed in 1987 as a way to control the spontaneous emission¹ or the localization² of light. Early work done at Ames Laboratory established the existence of a photonic band gap in the diamond structure.³ The Ames group produced designs that allowed three dimensional photonic band-gap crystals to be realized at high frequencies^{4,5}. In 1998, using the Ames Laboratory's patented, layered lattice design, S. Y. Lin and J. G. Fleming at Sandia National Laboratories successfully fabricated photonic crystals with band-gaps in the infrared and fiber-optics wavelengths^{6,7}. In 2002, they, in collaboration with Ames Laboratory scientists, extended the fabrication to photonic crystals made of tungsten⁸. These photonic crystals can be removed from the substrate and were found to be highly efficient light emitters in a specific frequency range⁹. However, conventional microfabrication techniques require high cost and expensive equipment for three-dimensional photonic crystals. Although a wide variety of novel approaches have been introduced to alleviate the difficulties in 3D microfabrication, they are not both low cost and tailorable.

We have proposed and demonstrated an economical technique to fabricate a three-dimensional layer-by-layer photonic band gap structure in the infrared wavelengths^{10,11}. A

polymer template of a photonic crystal structure is assembled using the microtransfer molding technique. This template is infiltrated with sol-gel or nanoparticle titanium oxide slurry, the template is later removed by heat treatment. Central problems with this method were production yield in template fabrication and the alignment of the structure between different layers.

We developed an advanced microtransfer molding technique, 2P- μ TM that shows an extremely high yield in layer-by-layer microfabrication sufficient to produce highly layered microstructures. The use of two different photo-curable prepolymers, a filler and an adhesive, allows for fabrication of layered microstructures without thin films between layers. The difference in surface energies between the polymers allows filling and selective coating of the two prepolymers with self-healing properties. The capabilities of 2P- μ TM are demonstrated by the fabrication of a wide-area 12-layer microstructure with high structural fidelity [see Fig. 1]

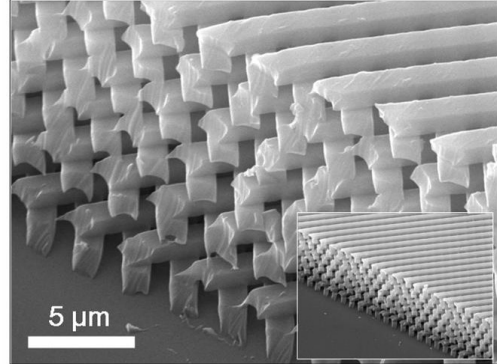


Fig. 1 12-layered polymer microstructure by 2P- μ TM

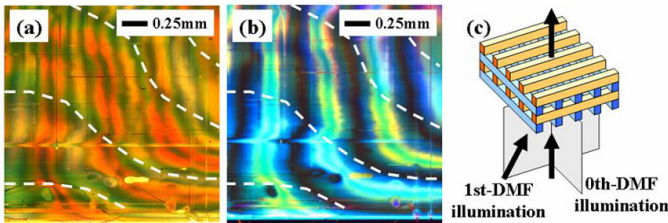


Fig. 2 Comparison of (a) conventional and (b) diffracted moiré fringes with (c) their imaging configurations.

structures comprised of irregularly deformed periodic patterns. By a comparison study of the diffracted moiré fringe pattern and detailed microscopy of the structure, we show that the diffracted moiré fringe can be used as a nondestructive tool to analyze the alignment of multilayered structures. The alignment method yields high contrast of fringes even when the materials being aligned have very weak contrasts [see Fig. 2].

An efficient method of fabricating free-standing three-dimensional metallic photonic crystals using 2P- μ TM was also developed. Low cost and ease of fabrication are achieved through gold sputter deposition on a free-standing woodpile polymer template [see Fig. 3(a)]. The photonic crystals behave as full metallic structures with a photonic band edge at a wavelength of $3.5 \mu\text{m}$. The rejection rates of the structures are about 10 dB per layer. By using ceramic infiltration of

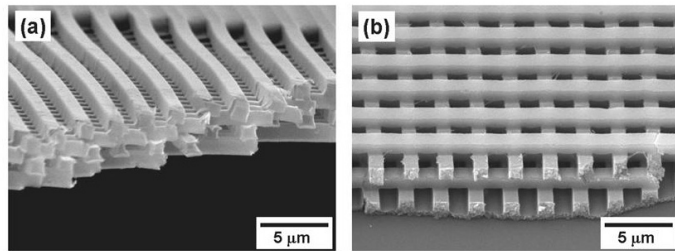


Fig. 3 SEM images of (a) metal-coated and (b) titania photonic crystals

polymer templates, ceramic woodpile structures were created. The ceramic infiltration technique for complex three-dimensional microstructures allows us to realize excellent structural fidelity and a low crack density [see Fig. 3(b)]. The fabricated photonic crystals have a photonic band gap at around $5\mu\text{m}$ and agree well with theoretical calculations. Since the structure of the crystals is fully controllable, diverse applications are expected by implanting functional defects.

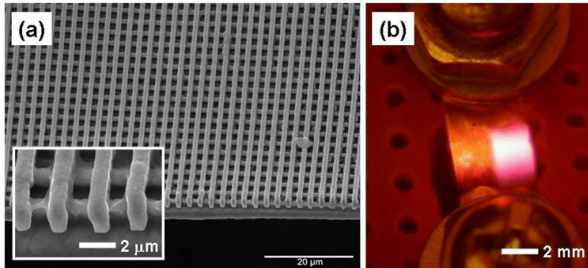


Fig. 4 (a) SEM images of a full metallic photonic crystal; (b) photograph of a glowing crystal by Joule heating.

We also found that polymer templates can be backfilled with metals by electro-deposition and removed by thermal decomposition. By doing so we can get woodpile-like full metallic structure [Fig. 4(a)]. And the metallic structure can be heated by passing an electrical current directly through the structure [Fig. 4(b)]. In Fig. 4(b), the bright region is the photonic crystal patterned region in our copper filament.

The emission of visible light is stronger than an unpatterned copper film with the same thickness. Based on this approach, we are designing efficient geometries for tailorable thermal radiation and investigating the emission behavior of full metallic photonic crystals with different configurations.

Future Plans

We will continue to develop new methods to align multiple layers (up to 32 layers). By solely using moiré fringe method, multilayer over four layers is difficult. To extend aligning capability, we will develop a fluorescence-based alignment method, complementing the developed moiré fringes technique. At present, we have been demonstrating our techniques with patterns with a $2.5\mu\text{m}$ pitch. We are developing an optical apparatus for 2D holographic lithography to reach higher frequencies with submicron pitch patterns. The resulting 2D structures will be used for master patterns for 2P- μTM and a modified layer-by-layer fabrication. With the smaller-pitch polymer templates, ceramic and metallic infiltration will be carried out. For thermal emission purposes, new metal-based composite photonic crystals will be studied for the potential of narrow emission peaks and high energy efficiency.

References

- (1) E. Yablonovitch, *Phys. Rev. Lett.* **1987**, 58, 2059-2062.
- (2) S. John, *Phys. Rev. Lett.* **1987**, 58, 2486-2489.
- (3) K. M. Ho, C. T. Chan, C. M. Soukoulis, *Phys. Rev. Lett.* **1990**, 65, 3152-3155.
- (4) K. M. Ho, C. T. Chan, C. M. Soukoulis, R. Biswas, M. Sigalas, *Solid State Commun.* **1994**, 89, 413-416.
- (5) E. Ozbay, E. Michel, G. Tuttle, R. Biswas, M. Sigalas, K. M. Ho, *Appl. Phys. Lett.* **1994**, 64, 2059-2061.

- (6) S. Y. Lin, J. G. Fleming, D. L. Hetherington, B. K. Smith, R. Biswas, K. M. Ho, M. Sigalas, W. Zubrzycki, S. R. Kurtz, J. Bur, *Nature* **1998**, 394, 251-253.
- (7) J.G. Fleming, S. Y. Lin, *Opt. Lett.* **1999**, 24, 49-51.
- (8) J. G. Fleming, S. Y. Lin, I. El-Kady, R. Biswas, K. M. Ho, *Nature* **2002**, 417, 52-55.
- (9) S. Y. Lin, J. G. Fleming, I. El-Kady, *Opt. Lett.* **2003**, 28, 1683-1685.
- (10) W. Leung, K. Constant, K. –M. Ho, M. Sigalas, H. Kang, C. –H. Kim, D. Cann, J. –H. Lee, *US Patent No. 6,555,406 B1* **2003**.
- (11) W. Leung, H. Kang, K. Constant, D. Cann, C. –H. Kim, R. Biswas, M. Sigalas, K. –M. Ho, *J. Appl. Phys.* **2003**, 93, 5866-5870.

DOE Sponsored Publication in 2004-2005

Diffraction moiré fringes as analysis and alignment tools for multilayer fabrication in soft lithography, J. –H. Lee, C. –H. Kim, Y. –S. Kim, K. –M. Ho, K. Constant, W. Leung, C. H. Oh, *Appl. Phys. Lett.* **2005**, 86, 204101.

Two-polymer microtransfer molding for highly layered microstructures, J. –H. Lee, C. –H. Kim, K. –M. Ho, K. Constant, *Adv. Mater.* **2005**, 17, 2481-2485.

Photonic band gaps of conformally coated structures, R. Biswas, J. Ahn, T. Lee, J. –H. Lee, Y. –S. Kim, C. –H. Kim, W. Leung, C. –H. Oh, K. Constant, K. –M. Ho, *J. Opt. Soc. Am. B* **2005**, 22, 2728.

Author Index

Author Index

Abrams, Billie L.	25	Leung, Wai-Y 91
Alivisatos, Paul 19		Liu, Feng..... 72
Amy, Fabrice..... 48		Malliaras, George G. 2,44
Bernholc, Jerry 83		Martin, Richard L. 7
Biswas, Rana..... 91		McBride, James R. 50
Braun, Paul V. 27		McGehee, Michael 12
Bredas, Jean-Lue..... 2		Mele, Eugene J. 76
Bowers, Michael J. II 50		Melosh, Nicholas 12
Brongersma, Mark 12		Millis, Andrew..... 87
Constant, Kristen..... 91		Muenchausen, Ross E..... 54,58
Cooke, D. Wayne..... 54,58		Munkholm, Anneli 62
Campbell, Ian H. 7		Nuckolls, Colin P..... 11
Chelikowsky, James R. 21		Okamoto, Satoshi 87
Crawford, Mary H. 66		Papadimitratos, Alexis..... 44
Crone, Brian K. 7		Park, Joong-Mok 91
Deng, Lan..... 15		Poulsen, Daniel..... 15
Duggal, Anil..... 2		Provencio, Paula P. 25
Exarhos, Greg 79		Ramirez, Arthur P. 11
Ferris, Kim 79		Roland, Christopher..... 83
Fink, Yoel 90		Rosenthal, Sandra J. 50
Fischer, Art J. 66		Russell, Tom P. 31
Follstaedt, David M. 66		Sapochak, Linda 79
Fong, Hon Hang..... 44		Segalman, Rachel 15
Forrest, Stephen 1		Shi, Jing 6
Fréchet, Jean M.M. 15		Shinar, Joseph..... 40
Ho, Kai-Ming..... 91		Siegrist, Theo..... 11
Howard, Andy 72		Smith, Darryl L..... 7
Hwang, Jaehyung..... 48		So, Woo-Young..... 11
Jacobsohn, Luiz G..... 54,58		Soukoulis, Costas M. 26
Jiang, Fan 62		Stephenson, G. Brian..... 62
Joannopoulos, John D. 90		Streiffer, Stephen K. 62
Kahn, Antoine 2,48		Stringfellow, Gerald B. 72
Kane, Charles L. 76		Thoma, Steven G. 25
Kaplar, Robert J. 66		Tolbert, Laren M. 35
Kim, Chang-Hwan 91		Vardeny, Z. Valy 6,32
Kim, Yong-Sung..... 91		Virgili, Justin 15
Kloc, Christian 11		Wang, Li-Qiong..... 79
Koleske, Daniel D. 66		Wei, Su-Huai 70
Kowalik, Janusz 35		Wilcoxon, Jess P. 25
Kuang, Ping..... 91		Yao, Chunhua 81
Kurtz, Steven R. 66		Zhang, Shengbai 70
Lang, David..... 11		Zhu, J. 72
Lauterwasser, Frank..... 15		Zunger, Alex..... 20
Lee, Jae-Hwang..... 91		
Lee, Stephen R. 66		